# Linear Static and Nonlinear Dynamic Analyses on Collapse Behaviors of Staggered-Truss Systems

**Chia Mohammadjani**

Submitted to the
Institute of Graduate Studies and Research
in partial fulfillment of the requirements for the Degree of

Master of Science
in
Civil Engineering

Eastern Mediterranean University
February 2015
Gazimağusa, North Cyprus

Approval of the Institute of Graduate Studies and Research

Prof. Dr. Serhan Çiftçioğlu
Director (a)

I certify that this thesis satisfies the requirements as a thesis for the degree of Master of Science in Civil Engineering.

Prof. Dr. Özgür Eren
Chair, Department of Civil Engineering

We certify that we have read this thesis and that in our opinion it is fully adequate in scope and quality as a thesis for the degree of Master of Science in Civil Engineering.

Asst. Prof. Dr. Shahram Derogar
Co-Supervisor

Asst. Prof. Dr. Mürüde Çelikağ
Supervisor

Examining Committee

1. Asst. Prof. Dr. Tülin Akçaoğlu
2. Asst. Prof. Dr. Mürüde Çelikağ
3 Asst. Prof. Dr. Shahram Derogar
4. Asst. Prof. Dr. Giray Özay
5. Asst. Prof. Dr. Serhan Şensoy

# ABSTRACT

The thesis investigates the linear and nonlinear collapse mechanism in Staggered Truss Systems using two computational programs (SAP2000 and ABAQUS finite element software). The thesis particularly focuses on the understanding and modelling of the collapse mechanisms of Staggered Truss Systems when a critical column was removed from the structure. AISC-LRFD steel structures design code and AISC 14 guidelines for staggered truss systems were used to design a full 3-D 10-story model by SAP 2000. The structure was built with Staggered Truss System (STS) in transvers direction and Moment Resistance Frame (MRF) in longitudinal direction. Linear Static and Nonlinear Dynamic Time-History analyses were then performed in accordance with UFC 2013 and GSA 2013 codes to determine the collapse potential in the existing model following removal of a load bearing element from different locations. When the results of Linear Static and Nonlinear Dynamic time-history analyses were studied in detail, it was observed that the nonlinear dynamic analysis not only yields more accurate results in revealing the collapse potential at different portions of the structure, but also is more economical in allocating this method for designing structures against progressive collapse.

Based on the software results, some indices of linear and nonlinear behavior of the systems such as yield load, vertical deformations, ductility, concrete deck effect, damping percentages, plastic rotations were analyzed. However due to limitations of SAP2000 software, the results were not comprehensive enough to provide insight understanding to the failure mechanisms. Therefore, a more advanced

finite element model using ABAQUS software was then developed. The finite element model was a full 3-D truss located between 5th and 6th floors of the existing model designed by SAP2000 with the same dimensions and the same sections using the Solid Part option in ABAQUS. The material properties, geometric and material nonlinearity and the loads were identical to the model developed using Sap 2000. The results indicates that the failure zones of the Staggered Truss Systems using both finite element software were comparable, however, the finite element model using ABAQUS also provided insights to the failure mechanisms such as plastic hinges on gusset plates and the exact location of plastic higes on truss chord were also obtained.

**Keywords**: Progressive Collapse, Linear Static, Nonlinear Dynamic, Time History, Plastic Hinges, Plastic Rotation, Vertical Deflection

# ÖZ

Bu tez, Çakışmayacak Şekilde Düzenlenmis Makas Sistemlerinde, doğrusal ve doğrusal olmayan çökme mekanizmasını, SAP2000 ve ABAQUS sonlu elemanlar yazılımlarını kullanarak incelemiştir. Tez, yapıdan bir kolon kaldırılması durumunda, Çakışmayacak Şekilde Düzenlenmis Makas Sistemlerinin çökme mekanizmasının modellenmesini anlamaya odaklıdır. AISC-LRFD çelik yapıların tasarımı standardı ve Çakışmayacak Şekilde Düzenlenmis Makas Sistemleri için hazırlanmış AISC 14 ilkeleri kullanılarak 3 Boyutlu 10 kat bir model SAP 2000 yazılımında modellenerak tasarlanmıştır. Bu yapının enine Çakışmayacak Şekilde Düzenlenmis Makas Sistemleri (ÇDMS) boyuna ise Moment Dayanımlı Çerçeve (MDÇ) kullanılarak inşa edilmiştir. Mevcut modelde, farklı konumlarda bulunan yük taşıyıcı elemanların kaldırılması sonucu oluşacak çokme mekanizmasını bulmak için UFC2013 ve GSA 2013 standardlarına göre Doğrusal Statik ve Doğrusal Olmayan Dinamik zaman-tanım alanında analizleri yapıldı. Doğrusal Statik ve Doğrusal Olmayan Dinamik zaman-tanım alanında analizler detaylı bir şekilde incelendiği zaman Doğrusal Olmayan Dinamik analizin yapının farklı kısımlarındaki çökme potansiyelini daha doğru verdiği gibi yapıların kademeli çökmeye karşı tasarımını da daha ekonomik olarak çözdüğü gözlemlenmiştir.

Program çıktılarına bakarak, doğrusal ve doğrusal olmayan sistem davranışlarının bazı endeksleri, örneğin akma yükü, düsey deformasyon, süneklik, betonarme ve çelik saç katının etkisi, sönümleme yüzdeleri, plastik rotasyon gibi, analiz edilmiştir. Halbuki SAP2000 yazılımının kısıtlamalarından dolayı, elde edilen sonuçlar çökme mekanizmasının içten anlaşılabilmesi için yeterli kapsamda

değildi. Bundan dolayı ABAQUS yazılımı kullanılarak daha gelişmiş bir sonlu elemanlar modeli hazırlanmıştır. Sonlu eleman modeli 3-boyutlu bir makas olup SAP2000 tarafından tasarlanmış 5. ve 6. katlar arasına ayni ebadlar ve ayni çelik kesitlerle ABAQUS yazılımının Solid Part seçeneği kullanılarak yerleştirilmiştir. Malzeme özellikleri, geometrik ve malzeme doğrusal olmayan özellikleri SAP2000 tarafından tasarlanmış ve geliştirilmiştir. Elde edilen sonuçlar Çakışmayacak Şekilde Düzenlenmis Makas Sistemlerinde çökme bölgeleri için her iki sonlu elemanlar yazılımı karşılaştırılabilir. Diğer yandan ABAQUS kullanılarak yapılan sonlu elemanlar modeli de kırılma mekanızmasının anlaşılmasına yardımcı oldu, örneğin bağlantı levhasında oluşan plastik mafsal ve bu plastik mafsalların makas elemanlarındaki tam yeri elde edildi.

**Anahtar sözcükler:** Kademeli çökme, Doğrusal Statik, Doğru olmayan dinamik, Zaman-Tanım, Plastic mafsallar, Plastik rotasyon, Düşey sapma

:

# ACKNOWLEDGEMENT

I would like to express my gratitude to my supervisor *Asst.Prof.Dr.Murude Celikag* and my co-supervisor *Asst.Prof.Dr. Shahram Derogar*.

My sincere appreciation goes to my family members and my friends for their kind support during accomplishment of this research.

**Science is**

***The Only***

**Twilight**

Provisional Winds blowing from Ideological Fanaticisms Can Not Shut it off as it is raised by the Dedication of Generations who believed in the Soul of Democracy and Freedom

# TABLE OF CONTENTS

# LIST OF TABLES

# LIST OF FIGURES

# Chapter 1

# INTRODUCTION

## 1.1 Overview

For decades, designers especially in the field of mid to high-rise buildings, concentrated on the performance of the structures against the forces affecting them. However, the main challenge for mid-rise buildings is the lateral loads caused by earthquakes and the ability of the structure to withstand against the collapse and maintain its serviceability after the earthquake. In high-rise structures, wind loads with large P-Δ ratios can be dominant when the structure is designed against lateral loads.

Different analysis and design methods were proposed in the literature, however, these methods are in the agreement that the load bearing and resisting members must remain stable under acceptance criteria during the structure's entire life. The concept of progressive collapse came to the attention of structural engineers after the collapse of the Ronan Point, a 22-story tower block in Newham, East London, on 1968. The building was collapsed due to a gas tank explosion in the kitchen of a flat located on the $18^{th}$ floor, continued by the removal of a neighboring column. The removal of the column eventually led to the collapse of the floor above the removed column location and then triggered all floors below to collapse.

The collapse of the Twin Towers in the New York City on September 11, 2001 again stressed to structural engineers the need to re-evaluate the importance of

collapse mechanism and the behavior of the structure when some critical elements may fail to retain their function.

Although all famous collapse phenomena due to such member loses happened by a blast load effect or by an unexpected terrorist activity, even during the structures normal life it could happen. A past earthquake shock or a vehicle impact or even a construction error may cause a critical column to buckle or lose a part or whole of its load bearing capacity.

Various definitions are determined for the term ‘progressive collapse’. NIST, the United States National Institute of Standards and Technology proposed that the professional community should adopt the following definition: ‘Progressive collapse is the spread of local damage, from an initiating event from element to element, resulting eventually in the collapse of an entire structure or a disproportionately large part of it, also known as disproportionate collapse’ [1].

## 1.2 Guidelines for Progressive Collapse Design

Several handbooks have been published to assess the potential for progressive collapse in buildings. Examples of those are the “Best Practices for Reducing the Potential for Progressive Collapse in Buildings” presented by the NIST (US Department of Commence) and the “Review of international research on structural robustness and disproportionate collapse” presented by UK Department for communities and local Government. Although these handbooks are among the best studies in the progressive collapse resistance field, they do not describe the necessary design procedures in the design process.

By contrast the UNIFIED FACILITIES CRITERIA (UFC) prepared by the U.S. ARMY CORPS OF ENGINEERS (DoD) and the GSA prepared by GENERAL SERVICES ADMINSTRATION, provide comprehensive data about the progressive collapse concept and about designing buildings against it.

Both the UFC and GSA design guidelines were modified and the new versions were republished in 2013. Examples of the changes for UFC include: Revised tie force equations; removed 0.9 factor and the lateral loads from alternate path load combination; clarified definition of controlled public access; clarified live load reduction requirements; revised reinforced concrete and structural steel examples; added cold-formed steel for example. The Tie Force method in GSA has been removed and it relates to Alternate Path method only.

For existing and new construction, the UFC defines the level of progressive collapse design correlated to the Occupancy Category (OC). The design requirements in the UFC are developed in such a way that varying levels of resistance to progressive collapse are specified, depending upon the OC. The UFC employs these levels of progressive collapse design as [2]:

- "Tie Forces, which prescribe a tensile force strength of the floor or roof system, to allow the transfer of load from the damaged portion of the structure to the undamaged portion,
- Alternate Path method, in which the building must bridge across a removed element, and.
- Enhanced Local Resistance, in which the shear and flexural strength of the perimeter columns and walls are increased to

provide additional protection by reducing the probability and extent of initial damage."

## 1.3 Research Importance and Progressive Collapse Mechanism in Staggered-Truss Systems

Progressive collapse can be viewed as a domino effect because a local failure triggers bigger failures, progressing in time to a collapse surrounding a large portion of a building. After removal of an element in a structure, the force contributed to that element will be redistributed to the other structural members. These are mainly the surrounding members while the beams and columns situated more remotely from the removed element would not be affected. The reason is that, the energy produced from removing an element will be absorbed and dissipated only in proximity of the removed elements. After removing a member, for instance a column, plastic hinges will occur at some surrounding members. Excessive plastic deformation in the plastic hinge regions forces the material to fail. Therefore, once plastic hinge fails in an adjacent element, the elastic energy drops to zero in the element and the progressive collapse will happen. By removing a column of the building, the formation of plasticity will directly trigger the failure progress in that building. For the structural members like the beam, column and brace, it can be seen that after the sudden removal of the column, the axial forces are more or less doubled. Moreover, progressive collapse depends on the position of the removed member and the type of loads affecting it. For example, by comparing one corner column at ground level and one corner column at higher levels, the column located at higher levels will produce larger vertical displacement than the column removed at ground level. This is because, for the column removed at the ground floor, more floors participated in absorbing the

released energy than that occurred in higher level. Consequently, as the number of stories and bays increase, the capacity of the structure to resist progressive collapse also increases, because additional elements will participate against progressive collapse.

Generally, sudden removal of a member will lead to a sudden release of its gravitational energy and this energy will result in motions and kinetic energy. Almost all investigations for progressive collapse occurrence in common structural frames have been done on column removal scenarios. Because in a moment resistance frame (MRF) or in a braced frame (BF) the most important structural elements to ensure the stability, axial and lateral load resistance and stiffness of the structure, are columns. However in staggered-truss frames, the truss members especially the diagonals and verticals have long lengths to be considered as lateral load resistance members. According to previous experimental study on staggered-truss systems [3], the response of the steel staggered truss systems (STS) are much more complicated compared to the ordinary steel frame structures. The main reason is that, as mentioned above, the truss consists of several members, which will resist against both lateral and gravitational loads. Moreover, due to the fact that trusses are arranged alternately in the staggered-truss system, potential progressive collapse is more likely to occur in a fire, explosion or sudden impact, and the consequence could be even greater compared to the ordinary steel frame structures. Thus, for the purpose of proposing a rational progressive collapse protection design strategy for the STS, potential progressive collapse under different conditions should be given more attention to and investigated in detail in further studies.

## 1.4 Outline of the Thesis

This thesis focuses on linear static and nonlinear dynamic analyses of collapse behaviors of staggered truss systems. Chapter 2 of this research belongs to some basic definitions and the literature review. Two structures were modeled in this thesis, therefore, in chapter 3 all necessary details about designing and modeling is expanded.

Then, the linear static method and the results about linear static progressive collapse analysis are presented in chapter 4. Because of complexity of nonlinear dynamic time-history analysis, chapter 5 is dedicated to this method's procedure description and required steps to do a time-history progressive collapse analysis with SAP2000. The results of nonlinear dynamic time-history analysis are presented in chapter 6 of this context. Finally, the results of both above mentioned analyses procedures on staggered truss buildings made in this thesis are described in the last chapter, chapter 7.

# Chapter 2

# BASIC DEFINITIONS AND LITERATURE REVIEW

## 2.1 Introduction

This research focuses on the progressive collapse potential and progressive collapse analysis of staggered truss systems. In order to reach this goal, in the first step a model prototype equipped with both Staggered Truss System (STS) and Moment Frame System (MRF) was designed. The AISC LRFD [4] Steel Design Code was used for designing the steel section. The ASCE 7-10 [5], UBC 97[6] and ASCE 41[7] were the main guidelines used to find the required seismic and wind load coefficients and factors. Overall the whole context is comprised of two main phases. In the first step the model was designed using conventional methods and codes. In the second step, the structure's vulnerability against the removal of different column scenarios was investigated. This included Linear Static analysis plus Plastic Hinge definitions and Time History analysis of the model. In this step, the original structure showed multiple failures due to progressive collapse. Therefore, the structure seemed to need redesigning for stronger sections to prevent from such failures.

As described above, a structure may be vulnerable to collapse due to column removal in spite of its well-designed components. Earlier, structural design concept was based on resistance against gravity and lateral loads with all necessary components in place. However unexpected disasters like the September

11 tragedy of the New York Twin Towers triggered the necessity of involving sudden removal of some elements in our design procedures. There are many researches that have focused on progressive collapse analysis in moment frames (MRF) or braced frames (BRF). But as many other structural systems exist, this kind of analysis needs to be taken into account in order to ascertain their behavior. Nowadays the use of STS (Staggered Truss System) structures is increasing worldwide, and no research has reported on a collapse analysis for STS systems. That is why this research is dedicated to progressive collapse analysis in staggered truss systems.

## 2.2 Staggered Truss System (STS)

The Staggered-Truss Systems became famous as a steel structural system from 60s.this system will be made by a series of story-height trusses spanning the total width between two rows of exterior columns and arranged in a staggered pattern on adjacent column lines (Figure 2.1). This system was developed at the Massachusetts Institute of Technology in the late 1960s under the auspices of the US Steel Corporation. It was championed for being very economical, highly effective and simple to fabricate. The goal of their study was to find out a new, reliable, structural steel system that would also provide architectural benefits.. After they research, the MIT scholars proposed the staggered truss structure which since then widely used in mid-rise (15 to 20 story) buildings like Hotels and Offices. The AISC 14 steel design guide for Staggered Truss Systems [8] stresses the benefits of staggered trusses over other systems. This is what prompted the designers to develop a guideline for such structural systems. In staggered-truss buildings, trusses are normally one-story deep with a Vierendeel panel at the corridors. The trusses are prefabricated in the shop and then bolted to the columns

at the construction site. Spandrel girders are bolted to the columns and field welded to the concrete slab. Theoretically, the staggered truss system could be compared to a cantilever beam when it is resisting against shear forces resulting from lateral loads. In this thesis, all columns are erected on the exterior parts of the building and common without presence of interior columns, therefore a big free corridor will be available. The floor system starts from the top chord of one truss to the bottom chord of the neighboring truss. Therefore, the floor plays an important role in the structural framing system serving as a diaphragm transferring the lateral shears from one column line to another, thus enabling the structure to perform as a single braced frame. The cantilever action of the double-planar truss system, due to lateral loads, reduces the bending moment effect in the columns. Therefore, in general, the columns will be designed for axial loads only and the truss should be attached to the columns web. The truss chords should be connected to the column webs because, the flanges which are located in strong axis of I shape columns will be used along moment frame direction.

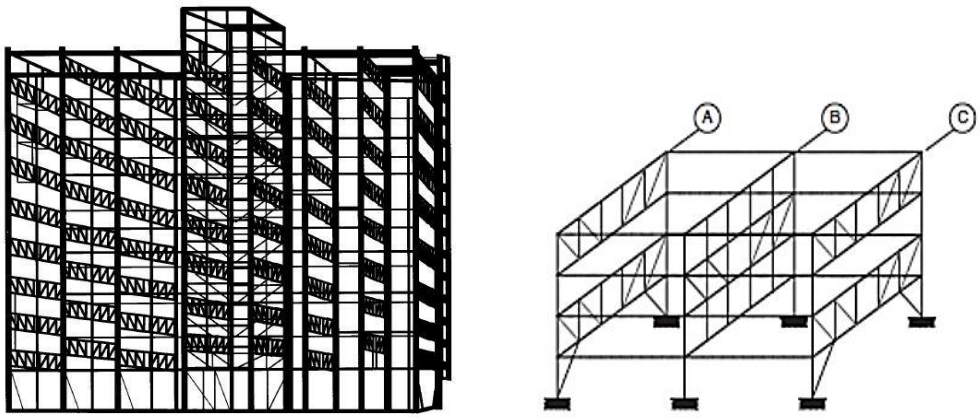

Figure 2.1: Staggered Truss pattern in a building

### 2.2.1 Advantages of Staggered Trusses

In recent years, the steel staggered truss system (STS) has been widely praised by the international engineering and academic world for its advantages of being economic, practical and cost-effective. Such a system has been applied more frequently in recent projects. For example: the Adam's Landing *Marriot Hotel* in Hartford with 20 stories built in 2003, the Legacy Tower apartment complex in Ames with 7 stories built in 2004, the *Shangrila Hotel* built in Seoul with 48 story in 2004, etc. [9]. Especially the *Stay Bridge Suites Hotel* which was constructed in 2008 in Chicago has been recognized as a classic project prototype by the American Institute of Steel Construction (AISC). This system is efficient for mid-rise apartments, hotels, motels, dormitories, hospitals and other structures for which a low floor-to-floor height is desirable. By applying floor-height steel trusses in a staggered pattern a large column free area is made available for each span. Furthermore, this system is normally economical, simple to fabricate and erect, and as a result, often cheaper than other framing systems [8]. The strongest point of this system is its high stiffness level against lateral loads distributed along trusses. In long, slender rectangular buildings of this type, lateral resistance in the transverse direction is often a problem due to the impact of wind forces on the longer dimension of the structure which must be resisted by the smaller building dimension or weak axis. The specific benefit of the staggered truss system is that the entire building weight is armed to resist against the overturning moment.

*Michael P.Cohen* did a presentation in AISC National Engineering conference in 1986 [10]. The study follows the conceptual design and selection process for a specific project between several structural framing systems. The Steel Frame and

Shear Wall, Concrete Frame Tube and the Steel Framed Tube systems were evaluated. The structural unit costs per square foot of building area, on a relative basis, were determined to have been as follows:

| | |
|---|---|
| 1. Steel staggered-truss | 1.0 |
| 2. Concrete frame to shear wall | 1.25 |
| 3. Concrete-framed tube | 1.10 |
| 4. Steel-framed tube | 1.4 |

This study shows that the staggered truss system was the most cost effective choice for this project. Some important advantages are as follows:

1- Due to double-planar system of framing, columns have minimum bending moments. Two kinds of structural framing systems exist in staggered truss systems, staggered trusses are located in transverse direction and in longitudinal direction a moment frame portal is placed. In transverse direction the trusses are connected to the web of column directly because the flanges of columns had to be located in moment frame direction (Figure 2.2). Therefore Columns will resist lateral loads with their strong axis in the longitudinal direction of the building.

2- The project-scheduling pace of such system makes it quite cost effective, because the truss will be shop welded off the construction site and then it will be transported and erected in its place. The staggered-truss framing system is one of the quickest available methods to use for construction during winter. Erection of the buildings is not affected by prolonged freezing weather. Steel framing, including spandrel beams and precast floors, are projected to be erected at the rate of one floor every five days.

Once two floors are finished, windows can be installed to insulate the inside of the structure and protect indoor structural activities from frostbite.

3- AISC 14 suggest maximum live load reduction factor of 50% [8] because tributary areas may be corrected to comply with code guidelines.

4- At the first floor, large column free areas will be available, because columns will be placed only on the exterior parts of the building.

5- Drift is small, because the total frame is acting as a stiff truss with only direct axial loads acting in most structural members. Secondary bending occurs only in the chords of the trusses.

Figure 2.2: Truss Chord and gusset plates will be connected to the column web

Because columns exist only in outer parts of the building, the vertical loads concentrate on fewer columns; therefore, these forces exceed the uplift forces generated by lateral loads. As a result uplift anchors are not required. These all will result in a considerable amount of reduction of foundation formwork and related construction costs.

6- The researches at M.I.T [10] also showed that the steel consumption of the staggered-truss system was less than that of the steel frame by 50%, and less than that of the braced steel frame by 40%, for multi-story or high-rise hotels and resident buildings.

### 2.2.2 Disadvantages of Staggered Trusses

Although the shallow floor-to-floor height of building proposed by AISC creates a rigid frame easily capable of resisting lateral loads, this can create some complications. On the first hand, fire suppression hardware, electrical cables and mechanical pipelines need to run horizontally through each level. This presents some problems because of the relatively small floor-to-floor height and the inability of these pipes to bend around the truss chords.

Secondly, according to the research done by *Jinkoo Kim* and *J.Lee* [11], the staggered truss system displayed superior or at least equivalent seismic load-resisting capacity in low-rise structures when compared to conventional ordinary concentric braced frames. However, this was not the case for mid- to high-rise structures due to localization of plastic damage in a vierendeel panel that was used in the corridors is not reinforced with a diagonal member, this caused week story and resulted in brittle failure of the structure. Figure 2.3 illustrates a typical truss with a vierendeel panel at the middle of the truss.

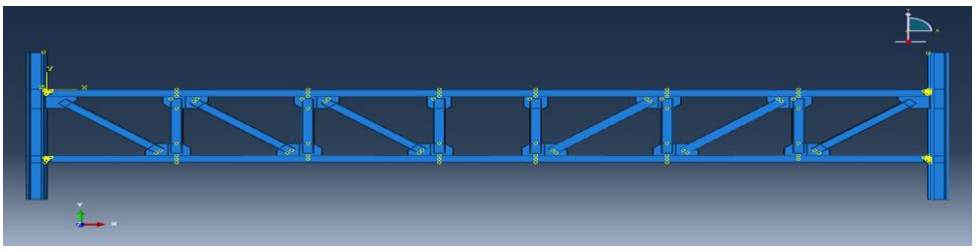

Figure 2.3: A typical staggered truss elevation view

### 2.2.3 Structural Frame Layout

Staggered trusses consist of two different structural frames. Staggered truss frames plus moment frames will act along transvers direction while moment frames only have to resist lateral frames in longitudinal direction (Figure 2.4).

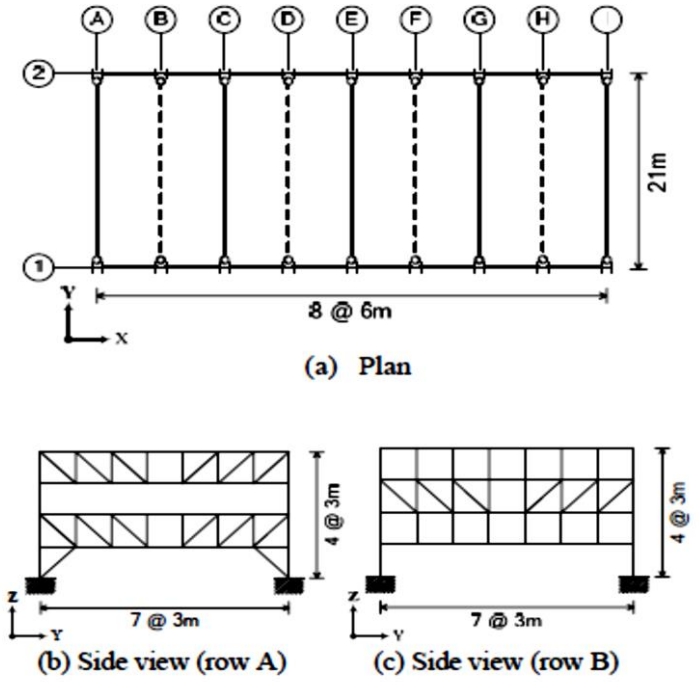


Figure 2.4: Staggered truss framing. Adopted from reference [11]

The vertical and diagonal members should be hinged at each end. The top and bottom chords are continuous beams and only need to be hinged at the ends where they are connected to the columns [8].

#### 2.2.3.1 Trusses

Generally, the trusses are required to transmit the gravity loads of the slabs to the columns and provide the necessary resistance against lateral loads. The trusses have openings at the mid span to permit a width and height to be used as a corridor (Figure 2.3).Truss chords should provide necessary width in order to allow the floors to easily seat on them. By using identical trusses throughout the

building, the cost of production will decrease and the project will be more efficient. The number of panels in the truss depends on the depth and the span in which diagonal members have an inclination of 45 to 60 degrees [8]. Theoretically, staggered-truss frames are treated as structurally determinate, pin-jointed frames. It is assumed that no moment is transmitted between members across the joints. However, the chords of staggered trusses are continuous members that do transmit moment, and some moment is always transmitted through the connections of the web members. The typical staggered-truss geometry is that of a "*Pratt truss*" with diagonal members intentionally arranged to be in tension when gravity loads are applied. Other geometries, however, may be possible. The gravity loads coming from floor system should be applied as concentrated loads at top and bottom panel joints of the chords. In a staggered truss system, a great portion of the lateral loads will be shouldered by the trusses and within a truss the diagonals are assumed to resist all corresponding lateral load. Therefore, the wind shears are transmitted by the floor system to the top chord of the truss and reacted horizontally at the lower chord into the floor system at that level.

The connection of top chord to the column will cause local bending in the column. A research study done by *John B.Scalzi* [12] found that the stiffness of the truss and floors is greater than the column stiffness; therefore, the local buckling in columns will decrease to an insignificant level in many structures. At the top and second stories where there are no trusses, posts and hangers are used to support these floor.

#### 2.2.3.2 Columns

The general duty of columns is to carry the total gravity loads and lateral loads from earthquake and wind force. The gravity loads are usually applied as direct axial forces to the columns, because the truss connection is on the web of the column. The forces acting on the building produce direct loads in the columns as a result of the truss action of the double-planar system. For the longitudinal frames wind will be resisted by moment frames, but if it is necessary and/or architectural features permit, braces could be used in this direction. The effective length of the column can be found by using the common methods. In the transverse direction, the truss can be connected to the web of column. Therefore the unbraced story can be the effective length of the column. However, in the longitudinal direction, buckling of the column relies on the portal or braced frame systems. AISC determines the effective length of columns in a portal frame by alignment charts or by rotational methods. Finally for a braced frame, the actual unbraced story height is the effective length.

### 2.2.4 Floor System

All types of floor systems could be used but precast concrete planks are the most economical options. According to AISC 14, 8 inch (20*cm*) concrete slabs with reinforcement should be used for spans up to 30 *ft* (900*cm*), while 10-in 25*cm*) planks can be used for spans up to 36 *ft* (1100 *cm*). In general, the total lateral load is distributed equally among trusses. Therefore, each truss will receive lateral forces from two bays, and consequently, the floor should provide enough strength to resist such loads (Figure 2.5). The floor system is acting as a deep beam and must be designed to resist the in-plane shears and deflections and the resulting in-plane bending moments. The longitudinal shear reinforcement must be able of

evolving the contact between floor panels to let them to act as a lone unit. Researchers at M.I.T. University found that, for a special building geometry, the shear capacity of the floor system may limit the height of the building. The connection of the floor system to the trusses should be strong enough to handover the axial and lateral loads to the trusses.

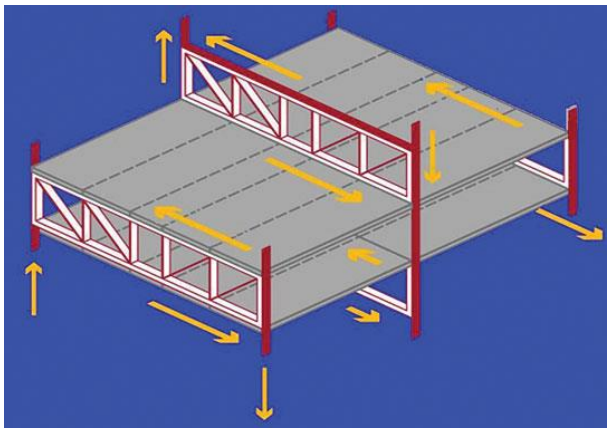

Figure 2.5: STS Floor system

The in-plane shears are conveyed by straight welding (if a steel deck is used) or by a welded shear plate (if concrete slabs or planks are used). The assembly to the chord member had to be made according to the shear spreading beside the truss in the transverse direction of the building.

**2.2.4.1 Diaphragm Design**

The floor system is a part critical to the correct operation of the staggered-truss system. As before labeled, the flat should act as a shear diaphragm to tolerate side loads. A truss at any level conveys the all lateral load from the entire structure above to a two-bay width. The flat zone on each side of the truss must handover half of this load to the top chord of the neighboring truss in the story under (Figure 2.5). The floor system must be planned to afford adequate diaphragm strength and stiffness to endure these horizontal forces as well as gravity loads. Diaphragms are

most of the time supposed to be rigid floors. Regarding the AISC 14 [8], for buildings located in a low-seismic risk area, a rigid diaphragm can be assumed. If the building is located in a mid to high risk seismic region, AISC recommends flexible floor system with plate-element and computational analysis.

### 2.2.5 Design Methodology

The design of staggered trusses will be done in several stages. All gravity loads and lateral loads resulting from wind and seismic forces should be calculated. Then manual calculations primarily lead to obtain member sizes. Computational calculations are needed at the end to evaluate the capacity of obtained member sizes and do corrections [8]. The method of coefficients for truss design is useful because of the repetition of the truss geometry and because of the shearing behavior of the trusses under lateral loads. Initially, staggered trusses are assumed to have hinged connections and consequently are treated as a determinate truss in which there will be no moment transition. However, the top and bottom chords are continuous and therefore, there will be moment transmission along the web members.

#### 2.2.5.1 Design of Truss Members

All the vertical and diagonal members have hinged connections at their ends. The truss chords are continuous; otherwise in the vierendeel panel, which has no diagonals due to an opening for corridor, the system will be unstable (Figure 2.3). For diagonal and vertical members, AISC 14 guideline suggests the HSS hollow sections and for connecting them to the truss chords, gusset plates be used. The design methodology that follows is based upon the recommendations listed in the AISC Hollow Structural Sections Connections Manual (AISC, 1997). Shown in Figure 2.6 is a typical slotted HSS to gusset plate connection. Truss chords mainly

are mainly selected from wide flange sections. Because of limited height in a staggered truss system I, sections that have bigger web height are not suitable. Wide flange sections can show good bearing and bending resistance capacity in spite of their low webs.

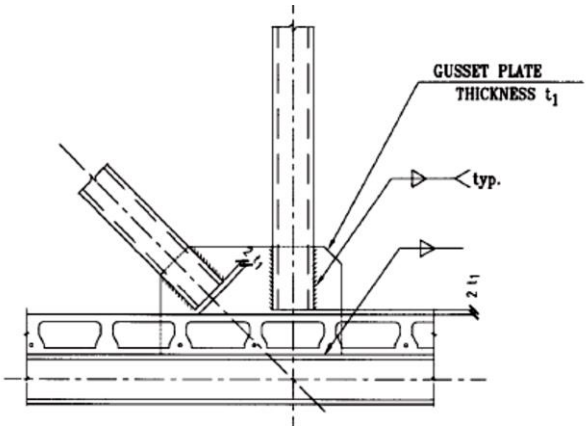


Figure 2.6: HSS section connected to truss chords with gusset plates adapted from [8]

#### 2.2.5.2 Columns Design

Column design will be done by applying shear and moments figures obtained from construction load's analysis. Column forces are due to dead and live loads and lateral loads are computed from a composite truss. Since columns cover a large area due to lack of internal columns, AISC 14 permits a 50% reduction for live loads [8]. Therefore the load combination for designing columns will be:

$$1.4\,D + 1.6\,L \qquad (2.1)$$

#### 2.2.5.3 Ductility

With large lateral stiffness due to their low height and little lateral displacement, staggered-truss system is a very reasonable and efficient lateral force resisting system. The floor system is acting like a deep beam and must be designed to resist in-plane shear and in-plane bending moments. In order to increase the stiffness

and shear resistance of staggered truss frames, AISC 14 suggests bracing diagonals and hangers in the frames where a staggered truss does not exist. These braces will normally be installed on the first floor and top floor of transverse frames and in longitudinal frames where architectural geometries permit. Staggered trusses normally use rectangular HSS for diagonals and verticals, which act like a braced frame (CBF). These sections may face local buckling which consequently will decrease the HSS plastic moment resistance and axial compressive strength. To compensate for this problem the AISC 14$^{th}$ steel guide series [8] recommends using stiffener plates around these sections. In high seismic applications, from the AISC Seismic Provisions, the b/t ratio for HSS should be limited to $\frac{110}{\sqrt{Fy}}$. The AISC 14 guideline suggests that, the behavior of staggered trusses be evaluated using Time History analysis. In high-seismic activity regions, the response of a staggered-truss structure that dissipates energy mainly through Vierendeel panels is similar to a ductile moment frame or an eccentrically braced frame. Therefore an R factor of 7 or 8 could be used for the design in the transverse direction of the building [8]. However in mid-seismic activity regions R=4 to 5 would be appropriate.

*Xuhong Zhou* et.l (2009) in their experimental study on seismic behavior of staggered-truss systems [13] found that, the seismic behavior of the staggered-truss system with ground floor trusses is better than that of the system without ground floor trusses because the stiffness of the ground floor of the staggered-truss system with ground floor trusses is higher than that of the system without ground floor trusses. Likewise the whole stiffness of the system with ground floor trusses is higher along the vertical direction than that of the system without

ground floor trusses. Also they have found that with increase of the open-web panel length, the ductility of the structure increases, however simultaneously the ultimate displacement grows more rapidly than the ductility. Therefore the open-web panel length of the truss should be as small as possible to prevent vertical web members failure and increase the seismic behavior of the system. Figure 2.7 illustrates a staggered truss prototype with presence of Hybrid truss and open-web truss.

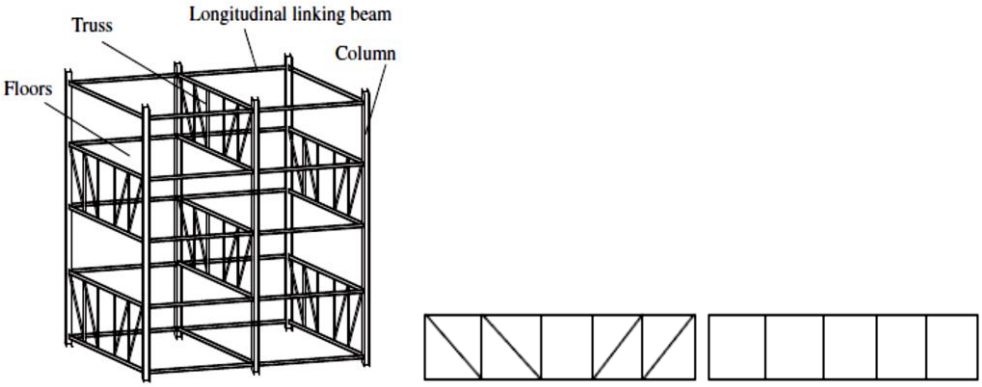


a) Hybrid truss b) Open-Web Truss

Figure 2.7: Typical Staggered-Truss Structure Adopted from [13]

Most findings indicate that, as the structure height increases, the ductility coefficient increases first and then decreases. The AISC guideline suggests that the reasonable and economical maximum story number of staggered-truss systems is 30-40. By increasing the structural height-width ratio, the maximum lateral displacement increases significantly but at the same time the ductility coefficient decreases gradually. Consequently the steel consumption increases in order to compensate for the problem. So by increasing the height-width ratio, the expenses will increase and the project would not be as economical.

## 2.3 Progressive Collapse Concept

A progressive collapse includes a sequence of failures that lead to limited or overall breakdown of a building. The US National Institute of Standards and Technology (NIST) [1] categorizes the potential abnormal load hazards that can lead to progressive collapse as: aircraft impact, design/construction error, fire, gas explosions, accidental overload, hazardous materials, vehicular collision, bomb explosions, etc. Because these hazards occur seldom during the life of a structure, many codes did not consider them or paid less attention to them as important criteria for designing and implementing members. Most of these impact loads have features of performing over a short period of time and result in dynamic reactions.

In the United States the General Services Administration (GSA) 2013 [14] and the Department of Defense (DoD), UFC 2013 [2] have detailed information and guidelines about progressive collapse in building structures. Both guidelines recommend the Alternate Path Method (APM) as a design code against progressive collapse. In this method, the structure is designed so that if one Element fails, alternate paths exist for the load and an overall failure does not take place. This method has the benefit of easiness and directness. In Alternate Path Method, structures should be designed to endure loss of one column without suffering additional failure.

### 2.3.1 Analysis Procedures for Progressive Collapse

The analysis techniques suggested by guidelines for alternate path method are: Linear Elastic Static (LS), Linear Dynamic (LD), Non-Linear Static (NS), and Non-Linear Dynamic (ND) methods. All these methods are recommended for

seismic analysis and design for structures in FEMA 356 [15]. Although both GSA and UFC guidelines recommend a linear static analysis to mitigate the analysis and computational costs, different research indicate that the linear static analysis might result in conservative results. This is probably because static analysis may not reflect the dynamic effect by sudden removal of columns. More studies prove that the static and the dynamic analysis should be combined together to get an adequate result for progressive collapse analysis. In general both methods have their advantages and disadvantages.

#### 2.3.1.1 Demand Capacity Ratio (DCR)

The GSA 2013 suggests the use of the Demand-Capacity Ratio (DCR), which is the member force over member strength ratio by linear analysis procedure. [14]

$$DCR = QUD/QCD \tag{2.2}$$

Where:

QUD: The acting force determined in component (moment, axial force, shear force etc.).

QCE: The expected ultimate capacity of the member (moment, axial force, shear force etc.).

The acceptance value of DCR ratio differs relating to the width/thickness ratio of the component. Based on the GSA 2013 guideline [14] limit values for DCR in girders and in columns depends on the width/thickness ratio. For non-linear analysis techniques, the guidelines use full plastic hinge rotation and ductility as acceptance criteria for progressive collapse. In table 2.1 the acceptance criteria for progressive collapse recommended by the GSA 2013 are presented. In this table the ductility ratio is the ratio of the ultimate deflection in a location where a

column is removed to the yield deflection at that point. The rotation angle is obtained by dividing the maximum deflection over the length of the beam.

Table 2.1: Acceptance criteria for Progressive Collapse (GSA)

| Component | Ductility | Rotation |
|---|---|---|
| Steel beams | 20 | 0.21 |
| Steel columns (tension controls) | 20 | 0.21 |
| Steel columns ( compression controls) | 1 | --- |

#### 2.3.1.2 Procedure for Linear-Static Analysis

The step-by-step procedure for conducting the linear-static analysis recommended in UFC 2013 is as follows:

**Step 1**

A column should be removed from its position and then the linear static analysis will be carried out. For such analysis the gravity load affecting the area close to removed column should be calculated from below formula:

$$\mathbf{G_{LD} = \Omega_{LD}\,[1.2\,D + (0.5\,L \text{ or } 0.2\,S)]} \qquad (2.3)$$

Where $G_{LD}$ = Increased gravity loads for deformation- controlled actions for Linear Static Analysis

D = Dead load including facade loads (lb/ft2 or kN/m2)

L = Live load (lb/ft2 or kN/m2)

S = Snow load (lb/ft2 or kN/m2)

$\Omega_{LD}$ = Load increase factor for calculating deformation-controlled actions for Linear Static analysis

**Step 2**

The DCR ratio in each structural component has to be measured. If the DCR ratio of an element surpasses the acceptance rate in shear, the member will be reflected to have failed. If the DCR ratio of an element end surpasses the acceptance value in bending, a plastic hinge at the end of the member will form as shown in figure 2.8. If hinge creation leads to failure of a component, it is detached from the model and all live and dead loads related to failed member had to be scattered to the neighboring members.

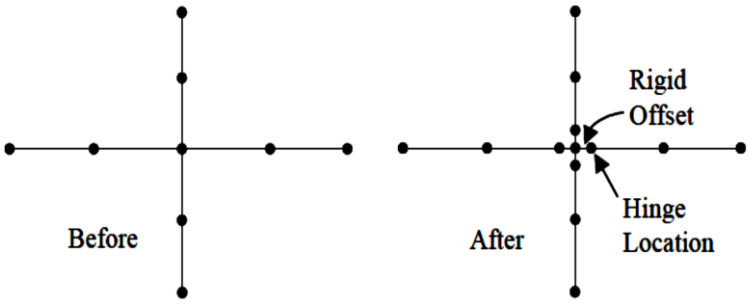


Figure 2.8: plastic Hinge Formation (GSA2013)

**Step 3**

At each emerged hinge, equal-but-opposite bending moments are applied parallel to the anticipated flexural strength of the member (nominal strength multiplied by the over strength factor of 1.1) as shown in Figure 2.8.

**Step 4**

Again the procedure from step 1 through step 3 is duplicated till the phase that the DCR of any component does not surpass the limit rate explained above. If the moments have been redistributed all over the whole building and the DCR values are still bigger than limited values in zones outside of the acceptable collapse region, the structure has a better chance of fronting progressive collapse.

### 2.3.2 Loads for Static and Dynamic Analysis

#### 2.3.2.1 Static Analysis

Both GSA 2013 and UFC 2013 guidelines recommend static load combinations equal to equation 2.2. The UFC 2013 guideline insists on more gravity loads in comparison with GSA 2013 and uses wind forces in load combinations.

#### 2.3.2.2 Dynamic Analysis

Both guidelines do not suggest dynamic increase factor. But to precede the dynamic analysis, the axial force belonging to the column that had to be removed will be calculated. Then the column had to be replaced by point loads equivalent of its internal load as shown in Figure 2.9. In the UFC 2013, wind load is applied to the load combinations as shown in Figure 2.9.

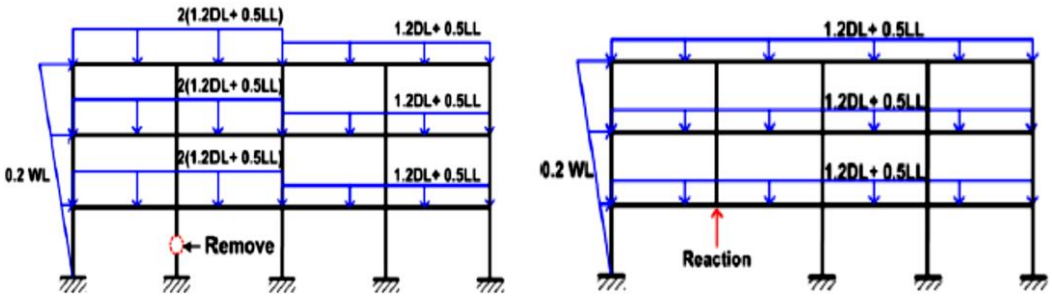


(a) Static Procedure (UFC 2013). (b) Dynamic Procedure (UFC 2013)

Figure 2.9: Load combinations for analysis of progressive collapse

GSA code suggests the same load coefficients for static and dynamic analysis as UFC 2013. *Feng Fu* [16] did a 3D finite element modeling to investigate the progressive collapse process in a 20-story building. The author used a real experiment from another study and then modeled it with ABAQUS. They used visual basic program to transfer output data from ETABS to ABAQUS. This convertor program can transform exactly all the information of ETABS to ABAQUS including the concrete slab properties.

In the study 2 different 20-story buildings were modeled, one with central shear walls as lateral load bracing system. The other one was equipped with braces as lateral bracing. The vertical columns were removed in different scenarios in both buildings and the failure mechanism and load distribution to other surrounding elements was investigated. This was done by following the alternate path method (APM) which is proposed by UFC 2013 [2] and GSA 2013 [14] guidelines. There are four procedures for alternate path method: linear elastic static (LS), linear dynamic (LD), nonlinear static (NS), and nonlinear dynamic (ND) methods. The methodology is based on the context of a missing column scenario to find out about progressive collapse probabilities in the structure. This method was also adopted by many researchers who did probes in this field. Figure 2.10 shows the modeled structure by *Feng.Fu* [16] with 2 removed columns at ground floor.

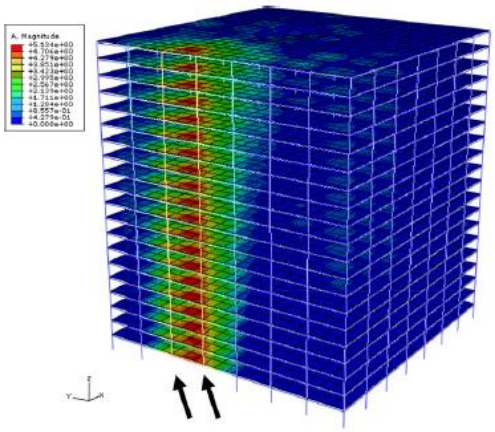

Figure 2.10: 20 story building with 2 columns removed adopted from [16]

Moreover, for designers, the most important issue is to check whether a building can successfully absorb the loss of a critical column and prevent progressive collapse. Therefore, the ability of the building under sudden column loss was assessed using non-linear dynamic analysis method with 3-D finite element

technique. The loads were computed as dead loads (which is the self-weight of the floor) plus 25% of the live load (which is 2.5 KN/m2) [16]. This is determined from the non-linear dynamic analysis for comparison with the acceptance criteria outlined in Table 2.1 of the GSA 2013 guideline [14].

By comparing the results of different column removal scenarios, it can be seen that the buildings are more vulnerable to 2 column removal instead of a single column. The reason is due to bigger affected loading area after losing 2 columns. In Fung [16] study, the dynamic response of beams and columns were almost identical for the building with shear wall and the building with braces. This is because the response of the structure is only related to the affected loading area after column removal. Finally studies show that, under the same general conditions, removing a column at higher levels will result with more vertical displacement in comparison with a column removal at the ground level.

Generally, plasticity is observed in more than two column removal scenarios and plasticity normally happens when 2 columns have removed from structural system. In many studies this process was done by removing 2 columns simultaneously, however, this is a conservative approach. In reality the chance for 2 columns to be damaged at the same time is rare. When attacks like car bomb or an airplane impact happen, it will hit one column first, then another. The columns are normally destroyed one after the other. Therefore, the structural behavior will be different. Regarding this fact, the sequential column removal scenarios should be followed instead of removing both columns suddenly. After the removal of the columns, the forces are mainly redistributed to the adjacent beams; the beams

situated far from the removed column would be less affected. Therefore, to resist progressive collapse, the beams in the lower level should be designed with stronger sections than those in the upper levels. This is because the beams will withstand more force redistribution from the columns removed at a lower level than the columns removed at a higher level.

*Xinzheng Lu* and his colleagues modeled a high-rise building in their study: Earthquake-induced collapse simulation of a super-tall mega-braced frame-core tube building in 2012 [17]. The study presents an earthquake-induced collapse simulation of a super-tall building to be built in China in a high risk seismic region with a maximum spectral acceleration of 0.9 *g*. A FE model of this building was constructed based on the fiber-beam and multi-layer shell models. The dynamic characteristics of the building were analyzed and the earthquake-induced collapse simulation was performed. The building has 119 stories above the ground with a total height of 550 *m*. A hybrid lateral- load-resisting system known as the mega-braced/frame-core tube/outrigger Figure 2.11 shows the elevation and plan views of the hypothetical model.

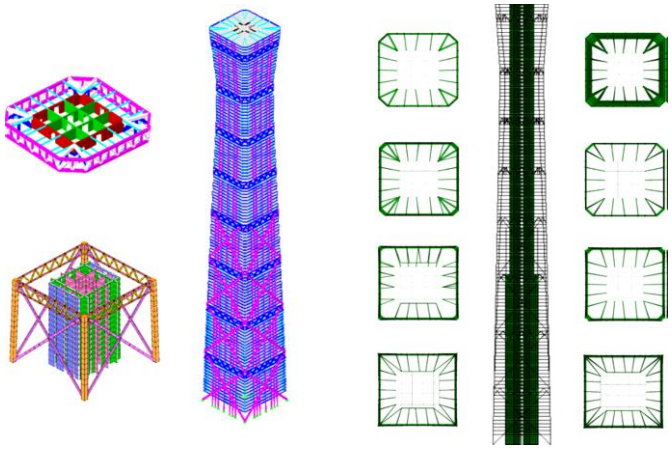

Figure 2.11: The FE model of the super-tall building adopted from [17]

In their study to fully understand the collapse process and failure mechanism, the intensity of ground motion increased until the tall building structure collapses. Although such a scale of earthquake might be very unlikely, however this method could be helpful to understand the reaction of super tall buildings under strong lateral shocks. To obtain the basic dynamic properties of tall buildings, a dynamic modal analysis by applying data from previous earthquakes could be performed. These earthquakes could be *El-Centro* earthquake, which took place in the USA in 1940 or the *Kobe* earthquake, which happened in Japan. Ground motion can be scaled up incrementally until one attains the collapse stage of the structure. Figure 2.12 shows that vertical displacement resulting from ground motion was much larger than horizontal displacement at the stage of collapse.

*Xinzheng Lu* and his colleagues[17] found that the overall collapse process of this building under Kobe ground motion data as "At the initial stage of t=12.310 *s*, the shear wall at the bottom of the building begins to fail due to concrete crushing, and the failure region expands rapidly. When t=12.410 *s*, the coupling beams located in higher zones begin to fail due to shear. Next, when t=12.810 *s*, more than 50% of the shear walls at the bottom of Zone are destroyed and the internal forces are redistributed to other components. The mega-columns begin to fail under combined over-turning moment and compression. When t=13.500 *s*, most of the mega-columns and shell walls at the bottom of Zone are destroyed. All these failures lead to the collapse of the entire building."

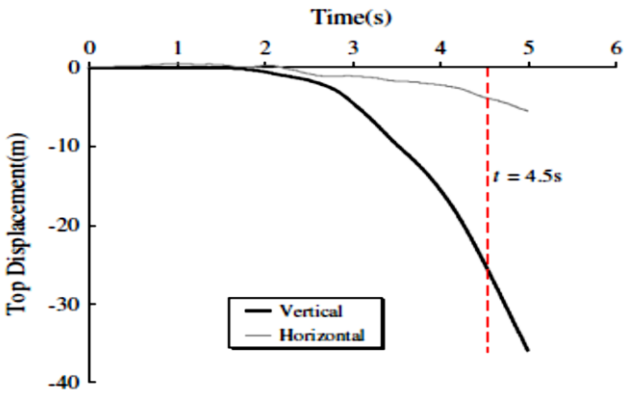


Figure 2.12: The vertical and horizontal roof displacement of the super tall building adopted from [17]

The earthquake-induced collapse simulation for super tall buildings shows that, the actual collapse zones do not necessarily coincide with the initial plastic zones predicted by the traditional nonlinear time-history analysis. Therefore, the collapse simulations are quite important in establishing the critical and vulnerable zones of a super-tall building.

*Jinkoo Kim* and *Taewan Kim* [18] assessed the progressive collapse-resisting capability of steel moment frames by using alternate path method. They modeled two types of steel moment frames with identical dimensions; however one of frames had stronger member sections as its structural elements. Then the potential progressive collapse probabilities in both frames regarding GSA 2003 and DoD 2005 guidelines were investigated. In the first attempt they did linear static analysis on both frames and found that by applying this analysis method, the DCR ratio in all girder ends in the left-hand side bay exceeded the limit value 3. This means that there is an excessive probability of progressive collapse incidence. The study has accomplished by two different column removal scenarios. First a corner column has been removed and plastic hinge formation in different steps was

recorded. Then the same scenario was duplicated by removing a column from a middle frame. The result showed that, in the first step the number of plastic hinges was smaller for a middle column removal scenario. However, after the 3 steps DCR in all of the girders situated in the bay in which a column was uninvolved surpassed the boundary value.

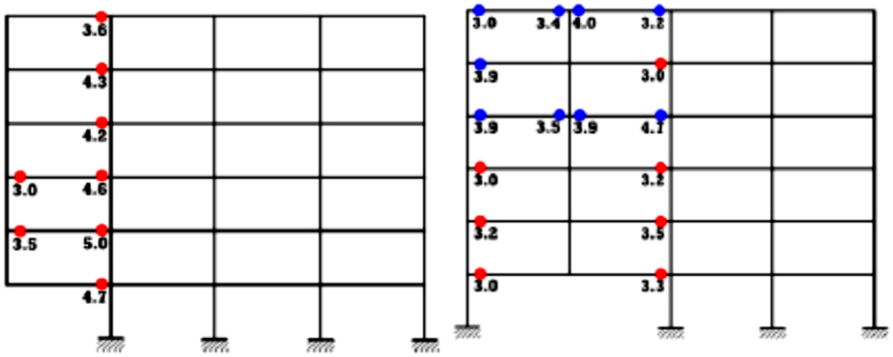


*(a) Corner column removed* *(b) Second column removed*

Figure 2.13: plastic hinge formation of a 6 story frame under 2 different column removal scenarios adopted from [18]

In the linear dynamic analysis less hinges formed throughout the areas close to removed column and the DCR values got from dynamic analysis were also less than those calculated by static analysis. Figure 2.14 shows the time history graph of the perpendicular deflection at the girder detached column joint. It can be seen that the maximum displacement resulting from dynamic analysis is smaller than that attained from a static analysis using dynamic increase factor [18]. It can also be observed that at upper levels the extent of dislocation is smaller. The reason is that, at higher floors more structural members will participate in resisting against progressive collapse.

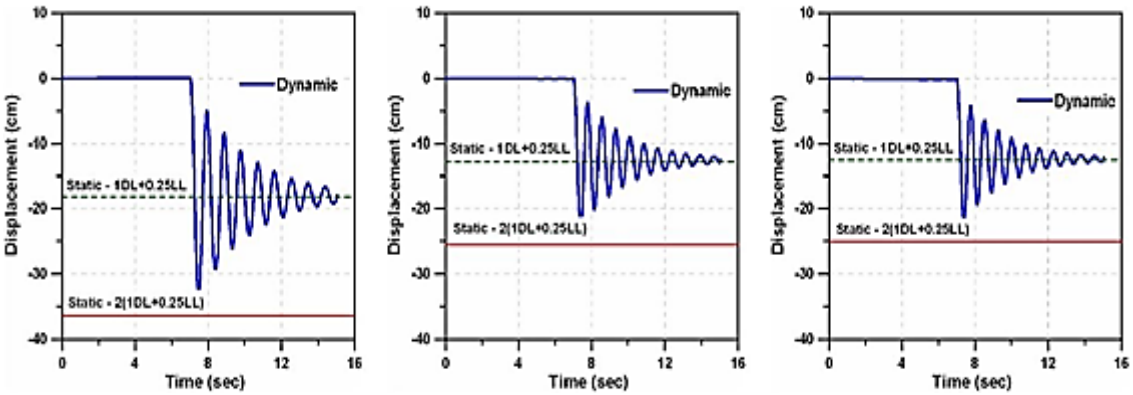

Figure 2.14: Movement time history at the joints when an angle column detached, adopted from [18]

Associated with linear analysis, the non-linear dynamic analysis delivers larger structural response and effects differ depending on applied load, location of removed column, and the number of building flats. Therefore, as the non-linear dynamic analysis for progressive collapse analysis does not need hysteretic behavior, it is a precise method for evaluating the progressive collapse potential within a structure. Such studies prove that, the potential of progressive collapse is higher when a corner column is removed, and the progressive collapse occurrence decreases as the height of building increase.

## 2.4 Progressive Collapse in Staggered-Truss Systems (STS)

Different studies have been done on staggered-truss systems and they are investigated for cyclic loads, design solutions, seismic loads, inelastic and seismic behavior etc. However, it is evident that there are few reports regarding the study of progressive collapse process in staggered-truss systems consequently this analysis could be a pioneer study in this field.

### 2.4.1 Previous Research

*Jinkoo Kim et al. (2006)* [11] designed 4-, 10-, and 30-story staggered-truss structures and investigated their seismic performance by doing push over analysis and compared the result with conventional moment resisting and braced frames.

The strength of braced frame in low to mid- rise buildings (4-10 stories) drops rapidly right after the maximum strength is reached due to the formation of plastic hinges in the middle of the girders in the braced bays. The moment frame, as it was designed with the largest response modification factor, has the smallest stiffness and strength, however it shows the best ductile behavior. The STS in this range of height shows large strength and enough ductility to remain stable until the maximum inter-story drift exceeds 2.0% of the story height. For mid to high-rise levels, the STS has little ductility even smaller than braced frame.

*Jinkoo Kim* and *Joonho Lee* have found that, the failure mode is quite brittle compared with braced frames in mid to high-rise structures. In mid to high-rise STS, the plastic hinges will occur in vierendeel panels due to lateral loads [11] which finally will result in brittle failure of the structure. By using stiffeners for braces in the vertical members of the vierendeel panels as AISC 14 [8] suggests, the system ductility will enhance without increasing cross-section of these elements. *Jinkoo Kim and Joonho Lee (2007)* [19], also did a research on the same staggered-truss systems and investigated the inelastic behavior of low, mid and high-rise staggered-truss buildings. The results were similar to the previous paper. The low-rise staggered-trusses performed well and showed relatively satisfactory lateral load-resisting capability compared with conventional braced frames. By contrast, in mid to high-rise STS, plastic hinges formed at horizontal and vertical

chords of a Vierendeel panel, which subsequently led to brittle collapse of the structure.

*Michael P.Cohen (1986)* [10], sketches the theoretical design and selection procedure of staggered-truss system to a hotel project. The hotel was to be a high-rise, hotel situated on the oceanfront. The width of structure was 70 ft. (21.34 m) and being in an Atlantic zone limited the height of the structure to 420 ft. (128 m). A wind tunnel study was conducted for the proposed prototype. The results of wind tunnel showed that by linking integrally the slab and the spandrel beams, the spandrel performs as the flange of the deep beam [10]. This will increase the lateral stiffness of the system. However, the spandrel beam was also to be portion of the moment frame in the longitudinal direction so its design was to be established on the critical case of lateral loads in both directions.

*Yue Yin et al. (2005)* [20] compared multistory staggered-truss buildings with and without concrete slabs. This aimed to investigate the role of concrete floor on the behavior of staggered-truss systems. Their study showed that, the concrete floor slab plays a very important role in transferring lateral loads between different parts of structure and make their lateral displacement compatible. After comparing the 2 models, the one without concrete slab had different drift patterns for adjacent rows of the structure. This means that, the frames with staggered-truss have less pre-story drift than the open-web truss frames (frames without staggered-truss). By contrast in models with concrete slabs, the drift patterns are the same and the total drift of the structure is less than the first model.

*Chang Chen et al. (2010)* [9], investigated the simplified method for the fire resistance analysis on the staggered-truss systems (STS) under lateral loads by modeling a 3D model, a plan cooperative model and a planar model and by considering the effect of concrete slab on these models (Figure 2.15).

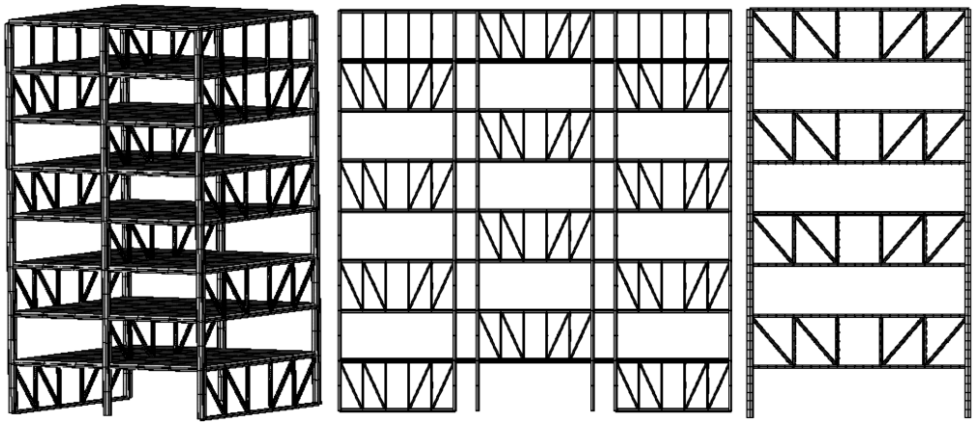

*a) 3D model b) Plane cooperative model c) Planar model*

Figure 2.15: Different models of STS adopted from [9]

Their analysis results show that, the adjacent trusses in staggered truss system under lateral force could keep good coordination at elevated temperature. The study shows that, the impact of the fire will be only on the truss exposed to the high temperature and the effect of fire on the adjacent trusses is negligible. Secondly, the slabs of the floor exposed to fire may be destroyed by high temperature, so the transmission of force of the slab at this floor can be ignored. But the effect of the slab on the other floors should be considered in the analysis. This shows that, the even the slab may face progressive collapse under the impact of fire.

# Chapter 3

# DEFINITION OF THE MODEL STRUCTURE

In this chapter all the primary information about the investigated model is described in detail. A 10-story Steel Staggered Truss structure was modeled and designed based on AISC 14 Steel Design Guidelines. This structure was supposed to be located at North East of t United States. Because for modeling process, the original Structure was compared to the apartment building described in the AISC 14 Design Gridline which is located at the same location (North-East of the United States). The designed structure in X direction consists of trusses which have been placed in a staggered formation and in Y direction is moment frame. Figure 3.1 shows a schematic of the proposed structure. In this chapter SI units are used however, the sections are selected using American Standard sections in AISC 14 [8].

## 3.1 The Structural System and Its Geometry

The structure is made of 2 kinds of framing systems. The moment resisting frames (MRF) are placed in longitudinal direction and the staggered truss systems (STS) are located along transverse direction as presented in Figure 3.2. In transverse direction, the trusses height is equal to the floor height and they are acting as a lateral load resisting system. Additionally, the gravity loads from floors will be transmitted to the bellow chords and then to columns through these members. In longitudinal (X) direction moment frames are the lateral load resisting systems.

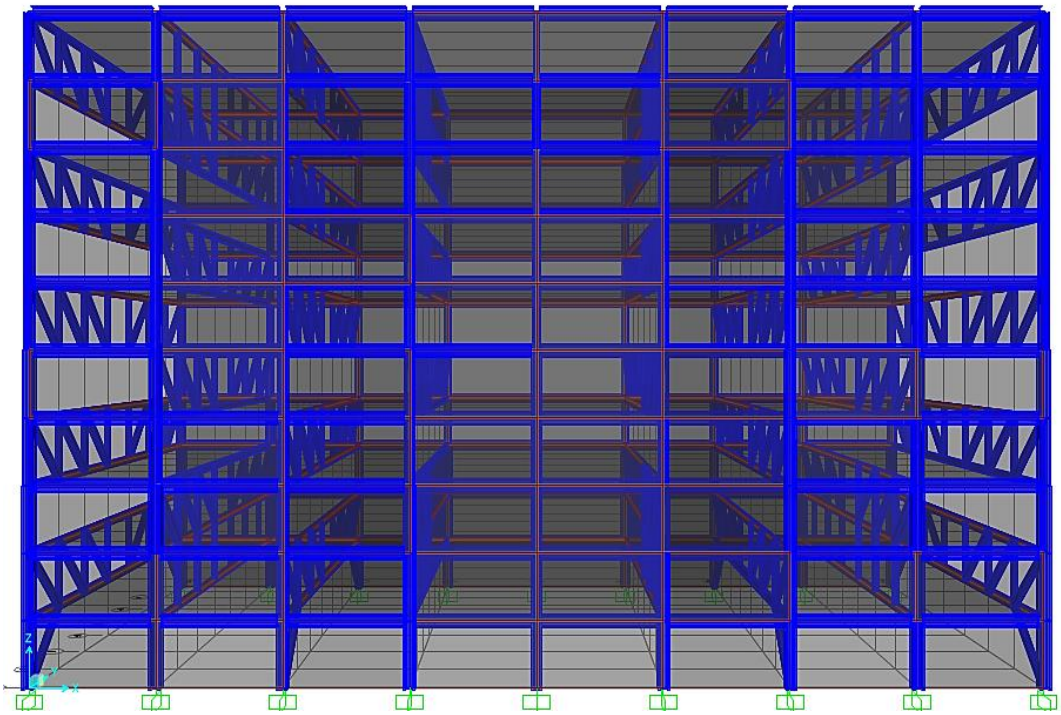

Figure 3.1: 3D view of 10 story Staggered Truss Structure (STS)

The chords of truss members are continuous beams and are not interrupted in truss member connections. The truss chords length is equal to 21 meters and vertical members are placed in 3 meter intervals. Diagonals are placed in each panel except the middle panel (Vierendeel panels). This panel is acting as a corridor for connection throughout the building (Fig 3.2).

As illustrated in Figure 3.2, two kinds of staggered truss systems were allocated in Y direction. The rows A, C, E, G, and I, (Fig3.2-c) start and finish with trusses every even floor, while in rows B,D, F,and H (Fig 3.2-d) trusses start from 3$^{rd}$ floor every odd floor.

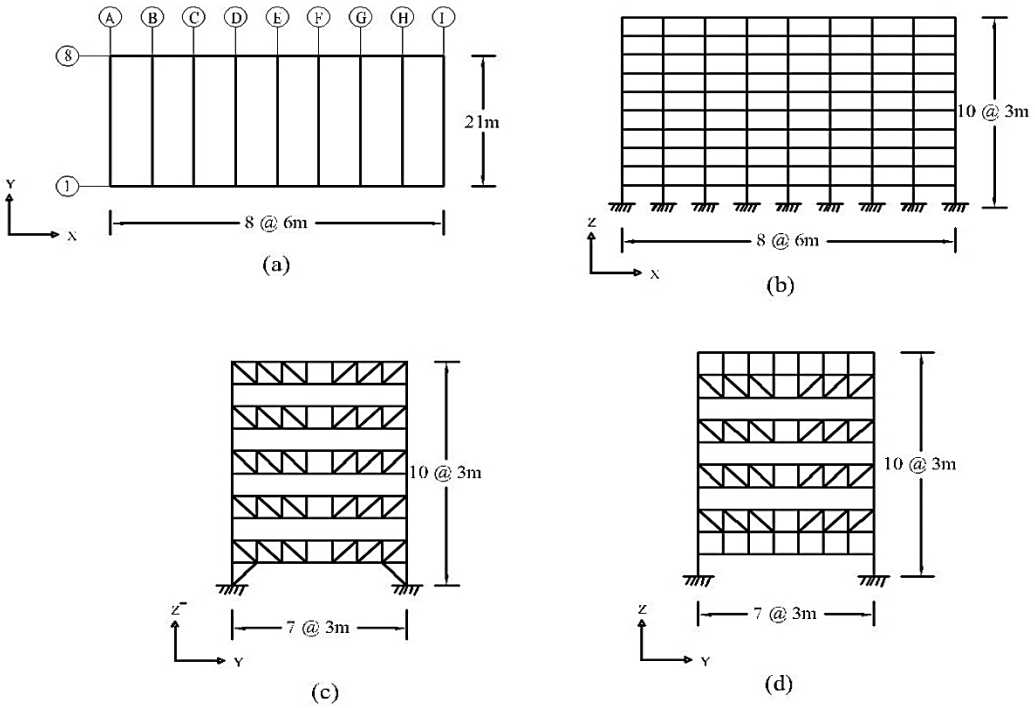


Figure 3.2: Structural Detail of the Model. (a): Plan - (b): Side View - (c):Trusses Located in Odd Rows - (d): Trusses Located in Even Rows

## 3.2 Material Properties

The assumed steel material properties which have been used for all columns, beams, braces and truss members were based on AISC-LRFD and AASHTO A992 specifications as follows:

- Modulus of Elasticity: E = 199947.98 $N/mm^2$
- Poisson's Ratio: $\nu = 0.3$
- Weight per Unit Volume: 7.69e-5 $N/mm^3$
- Mass per Unit Volume: 7.85e-9 $N/mm^3$
- Minimum Yield Stress $F_y$: 344.7 $N/mm^2$
- Effective Tensile Stress $F_u$: 448.15 $N/mm^2$
- Effective yield stress $F_{ye}$ : 379.2 $N/mm^2$

The flooring system consists of precast concrete slabs. The assumed concrete material specifications are as follows:

- Modulus of Elasticity: E = 24855.6 *N/mm2*
- Poisson's Ratio: ν = 0.2
- Weight per Unit Volume: 2.36e-5 *N/mm3*
- Mass per Unit Volume: 2.403e-9 *N/mm3*
- Shear modulus G : 10356.5 *N/mm2*
- Specified concrete compressive strength $f'_c$=27.6

## 3.3 Steel Sections Used in the Model Structure

For truss chords W10 sections were selected because these sections are H shape section which provides a good connection area with the slab. Columns are from W12 and W14 sections with H shapes. Diagonals and vertical truss members are mostly from HSS hollow sections.

## 3.4 Connections

As previously described in chapter 2, the AISC 14 [8] suggests that vertical and diagonals in the truss are assumed to be hinged at each end. Moreover the top and bottom chords are hinged at their end connections to the columns. But these chords are continuous beams and will not be interrupted by truss members.

In X direction all the beam to column connections are fixed to represent a moment frame (MRF) system. Due to long length of the frames in this direction, all perimeter frames designed as special moment resistant frames (SMF) with connections that are stronger than beams. This will decrease the period of the structure in the longitudinal direction and will direct the plastic hinge formation to the beams and not on the columns or connections. And finally all the columns to

baseplate connections and column to column connections are fixed at their ends. Fig 3.3 illustrates a typical View of row A and Row B frame connections.

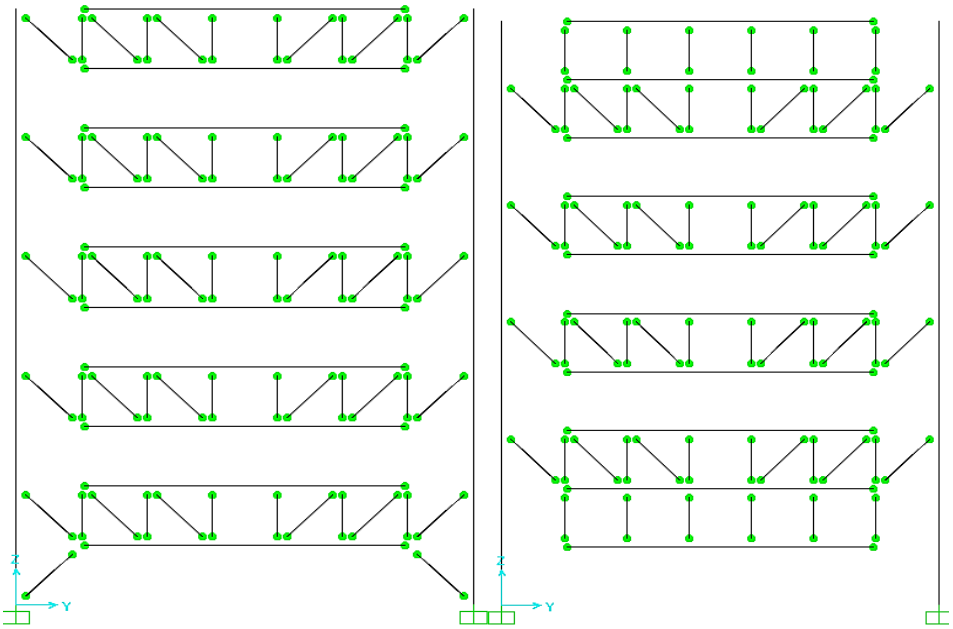

Figure 3.3: Member connections in Truss row A and Truss row B

## 3.5 Loading

There are 7 load cases defined in SAP2000 model for static analysis and design, DEAD – super dead – perimeter – Live – EX – EY and Wind Load.

### 3.5.1 Gravity Loads

Dead loads were introduced in three stages to the modelled structure in SAP2000 [5]. The dead load pattern with self-multiplier coefficient equal to 1 was used. The coefficient of 1 for dead load represents the gravity load produced from steel sections and the concrete plank floor.

The super dead load pattern was used to represent the partitioning and ceiling gravity loads while the perimeter load pattern was assigned to the perimeter beams as the gravity load resulting from outer walls. Table 3.1 shows details of all the

assigned loads in detail. Both the Dead and Live Loads were chosen from ASCE7-10 Minimum Design Loads for Buildings and Other Structures.

Table 3.1: Applied Gravity Loads

| Load Pattern | Type | Magnitude |
|---|---|---|
| Perimeter | Dead | 3.65 KN/m |
| Super Dead | Dead | 5.9 KN/m2 |
| Live | Live | 4.8 KN/m2 |

### 3.5.2 Earthquake and Wind Loading

Lateral loads including the earthquake loads were applied as a static load case. All seismic coefficient factors were calculated by following the Unified Building Code (UBC 97) volume 2, chapter 16 [6]. The seismic factors were calculated separately for X and Y directions based on UBC97 specifications, however the Response modification factors for both the MRF and STS frames were chosen from AISC 14 staggered truss system guideline [8].Finally the wind load was applied to the building by following the ASCE 7-10 guidelines [5]. Tables 3.2 and 3.3 show the calculated factors for earthquake and wind loading.

Table 3.2: Design Parameters for Seismic Load

| **Structural System** | **MRF** | **STS** |
|---|---|---|
| Peak Ground Acceleration | 0.11 | 0.11 |
| Soil Type | SD | SD |
| Importance Factor | 1.2 | 1.2 |
| Response Modification Factor | 3 | 6 |
| Seismic Zone Factor | 0.15 | 0.15 |
| Ct | 0.03 | 0.035 |

Table 3.3: Design Parameters for Wind Load

| | |
|---|---|
| Exposure | B |
| Basic Wind Speed | 100 |
| Importance Factor | 1 |
| Gust Factor | 0.85 |

### 3.5.3 Load Combinations

The load combinations were according to the LRFD specifications. [4].The load combinations are as follows:

1.4D (3.1)

1.2D + 1.6L (3.2)

1.2D + (0.5L or 0.8W) (3.3)

1.2D + 1.3W + 0.5L (3.4)

1.2D ± 1.0E + 0.5L (3.5)

0.9D ± (1.3W or 1.0E) (3.6)

Where,

D is the deal load, L is the live load, W is the wind load, and E is the Earthquake Load.

## 3.6 Yield Rotation, Plastic Rotation and Plastic Hinge Definitions

### 3.6.1 Yield Rotation

The yield rotation is identical to the flexural rotation at which the extreme fibers of the structural components touch their yield strength (ASCE 41) [7]. Flexural members answer elastically until the extreme fibers reach their full yield volume under loads. After the point at which these fibers have reached their full capacity, the response of the structure becomes nonlinear. Because the yield rotation $\Theta_y$ happens in this moment, it is similarly named the elastic rotation.

According to the ASCE 41 [7], the yield rotations for column and beams are determined using the equations 3.7, and 3.8. These equations are used to determine the yield rotation of beam and column elements in SAP2000 model as well.

Beams: $\Theta_y = \frac{Z.F_{ye}.L_b}{6.E.I_b}$ (3.7)

Columns: $\Theta_y = \frac{Z.F_{ye}.L_c}{6.E.I_c} \times \left(1 - \frac{P}{P_{ye}}\right)$ (3.8)

Where:

- $\Theta_y$ = Yield Rotation.
- $P$ = axial force in the member at the target displacement for nonlinear static analyses, or at the instant of computation for nonlinear dynamic analyses,
- $P_{ye}$ = expected axial yield force of the member= $A_g.F_{ye}$,
- $Z$ = plastic section modulus,
- $L_b$ = beam length,
- $L_c$ = column length,
- $I$ = moment of inertia.

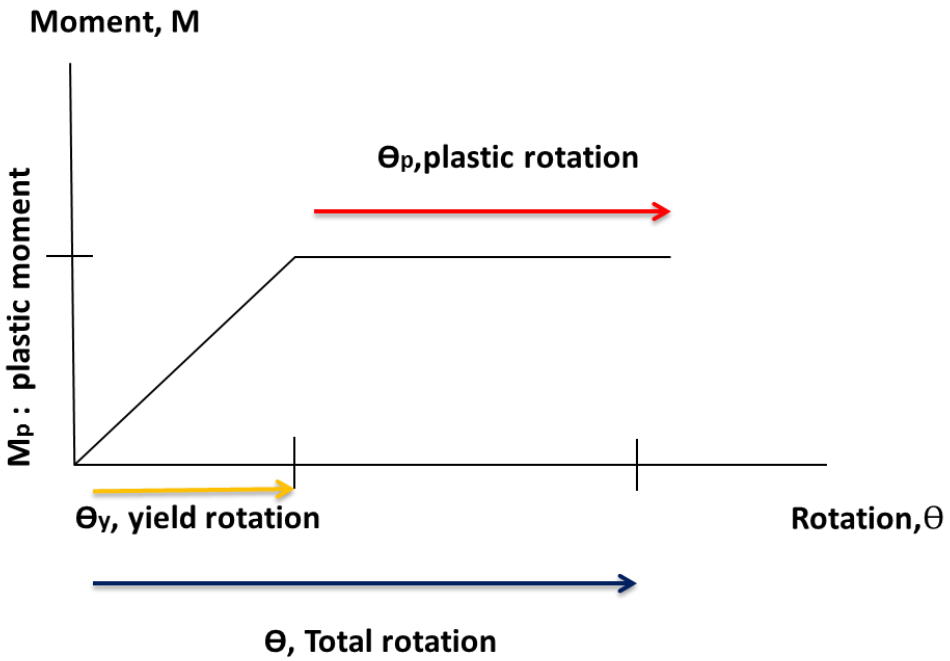


Figure 3.4: Yield Rotation and Plastic Rotation Curve

### 3.6.2 Plastic Rotation and Plastic Hinges

The stress-strain curve of the steel material used in the analytical modelling is shown in Figure 3.5. The yield strength ($F_y$) of 345 *MPa* and the ultimate strength ($F_u$) of 495 *MPa* was used for the further analysis. . As shown in Figure 3.5, the line connecting point O to the point A represents the elastic behavior of the steel. Line AB represents yielding of the material while the stress remains constant and it is equal to yield stress $F_y$**.** The yielding moment $M_y$ is at point A and afterward the Plastic Moment $M_p$ is located at point B. Member behavior between point A and B is still considered as elastic behavior. The plastic hinge happens when the material starts to yield and plastic moment $M_p$ is reached. Plastic hinge is defined as a yielded zone due to bending in a structural member at which an infinite rotation can take place at a constant plastic moment $M_p$ of the section. Strain hardening takes place between point B and point C. The strain at point C is equal to 0.1196 which is known as the summit strain hardening point.

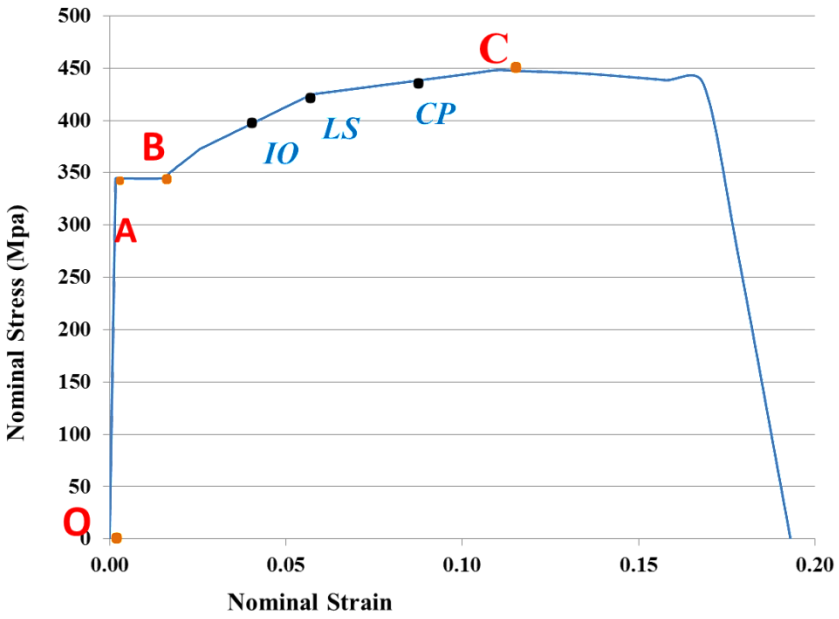


Figure 3.5: Strain-Stress curve for A992 Steel

The plastic rotation $\Theta p$ starts after the elastic rotation and is considered as inelastic or non-recoverable rotation. The plastic hinge includes both the elastic and plastic rotation (Fig3.4) .There are multiple possibilities to model the plastic hinge when this concept is used in structural analysis. FEMA356 and ASCE41 categorize the plastic hinge behavior to Immediate Occupancy (IO), Life Safety (LS), Collapse Prevention (CP) and Collapse (C) sections as shown in Fig. 3.5.

In this study the plastic hinge of M3 type is defined according to ASCE 41 [7] for Spandrel (longitudinal) beams and for chords of the truss members. P-M2-M3 type of the plastic hinge was used for the columns, while for the braces axial load P was used.

According to UFC 2013 [2] the nonlinear and linear acceptance criteria for structural steel beam members should meet the Collapse Prevention (CP) and for

the column members is the Life Safety (LS). Tables 5.5, 5.6, and 5.7 of ASCE 41 [7] are used to calculate the plastic hinge definitions for all the beams, columns, and braces.  41.

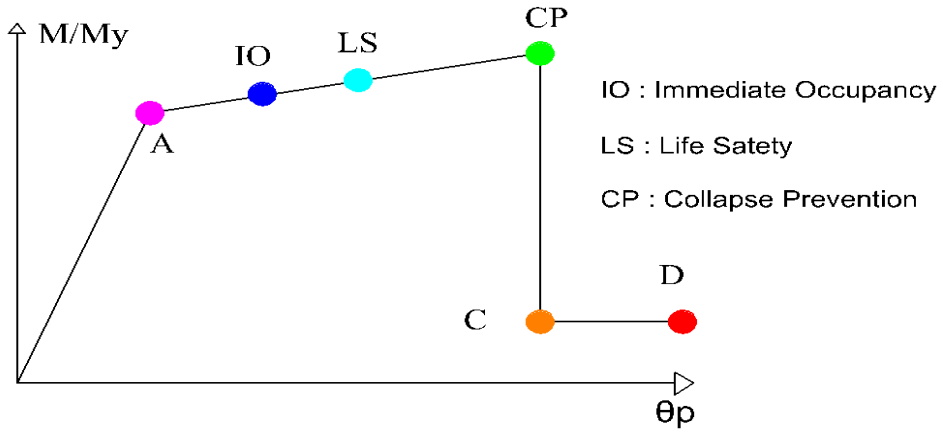


Figure 3.6: M3 plastic hinge behavior

### 3.6.2.1 Column Plastic Hinge Definitions

According to the analysis, W12 and W14 sections (ready sections in SAP2000 library) were used for column members. Table 5-6 of ASCE 41 was used to calculate the plastic hinge characteristics of columns.  It is vital to first calculate the lower bound strength of the steel columns ($P_{CL}$).  $P_{CL}$ is the minimum value found for the limit conditions of column buckling, local buckling or local web buckling calculated with the lower bound strength, $F_{YL}$. Table 3.4 shows the calculated plastic hinge definitions for all the column sections in the proposed model.

Table 3.4: Columns Hinge Parameters and Acceptance Criteria

| section | Θy | P1 (kips) | Pcl (kips) | P/Pcl | A (in^2) | Fye (ksi) | Pye (ksi) | Plastic Rotation Angles (Radiand ) | | | Acceptance Criteria | | |
|---|---|---|---|---|---|---|---|---|---|---|---|---|---|
| | | | | | | | | a | b | c | IO | LS | CP |
| W14*500 | 0.4761 | 3849.5 | 7699.4 | 0.500 | 147 | 55 | 8085 | 0.8646 | 1.3362 | 0.2 | 0.1310 | 0.6288 | 0.8646 |
| W14*455 | 0.4755 | 3504.7 | 7009.6 | 0.500 | 134 | 55 | 7370 | 0.8655 | 1.3376 | 0.2 | 0.1311 | 0.6295 | 0.8655 |
| W14*426 | 0.4791 | 3293.84 | 6587.6 | 0.500 | 125 | 55 | 6875 | 0.8594 | 1.3282 | 0.2 | 0.1302 | 0.6250 | 0.8594 |
| W14*398 | 0.4788 | 3081.3 | 6162.8 | 0.500 | 117 | 55 | 6435 | 0.8601 | 1.3292 | 0.2 | 0.1303 | 0.6255 | 0.8601 |
| W12*305 | 0.4670 | 2301.15 | 4602.3 | 0.500 | 89.6 | 55 | 4928 | 0.8795 | 1.3592 | 0.2 | 0.1333 | 0.6396 | 0.8795 |
| W12*279 | 0.4661 | 2099.55 | 4199.1 | 0.500 | 81.9 | 55 | 4505 | 0.8809 | 1.3614 | 0.2 | 0.1335 | 0.6407 | 0.8809 |
| W12*252 | 0.4654 | 1896.6 | 3683 | 0.515 | 74.1 | 55 | 4076 | 0.7326 | 1.1322 | 0.2 | 0.1337 | 0.5328 | 0.7326 |
| W12*230 | 0.4646 | 1729.9 | 3459.9 | 0.500 | 67.7 | 55 | 3724 | 0.8836 | 1.3655 | 0.2 | 0.1339 | 0.6426 | 0.8836 |
| W12*210 | 0.5427 | 1554.47 | 3109 | 0.500 | 61.8 | 55 | 3399 | 0.8955 | 1.3840 | 0.2 | 0.1357 | 0.6513 | 0.8955 |
| W12*190 | 0.5366 | 1422.18 | 2844.4 | 0.500 | 55.8 | 55 | 3069 | 0.8854 | 1.3683 | 0.2 | 0.1341 | 0.6439 | 0.8854 |
| W12*170 | 0.5375 | 1272 | 2544 | 0.500 | 50 | 55 | 2750 | 0.8868 | 1.3705 | 0.2 | 0.1344 | 0.6449 | 0.8868 |
| W12*152 | 0.5380 | 1135.78 | 2271.7 | 0.500 | 44.7 | 55 | 2459 | 0.8879 | 1.3723 | 0.2 | 0.1345 | 0.6458 | 0.8879 |
| W12*136 | 0.5388 | 1012.15 | 2024.2 | 0.500 | 39.9 | 55 | 2195 | 0.8887 | 1.3735 | 0.2 | 0.1347 | 0.6463 | 0.8887 |
| W12*120 | 0.5395 | 893.99 | 1788 | 0.500 | 35.3 | 55 | 1942 | 0.8903 | 1.3759 | 0.2 | 0.1349 | 0.6475 | 0.8903 |
| W12*106 | 0.5401 | 789.199 | 1578.4 | 0.500 | 31.2 | 55 | 1716 | 0.8912 | 1.3772 | 0.2 | 0.1350 | 0.6481 | 0.8912 |

### 3.6.2.2 Beam and Braces Plastic Hinge Definitions

For beams, the plastic hinge parameters had to be obtained from table 5-6 of ASCE 41. Regarding the $\frac{b_f}{2.t_f}$ and $\frac{h}{t_w}$ equations, the designer has to choose the plastic hinge angle and acceptance criteria from row a or row b or by interpolation between the two rows. ASCE 41 uses variety of plastic hinge parameters for braces under compression and tension. To calculate brace plastic hinge parameters, first it should be clarified that the brace or truss member is in tension or compression. Afterwards based on $\frac{KL}{r}$ ratio the plastic rotation angle and acceptance criteria will be calculated.

Table 3.5: Beams Hinge Parameters and Acceptance Criteria

| section | bf (in) | tf (in) | tw (in) | h (in) | Fye (ksi) | bf/2tf | h/tw | Plastic Rotation Angles Radiand | | | Acceptance Criteria | | |
|---|---|---|---|---|---|---|---|---|---|---|---|---|---|
| | | | | | | | | a | b | c | IO | LS | CP |
| W16*31 | 5.52 | 0.44 | 0.28 | 15.88 | 55 | 6.27273 | 57.745 | 9.09 | 10.77 | 0.58 | 0.97 | 5.81 | 7.77 |
| W18*35 | 6.00 | 0.43 | 0.30 | 17.70 | 55 | 7.05882 | 59 | 9.18 | 10.56 | 0.56 | 0.93 | 5.65 | 7.56 |
| W18*40 | 6.02 | 0.53 | 0.32 | 17.90 | 55 | 5.72857 | 56.825 | 9.00 | 11.00 | 0.60 | 1.00 | 6.00 | 8.00 |
| W18*46 | 6.06 | 0.61 | 0.36 | 18.06 | 55 | 5.00826 | 50.167 | 9.00 | 11.00 | 0.60 | 1.00 | 6.00 | 8.00 |
| W18*50 | 7.50 | 0.57 | 0.36 | 17.99 | 55 | 6.57895 | 50.676 | 9.00 | 11.00 | 0.60 | 1.00 | 6.00 | 8.00 |
| W18*60 | 7.56 | 0.70 | 0.42 | 18.24 | 55 | 5.43525 | 43.952 | 9.00 | 11.00 | 0.60 | 1.00 | 6.00 | 8.00 |
| W18*65 | 7.59 | 0.75 | 0.45 | 18.35 | 55 | 5.06 | 40.778 | 9.00 | 11.00 | 0.60 | 1.00 | 6.00 | 8.00 |
| W18*71 | 7.64 | 0.81 | 0.50 | 18.47 | 55 | 4.71296 | 37.313 | 9.00 | 11.00 | 0.60 | 1.00 | 6.00 | 8.00 |
| W18*76 | 11.04 | 0.68 | 0.43 | 18.21 | 55 | 8.11397 | 42.847 | 5.86 | 7.86 | 0.35 | 0.53 | 3.49 | 4.86 |
| W10*45 | 8.02 | 0.62 | 0.35 | 10.10 | 55 | 6.46774 | 28.857 | 9.00 | 11.00 | 0.60 | 1.00 | 6.00 | 8.00 |
| W10*49 | 10.00 | 0.56 | 0.34 | 9.98 | 55 | 8.92857 | 29.353 | 4.00 | 6.00 | 0.20 | 0.25 | 2.00 | 3.00 |
| W10*54 | 10.03 | 0.62 | 0.37 | 10.09 | 55 | 8.15447 | 27.27 | 9.00 | 11.00 | 0.60 | 1.00 | 6.00 | 8.00 |
| W10*60 | 10.08 | 0.68 | 0.42 | 10.22 | 55 | 7.41176 | 24.333 | 7.86 | 9.86 | 0.51 | 0.82 | 5.10 | 6.86 |
| W10*68 | 10.13 | 0.77 | 0.47 | 10.40 | 55 | 6.57792 | 22.128 | 9.00 | 11.00 | 0.60 | 1.00 | 6.00 | 8.00 |
| W10*77 | 10.19 | 0.87 | 0.53 | 10.60 | 55 | 5.85632 | 20 | 9.00 | 11.00 | 0.60 | 1.00 | 6.00 | 8.00 |
| W10*88 | 10.26 | 0.99 | 0.61 | 10.84 | 55 | 5.18182 | 17.917 | 9.00 | 11.00 | 0.60 | 1.00 | 6.00 | 8.00 |
| W10*100 | 10.34 | 0.99 | 0.68 | 10.34 | 55 | 5.22222 | 15.206 | 9.00 | 11.00 | 0.60 | 1.00 | 6.00 | 8.00 |
| W10*112 | 10.42 | 1.25 | 0.76 | 11.36 | 55 | 4.166 | 15.046 | 9.00 | 11.00 | 0.60 | 1.00 | 6.00 | 8.00 |
| W12*106 | 12.22 | 0.99 | 0.61 | 12.89 | 55 | 6.17172 | 21.131 | 9.00 | 11.00 | 0.60 | 1.00 | 6.00 | 8.00 |
| W12*120 | 12.32 | 1.10 | 0.71 | 13.12 | 55 | 5.6 | 18.479 | 9.00 | 11.00 | 0.60 | 1.00 | 6.00 | 8.00 |
| W12*136 | 12.40 | 1.25 | 0.79 | 13.41 | 55 | 4.96 | 16.975 | 9.00 | 11.00 | 0.60 | 1.00 | 6.00 | 8.00 |
| W12*152 | 12.48 | 1.40 | 0.87 | 13.71 | 55 | 4.45714 | 15.759 | 9.00 | 11.00 | 0.60 | 1.00 | 6.00 | 8.00 |

# Chapter 4

# LINEAR STATIC ANALYSES OF FALIURE MECHANISM FOR COLUMN REMOVALS

## 4.1 Introduction

In this chapter, the linear static analysis method will be performed to assess the collapse behavior of staggered truss structures. Both the GSA 2013 [14] and the UFC 2013 [2], suggest a Linear Static procedure for progressive collapse when the structure is not irregular and the component Demand Capacity Ratios are less or equal to 2. If the structure under evaluation for progressive collapse potential is asymmetrical or one or extra DCR ratios surpass 2, a linear static analysis is not recommended. For each element, a demand modifier or ***m*** factor should be calculated. These ***m*** factors are determined from table 5-5 in ASCE 41 guideline [7]. Before finding ***m*** factors, it is essential to clarify which elements are force-controlled and which elements are deformation-controlled actions. Table 5.1, which is adopted from the GSA 2013 [14], shows a summary of the different modeling requirements for deformation and force-controlled actions.

Table 4.1: Model Requirements for Deformation and Force-Controlled Actions

| **Design and/or Modeling Assumption** | **Deformation-Controlled** | **Force-Controlled** |
|---|---|---|
| Design Strength | Expected (QCE) | Lower Bound (QCL) |
| Load Increase Factor | 0.9 mLIF + 1.1 | 2.0 |
| Demand Modifier | m-factor | 1.0 |

## 4.2 m-Factors

For each structural element such as beams or columns, two ***m*** factors had to be calculated, one for the element itself and one for its connections. The governing *m* factor for each element is based on the smallest of the element or the element connection. The entire beam to column connections in the moment frames used in this study were assumed to be an improved WUF connection. This type of connection is introduced in appendix C of UFC 2013 [2] and appendix C of GSA 2013 [14].

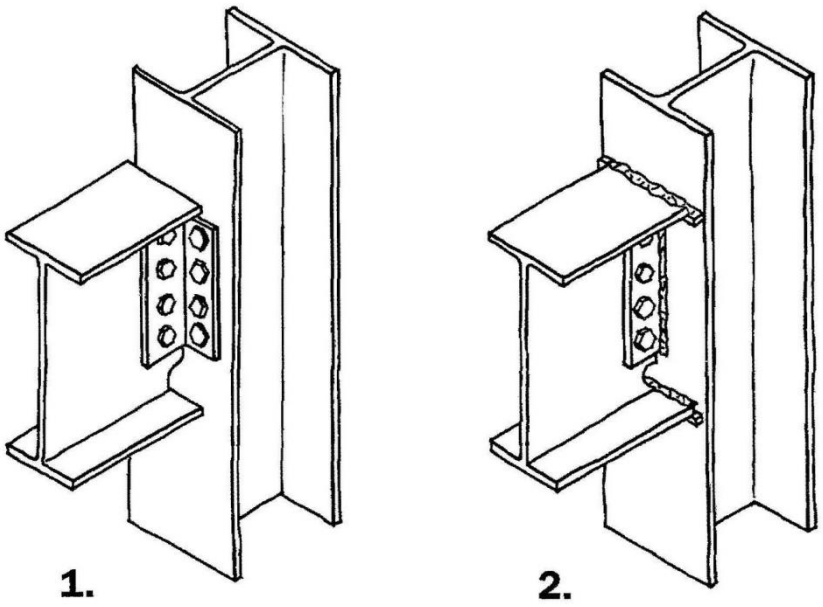


Figure 4.1: Typical Simple Shear Tab Connection (1) and WUF Connection (2)

Figure 4.1(2) shows a typical WUF connection used for moment connection frames. The beam flange welds transmit full flange strength to the column, therefore using both bolt groups and welding makes the connections behave like a moment connection. In trusses for the chord to column connections which are pinned connections, the Simple Shear Tab Connection definition was used (figure

4.1-1). In this type of connection beams are connected to the columns by using L shaped angles and bolt groups only.

### 4.2.1 Beam m-Factors

The m-factor for beam components is determined in accordance with the table 5-5 of ASCE 41 [7] guideline based on a Collapse Prevention (CP) level. For each beam section, its properties are defined per AISC-LRFD [4]. Then regarding $\frac{b_f}{2t_f}$ and $\frac{h}{t_w}$ equations, the designer has to decide which of the m-factors to use for beam components.

### 4.2.2 Connection m-Factors

To find out the connection ***m***-factor, table 4.2 adopted from GSA 2013 [14] are used. As shown in Figure 4.1, improved WUF connection type and Simple Shear Tab connections are used for moment frames and truss connections respectively.

### 4.2.3 Column m-Factors

Table 5.5 in ASCE 41 is used to determine the m factor values for the columns *m* factor; the same table used for beams (was used for Collapse prevention level. The ***m***-factor is a function of the section compactness of $\frac{b_f}{2t_f}$ or $\frac{h}{t_w}$ . The GSA (2013) requires categorizing the column whether it is force-controlled action or deformation controlled action. Accordingly, if the $0.2 \leq \frac{P}{\boldsymbol{P_{cl}}} \leq 0.5$ (*P* is the axial force in the column due to column removal scenario and $P_{CL}$ is the lower bound strength of the column) then the column is characterized as deformation control or else it is characterized as force-controlled action.

Table 4.2: Acceptance Criteria for Linear Static Modeling of Steel Frame Connection.

| Connection Type | Linear Acceptance Criteria | |
|---|---|---|
| m-factors | | |
| Primary(1) | Secondary(1) | |
| Fully Restrained Moment Connections | | |
| Improved WUF with Bolted Web | 3.1 - 0.032d | 6.2 - 0.065d |
| Reduced Beam Section (RBS) | 6.9 - 0.032d | 8.4 - 0.032d |
| WUF | 3.9 - 0.043d | 5.5 - 0.064d |
| SidePlate | 6.7 - 0.039d(2) | 11.1 - 0.062d |
| Partially Restrained Moment Connections (Relatively Stiff) | | |
| Double Split Tee | | |
| a. Shear in Bolt | 6 | 8 |
| b. Tension in Bolt | 2.5 | 4 |
| c. Tension in Tee | 2 | 2 |
| d. Flexure in Tee | 7 | 14 |
| Partially Restrained Moment Connections (Flexible) | | |
| Double Angles | | |
| a. Shear in Bolt | 5.8 - 0.107dbg (3) | 8.7 - 0.161dbg |
| b. Tension in Bolt | 1.5 | 4 |
| c. Flexure in Angles | 8.9 - 0.193dbg | 13.0 - 0.290dbg |
| Simple Shear Tab | 5.8 - 0.107dbg | 8.7 - 0.161dbg |

(1) Refer to Section 3.2.4 for determination of Primary and Secondary classification.
(2) d = depth of beam, in
(3) dbg = depth of bolt group, in

## 4.3 Load Increase Factors

According to GSA (2013) for steel frame structures, the load increase factor for Force-Controlled Actions is equal to 2 and for deformation-Controlled actions; the load increase factor is the smallest of *m*-factor of either the element or the connection.

## 4.4 Load Combinations

The load combinations applied to the structure are different based on the location of the elements and the force or deformation controlled actions. Generally there are three different load combinations required for linear static progressive collapse analysis:

- Load combination applied to the components directly above the removed column.
- Load combination applied to the surrounding components.
- Load combination applied to the Force-Controlled components.

For the components immediately above the removed element the GSA 2013 [14] suggests equations 4.1, 4.2 and 4.3:

$$\boldsymbol{G}_{LD} = \Omega_{LD}\,[1.2D + (0.5\,L \text{ or } 0.2\,S)] \quad (4.1)$$

$$\Omega_{LD} = 0.9\,m_{LIF} + 1.1 \quad (4.2)$$

$$\boldsymbol{G}_{LF} = \Omega_{LF}\,[1.2\,D + (0.5\,L \text{ or } 0.2\,S)] \quad (4.3)$$

where

$\mathbf{G}_{LD}$ = Increased gravity loads for deformation-controlled actions for Linear static analysis

$\mathbf{G}_{LF}$ = Increased gravity loads for force-controlled actions for linear static analysis

D = Dead load

L= Live load

S = Snow load

$\Omega_{LD}$ = Load increase factors for deformation-controlled actions

$\Omega_{LF}$ = 2.

For the components not immediately adjacent to the removed element the load combination is:

$$G = 1.2\,D + (0.5\,L \text{ or } 0.2\,S) \quad (4.4)$$

## 4.5 Column Removal Scenarios

To perform a Linear Static Analysis (LSA) for collapse potential in Staggered Truss Systems, two analyses were performed. The first model was based on regular design procedures offered by AISC-LRFD [4] manual of steel

construction. At this stage of the analysis, the effects of member loss have not been considered during the design procedure. In the second model, GSA 2013 and UFC 2013 guidelines are used to assess the effects of column removal scenarios (the Retrofitted Structure) and if required to retrofit the structure.

According to the UFC 2013, the location of element removal is given below:

1. First floor above grade
2. Floor right below roof
3. Floor at the enteral-height
4. Floor over the position of a column splice or alteration in column dimension.

### 4.5.1 Ground Floor and 6$^{th}$ Floor Columns Were Removed From the Original Model

In the first step a column from 5$^{th}$ frame (middle frame) – at the ground floor of the original structure as shown in Figure 4.2 was removed. Then the results of the linear static analysis will be compared together to investigate the probability of failure mechanism due to column removals. Figure 4.2 shows the location of the removed column at ground floor.

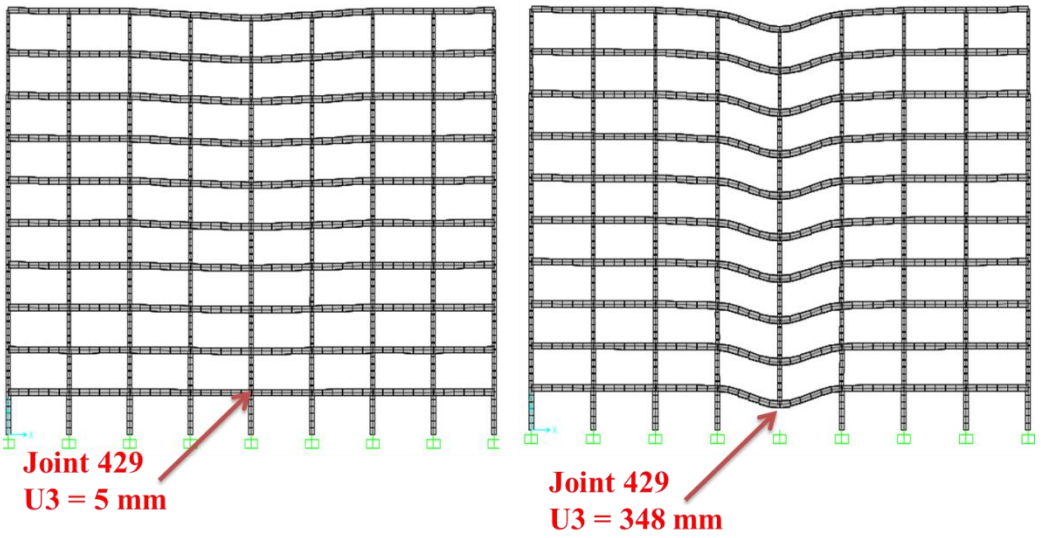


Figure 4.2: Vertical deflection of the joint 429 before and after removing the middle column in the original model

Because in the linear static analysis several load combinations had to be applied. Therefore the Staged Construction option in SAP2000 can be used for the formation of distinct analysis cases. To do this, while this is a linear static procedure, the nonlinear analysis check-box is selected and P-Delta effects were being allowed. In Nonlinear-Static Staged Construction menu, 2 stages had to be defined. In the first stage, all loads were assigned to different component groups following equations 4.1, 4.2, 4.3 and 4.4. In the second stage, a column will be removed under investigation and Remove Structure option in this Load Case (Figure 4.3). In the first stage as figure 4.2 illustrates, the vertical displacement of the joint 429 directly above the column which had to be removed is 5 mm. After removing the column under investigation, the vertical displacement of the joint 429 is equal to 348 mm.

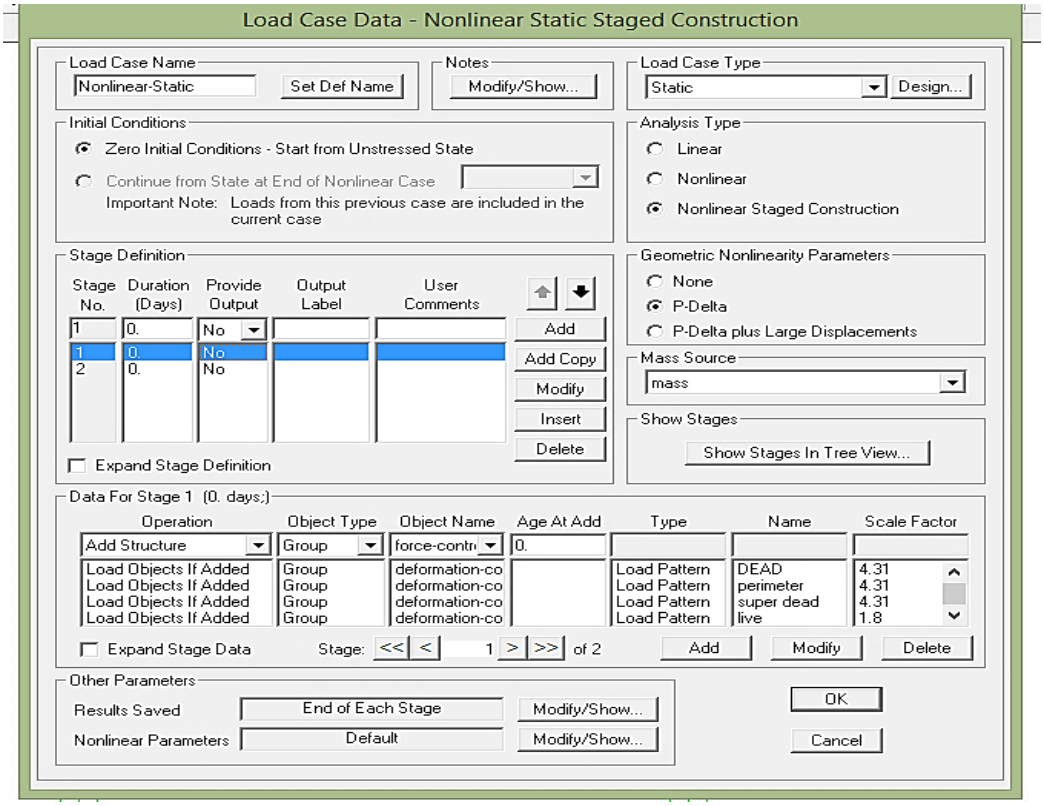

Figure 4.3: Analysis Case Definition

To find out which structural members have failed in the original model, the DCR ratios should be compared with the governing m-factors for the element and its component. The process of calculating the DCR ratio was already described in chapter 2. It should be noted that for Deformation-Controlled actions the equation 2.1 (DCR = QUD/QCD) should be used. For Force-Controlled actions the DCR must exceed 1 (GSA 2013[14]).

Using the above mentioned equation, the DCR ratios for beams were manually calculated based on the maximum moment in the beam in relation to its ultimate capacity as shown below:

$$\boldsymbol{DCR = \frac{M_{max}}{M_p}} \qquad (4.5)$$

DCR for columns can be found out as shown in the following equation:

$$\frac{\boldsymbol{P}}{\boldsymbol{P_y}} + \frac{\boldsymbol{M_{pc}}}{\boldsymbol{1.18M_p}} \leq 1 \qquad (4.6)$$

Where P = Column Axial Force

$P_Y$ = Yield Strength

$M_{PC}$ = Maximum moment acting in the member

$M_p$ = Ultimate moment capacity

Table 4.3 and 4.4 show the component m-factors, DCRs and the status of the beams and columns in the original model. The analysis showed that after removing the ground floor central column, most of the beams from left and right side of the removed column had DCR ratios bigger than acceptance criteria. These spandrel beams are W16×31 - W18×35 - W18×40 - W18×46 - W18×50 - W18×60-W18×65- W18×71 and W18×76 sections located in the moment frame direction. In this stage Truss Chords from 3rd to 10th floor were failed due to removal of first column.

In Table 4.4 it could be seen that after removing the column, many columns located in the left and right above the removed column have failed. These columns belong to the 4th and 6th frames where the beams connected to them have transferred the axial loads to them resulted from removing the 5th frame column. To expand this situation more, it should be indicated that, after demolishing a column, the axial forces coming from upper structural elements had to be transmitted by the connected beams to the neighboring columns. It is clear that, most of the failed columns were those which were categorized as Force-Controlled actions. In force controlled columns $\frac{\boldsymbol{P}}{\boldsymbol{Pcl}} > 0.5$, therefore generally the ratio of axial load to axial strength is high in these elements. When a column is

removed from structural system, the resulting redundant axial load makes the condition worse for those columns, which eventually leads to a member failure.

Table 4.3: Beam properties of the original structure after removing a column from middle frame- ground floor

| section | Location | DCR (Mu/Mp) | Acceptance Criteria | Linear Static Result |
|---|---|---|---|---|
| W18*35 | moment frame-1st floor, left | 9.55 | 2.831 | Failed |
| W18*35 | moment frame-1st floor,right | 9.57 | 2.831 | Failed |
| W18*65 | moment frame-2nd floor,left | 6.8 | 2.777 | Failed |
| W18*65 | moment frame-2nd floor,right | 6.78 | 2.777 | Failed |
| W18*65 | moment frame-3rd floor,left | 6.6 | 2.777 | Failed |
| W18*65 | moment frame-3rd floor,right | 6.63 | 2.777 | Failed |
| W18*65 | moment frame-4th floor,left | 6.5 | 2.777 | Failed |
| W18*65 | moment frame-4th floor,right | 6.5 | 2.777 | Failed |
| W18*65 | moment frame-5th floor,left | 6.2 | 2.777 | Failed |
| W18*65 | moment frame-5th floor,right | 6.2 | 2.777 | Failed |
| W18*50 | moment frame-6th floor,left | 6.13 | 2.807 | Failed |
| W18*50 | moment frame-6th floor,right | 6.14 | 2.807 | Failed |
| W18*50 | moment frame-7th floor,left | 6 | 2.807 | Failed |
| W18*50 | moment frame-7th floor,right | 6 | 2.807 | Failed |
| W18*46 | moment frame-8th floor,left | 6.9 | 2.801 | Failed |
| W18*46 | moment frame-8th floor,right | 6.9 | 2.801 | Failed |
| W18*40 | moment frame-9th floor,left | 7.4 | 2.814 | Failed |
| W18*40 | moment frame-9th floor,right | 7.4 | 2.814 | Failed |
| W16*31 | moment frame-10th floor,left | 7.7 | 2.982 | Failed |
| W16*31 | moment frame-10th floor,right | 7.71 | 2.982 | Failed |
| W12*152 | staggered truss frame-1st floor | 3.94 | 4.333 | Not Failed |
| W10*112 | staggered truss frame-2nd floor | 4 | 4.584 | Not Failed |
| W10*100 | staggered truss frame-3rd floor | 4.74 | 4.694 | Failed |
| W10*100 | staggered truss frame-4th floor | 4.5 | 4.694 | Failed |
| W10*88 | staggered truss frame-5th floor | 5.24 | 4.640 | Failed |
| W10*88 | staggered truss frame-6th floor | 5.23 | 4.640 | Failed |
| W10*77 | staggered truss frame-7th floor | 5.76 | 4.666 | Failed |
| W10*77 | staggered truss frame-8th floor | 5.9 | 4.666 | Failed |
| W10*49 | staggered truss frame-9th floor | 8.86 | 4.732 | Failed |
| W10*49 | staggered truss frame-10th floor | 9 | 4.732 | Failed |

Table 4.4: Column properties of the original structure after removing a column from middle frame-ground floor

| section | Location | bf (in) | tf (in) | tw (in) | h (in) | Fye (ksi) | bf/2tf | h/tw | P (kip) | Pcl (kip) | P/Pcl | m-factors | DCR | Column Status |
|---|---|---|---|---|---|---|---|---|---|---|---|---|---|---|
| W14*455 | moment frame-left column-1st floor | 16.84 | 3.21 | 2.02 | 19.02 | 55 | 2.6231 | 9.42 | 2873 | 7010 | 0.41 | 3.80 | 1.7 | Not Failed |
| W14*455 | moment frame-right column-1st floor | 16.84 | 3.21 | 2.02 | 19.02 | 55 | 2.6231 | 9.42 | 2874 | 7010 | 0.41 | 3.80 | 1.71 | Not Failed |
| W12*305 | moment frame-left column-2nd floor | 13.24 | 2.71 | 1.63 | 16.32 | 55 | 2.4428 | 10 | 2819 | 4602 | 0.61 | force controlled | 3.12 | Failed |
| W12*305 | moment frame-middle column-2nd floor | 13.24 | 2.71 | 1.63 | 16.32 | 55 | 2.4428 | 10 | 2409 | 4602 | 0.52 | force controlled | 0.173 | Not Failed |
| W12*305 | moment frame-right column-2nd floor | 13.24 | 2.71 | 1.63 | 16.32 | 55 | 2.4428 | 10 | 2820 | 4602 | 0.61 | force controlled | 3.13 | Failed |
| W12*279 | moment frame-left column-3rd floor | 13.14 | 2.47 | 1.53 | 15.85 | 55 | 2.6599 | 10.4 | 2777 | 4200 | 0.66 | force controlled | 3.17 | Failed |
| W12*279 | moment frame-middle column-3rd floor | 13.14 | 2.47 | 1.53 | 15.85 | 55 | 2.6599 | 10.4 | 2326 | 4200 | 0.55 | force controlled | 0.222 | Not Failed |
| W12*279 | moment frame-right column-3rd floor | 13.14 | 2.47 | 1.53 | 15.85 | 55 | 2.6599 | 10.4 | 2772 | 4200 | 0.66 | force controlled | 3.17 | Failed |
| W12*279 | moment frame-left column-4th floor | 13.14 | 2.47 | 1.53 | 15.85 | 55 | 2.6599 | 10.4 | 2005 | 4200 | 0.48 | 2.45 | 2.7 | Failed |
| W12*279 | moment frame-middle column-4th floor | 13.14 | 2.47 | 1.53 | 15.85 | 55 | 2.6599 | 10.4 | 2270 | 4200 | 0.54 | force controlled | 0.46 | Not Failed |
| W12*279 | moment frame-right column-4th floor | 13.14 | 2.47 | 1.53 | 15.85 | 55 | 2.6599 | 10.4 | 2006 | 4200 | 0.48 | 2.45 | 2.7 | Failed |
| W12*190 | moment frame-left column-5th floor | 12.67 | 1.74 | 1.06 | 14.38 | 55 | 3.6408 | 13.6 | 1955 | 2844 | 0.69 | force controlled | 3.5 | Failed |
| W12*190 | moment frame-middle column-5th floor | 12.67 | 1.74 | 1.06 | 14.38 | 55 | 3.6408 | 13.6 | 1739 | 2844 | 0.61 | force controlled | 0.55 | Not Failed |
| W12*190 | moment frame-right column-5th floor | 12.67 | 1.74 | 1.06 | 14.38 | 55 | 3.6408 | 13.6 | 1954 | 2844 | 0.69 | force controlled | 3.5 | Failed |
| W12*190 | moment frame-left column-6th floor | 12.67 | 1.74 | 1.06 | 14.38 | 55 | 3.6408 | 13.6 | 1430 | 2844 | 0.50 | 1.94 | 2.9 | Failed |
| W12*190 | moment frame-middle column-6th floor | 12.67 | 1.74 | 1.06 | 14.38 | 55 | 3.6408 | 13.6 | 1684 | 2844 | 0.59 | force controlled | 0.77 | Not Failed |
| W12*190 | moment frame-right column-6th floor | 12.67 | 1.74 | 1.06 | 14.38 | 55 | 3.6408 | 13.6 | 1431 | 2844 | 0.50 | 1.94 | 2.92 | Failed |
| W12*190 | moment frame-left column-7th floor | 12.67 | 1.74 | 1.06 | 14.38 | 55 | 3.6408 | 13.6 | 1382 | 2844 | 0.49 | 2.28 | 2.3 | Failed |
| W12*190 | moment frame-middle column-7th floor | 12.67 | 1.74 | 1.06 | 14.38 | 55 | 3.6408 | 13.6 | 1155 | 2844 | 0.41 | 3.88 | 0.55 | Not Failed |
| W12*190 | moment frame-right column-7th floor | 12.67 | 1.74 | 1.06 | 14.38 | 55 | 3.6408 | 13.6 | 1382 | 2844 | 0.49 | 2.28 | 2.32 | Failed |
| W12*190 | moment frame-left column-8th floor | 12.67 | 1.74 | 1.06 | 14.38 | 55 | 3.6408 | 13.6 | 856 | 2844 | 0.30 | 5.98 | 1.88 | Not Failed |
| W12*190 | moment frame-middle column-8th floor | 12.67 | 1.74 | 1.06 | 14.38 | 55 | 3.6408 | 13.6 | 1103 | 2844 | 0.39 | 4.24 | 0.7 | Not Failed |
| W12*190 | moment frame-right column-8th floor | 12.67 | 1.74 | 1.06 | 14.38 | 55 | 3.6408 | 13.6 | 857 | 2844 | 0.30 | 5.97 | 1.9 | Not Failed |
| W12*106 | moment frame-left column-9th floor | 12.22 | 0.99 | 0.61 | 12.89 | 55 | 6.1717 | 21.1 | 809 | 1578 | 0.51 | force controlled | 2.5 | Failed |
| W12*106 | moment frame-middle column-9th floor | 12.22 | 0.99 | 0.61 | 12.89 | 55 | 6.1717 | 21.1 | 574 | 1578 | 0.36 | 4.72 | 0.72 | Not Failed |
| W12*106 | moment frame-right column-9th floor | 12.22 | 0.99 | 0.61 | 12.89 | 55 | 6.1717 | 21.1 | 810 | 1578 | 0.51 | force controlled | 2.5 | Failed |
| W12*106 | moment frame-left column-10th floor | 12.22 | 0.99 | 0.61 | 12.89 | 55 | 6.1717 | 21.1 | 47 | 1578 | 0.03 | 11.40 | 1.57 | Not Failed |
| W12*106 | moment frame-middle column-10th floor | 12.22 | 0.99 | 0.61 | 12.89 | 55 | 6.1717 | 21.1 | 524 | 1578 | 0.33 | 5.36 | 0.9 | Not Failed |
| W12*106 | moment frame-right column-10th floor | 12.22 | 0.99 | 0.61 | 12.89 | 55 | 6.1717 | 21.1 | 525 | 1578 | 0.33 | 5.35 | 1.57 | Not Failed |

The truss diagonals and verticals are mostly HSS10×10×0.5 hollow sections. Table 5.5 of ASCE 41 [7], indicates an acceptance criteria equal to 6 and Collapse Prevention (CP) state for these members. The static analysis results on the original model revealed DCR ratios below the acceptance criteria for HSS sections. This proves that, removing a column from the ground floor in the original model will not lead the truss members to fail.

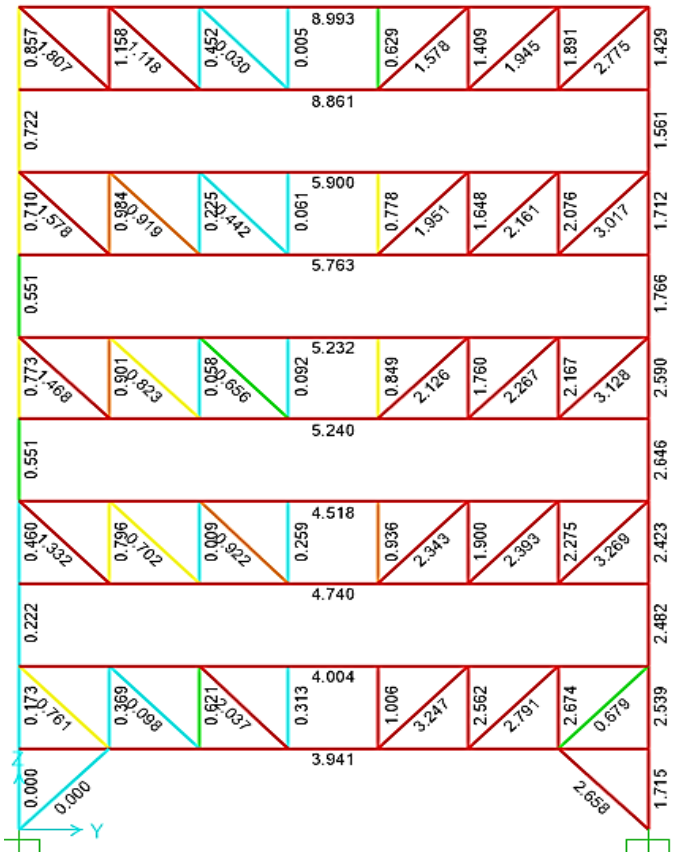

Figure 4.4: DCR ratios of truss members after removing 5th frame ground floor column

In the second scenario, a column at 6th floor from the same frame (middle frame) of the original structure was removed. The previous procedure accomplished for the ground floor was duplicated here under relevant investigations. Figure 4.5

shows the location of removed column and the vertical displacement of the joint 424.

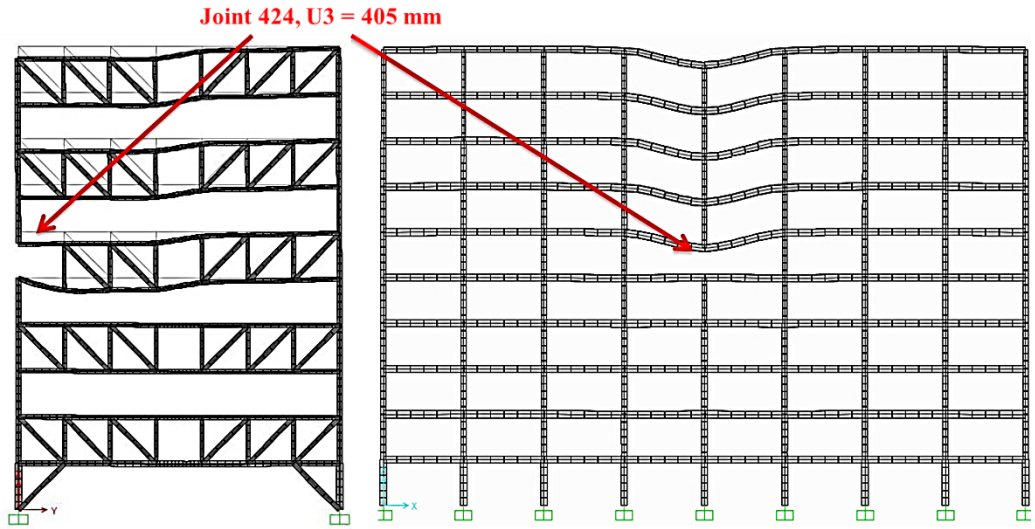


Figure 4.5: Vertical displacement of joint 424 after removing the 6th floor column

Table 4.5: Beam properties of the original structure after removing a column from middle frame- 6th floor

| section | Location | DCR (Mu/Mp) | Acceptance Criteria | Linear Static Result |
|---|---|---|---|---|
| W18*50 | moment frame-6th floor,left | 7.3 | 2.807 | Failed |
| W18*50 | moment frame-6th floor,right | 7.3 | 2.807 | Failed |
| W18*50 | moment frame-7th floor,left | 7.27 | 2.807 | Failed |
| W18*50 | moment frame-7th floor,right | 7.28 | 2.807 | Failed |
| W18*46 | moment frame-8th floor,left | 8.24 | 2.801 | Failed |
| W18*46 | moment frame-8th floor,right | 8.3 | 2.801 | Failed |
| W18*40 | moment frame-9th floor,left | 8.9 | 2.814 | Failed |
| W18*40 | moment frame-9th floor,right | 8.9 | 2.814 | Failed |
| W16*31 | moment frame-10th floor,left | 9.2 | 2.982 | Failed |
| W16*31 | moment frame-10th floor,right | 9.2 | 2.982 | Failed |
| W10*88 | staggered truss frame-5th floor | 7.9 | 4.640 | Failed |
| W10*88 | staggered truss frame-6th floor | 6 | 4.640 | Failed |
| W10*77 | staggered truss frame-7th floor | 7.4 | 4.666 | Failed |
| W10*77 | staggered truss frame-8th floor | 7.2 | 4.666 | Failed |
| W10*49 | staggered truss frame-9th floor | 11.3 | 4.732 | Failed |
| W10*49 | staggered truss frame-10th floor | 11.5 | 4.732 | Failed |

A summary of beam and column properties after removing the 6th floor columns are illustrated n in table 4.5 and 4.6. After cutting off the column, all spandrel beams and chords in both moment and staggered truss frames are failed. Additionally, some of the columns above the removed column have DCR ratios bigger than their acceptance criteria which means they also failed to resist against the increased axial loads.

Table 4.6: Column properties of the original structure after removing a column from middle frame-6th floor

| section | Location | bf (in) | tf (in) | tw (in) | h (in) | Fye (ksi) | bf/2tf | h/tw | P (kip) | Pcl (kip) | P/Pcl | m-factors | DCR | Column Status |
|---|---|---|---|---|---|---|---|---|---|---|---|---|---|---|
| W12*190 | moment frame-left column-6th floor | 12.7 | 1.74 | 1.1 | 14 | 55 | 3.641 | 14 | 1430 | 2844 | 0.5 | 1.944 | 2.7 | Failed |
| W12*190 | moment frame-right column-6th floor | 12.7 | 1.74 | 1.1 | 14 | 55 | 3.641 | 14 | 1431 | 2844 | 0.5 | 1.937 | 2.75 | Failed |
| W12*190 | moment frame-left column-7th floor | 12.7 | 1.74 | 1.1 | 14 | 55 | 3.641 | 14 | 1382 | 2844 | 0.49 | 2.281 | 2.96 | Failed |
| W12*190 | moment frame-middle column-7th floor | 12.7 | 1.74 | 1.1 | 14 | 55 | 3.641 | 14 | 1155 | 2844 | 0.41 | 3.878 | 0.32 | Not Failed |
| W12*190 | moment frame-right column-7th floor | 12.7 | 1.74 | 1.1 | 14 | 55 | 3.641 | 14 | 1382 | 2844 | 0.49 | 2.281 | 2.95 | Failed |
| W12*190 | moment frame-left column-8th floor | 12.7 | 1.74 | 1.1 | 14 | 55 | 3.641 | 14 | 856 | 2844 | 0.3 | 5.980 | 2.1 | Not Failed |
| W12*190 | moment frame-middle column-8th floor | 12.7 | 1.74 | 1.1 | 14 | 55 | 3.641 | 14 | 1103 | 2844 | 0.39 | 4.243 | 0.53 | Not Failed |
| W12*190 | moment frame-right column-8th floor | 12.7 | 1.74 | 1.1 | 14 | 55 | 3.641 | 14 | 857 | 2844 | 0.3 | 5.973 | 2.1 | Not Failed |
| W12*106 | moment frame-left column-9th floor | 12.2 | 0.99 | 0.6 | 13 | 55 | 6.172 | 21 | 809 | 1578 | 0.51 | force controlled | 2.88 | Failed |
| W12*106 | moment frame-middle column-9th floor | 12.2 | 0.99 | 0.6 | 13 | 55 | 6.172 | 21 | 574 | 1578 | 0.36 | 4.725 | 0.61 | Not Failed |
| W12*106 | moment frame-right column-9th floor | 12.2 | 0.99 | 0.6 | 13 | 55 | 6.172 | 21 | 810 | 1578 | 0.51 | force controlled | 2.9 | Failed |
| W12*106 | moment frame-left column-10th floor | 12.2 | 0.99 | 0.6 | 13 | 55 | 6.172 | 21 | 47 | 1578 | 0.03 | 11.403 | 1.8 | Not Failed |
| W12*106 | moment frame-middle column-10th floor | 12.2 | 0.99 | 0.6 | 13 | 55 | 6.172 | 21 | 524 | 1578 | 0.33 | 5.359 | 0.8 | Not Failed |
| W12*106 | moment frame-right column-10th floor | 12.2 | 0.99 | 0.6 | 13 | 55 | 6.172 | 21 | 525 | 1578 | 0.33 | 5.346 | 1.8 | Not Failed |

A comparison between the first and second scenarios reveals that at higher levels bigger vertical displacement happens when a column from the same frame is removed. After demolishing the column from the ground floor, *U3* at joint 429 became 348 mm whereas at 6th level the *U3* for joint 424 is 405 *mm*. This shows

that as the number of stories above the removed column decrease, the potential for progressive collapse increases. The reason is that, as the number of stories and bays increased, a larger capacity to resist progressive collapse under axial loading is obtained. In this case, more elements would participate to resist against progressive collapse. The process of removing a column in the ground floor and in the $6^{th}$ floor indicates that this structure is quite susceptible to collapse for a column removal scenario. It means that despite the fact that the Original Structure designed based on AISC-LRFD regulations and based on AISC 14 Steel Design guide for STS structures, still the structure is vulnerable to progressive collapse when it was statically analyzed. To prevent progressive collapse happening, a new model was designed using stronger sections. The section redesign procedure was attributed to the columns, moment frame beams (spandrels) and truss chords. To find the appropriate sections for all elements, the design option in SAP2000 could be used. Design load combination must be defined in order to evaluate the acceptance criteria. For the retrofitted model, the LRFD load combination described in chapter 3 adopted plus a new load case which was the Nonlinear Static load case assigned to the Original model for its progressive collapse analysis. This new model is called "Retrofitted Model" from now on during this study. A summary of changed sections in retrofitted structure is shown in the Table 4.7.

### 4.5.2 Ground Floor and $6^{th}$ Floor Columns Were Removed from Retrofitted Model

After redesigning the model, several column removal scenarios were done to see the new structure's vulnerability against the progressive collapse.

Table 4.7: Section changes comparison between the Original and the Retrofitted models

| Section | Location | Level | Original Structure | Retrofitted Structure |
|---|---|---|---|---|
| Spandrel Beam | Moment Frame | 10 | W16*31 | W21*132 |
| Spandrel Beam | Moment Frame | 1&9 | W18*40 | W21*147 |
| Spandrel Beam | Moment Frame | 1 | W18*35 | W21*147 |
| Spandrel Beam | Moment Frame | 8,9 | W18*46 | W21*132 |
| Spandrel Beam | Moment Frame | 6,7,8 | W18*50 | W21*132 |
| Spandrel Beam | Moment Frame | 7 | W18*60 | W21*147 |
| Spandrel Beam | Moment Frame | 2,3,4,5 | W18*65 | W21*147 |
| Spandrel Beam | Moment Frame | 6 | W18*71 | W21*147 |
| Spandrel Beam | Moment Frame | 2,3,4,5 | W18*76 | W21*166 |
| Column | All Frames | 1 | W14*455 | W14*605 |
| Column | All Frames | 2 | W12*305 | W14*605 |
| Column | All Frames | 3 | W12*279 | W14*605 |
| Column | All Frames | 4 | W12*279 | W14*455 |
| Column | All Frames | 5 | W12*190 | W14*398 |
| Column | All Frames | 6 | W12*190 | W12*305 |
| Column | All Frames | 7 | W12*190 | W12*305 |
| Column | All Frames | 8 | W12*190 | W12*305 |
| Column | All Frames | 9 | W12*190 | W12*305 |
| Column | All Frames | 10 | W12*106 | W12*106 |
| Truss Chord | 1st & 5th Frames | 3,4,5,7,8 | W10*77 | W10*112 |
| Truss Chord | 1st Frame | 6 | W10*68 | W10*112 |
| Truss Chord | 1st Frame | 7 | W10*68 | W10*88 |
| Truss Chord | 1st Frame | 8 | W10*60 | W10*88 |
| Truss Chord | 1st Frame | 9,10 | W10*45 | W10*88 |
| Truss Chord | 5th Frame | 3,4 | W10*100 | W10*112 |
| Truss Chord | 5th Frame | 5,6 | W10*88 | W10*112 |
| Truss Chord | 5th Frame | 10 | W10*49 | W10*88 |

Accordingly, six different models regarding to the six column removal scenarios are developed. The columns which had to be removed were selected from 1$^{st}$ and 5$^{th}$ (middle) frames. The columns were located at ground floor, 6$^{th}$ floor (middle height) and at the 10$^{th}$ floor (top) of the structure.

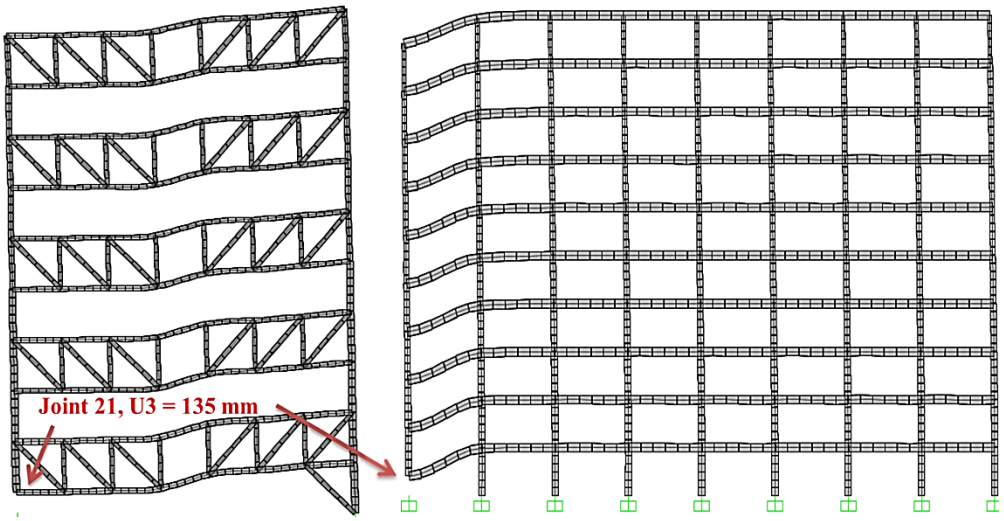


(a)

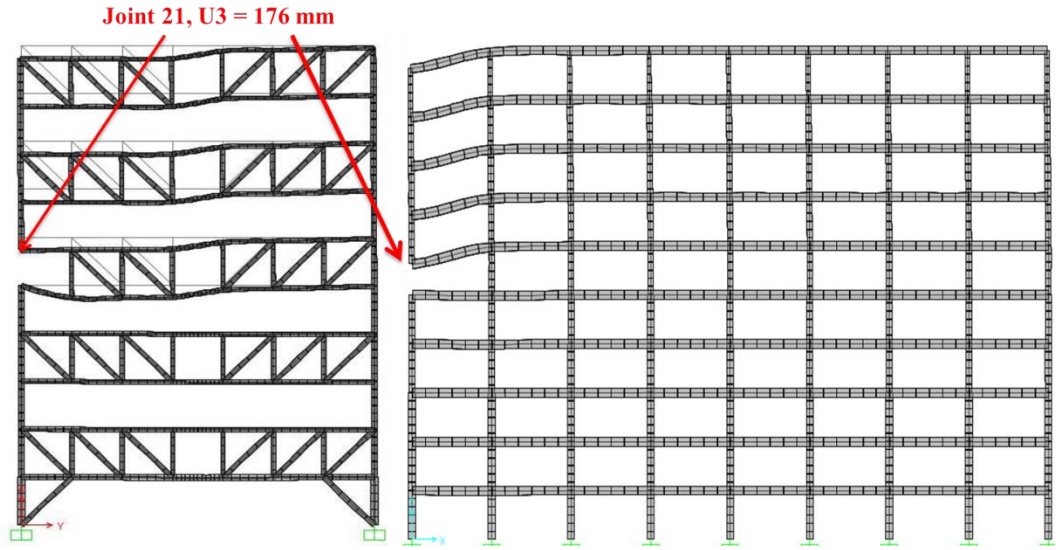


(b)

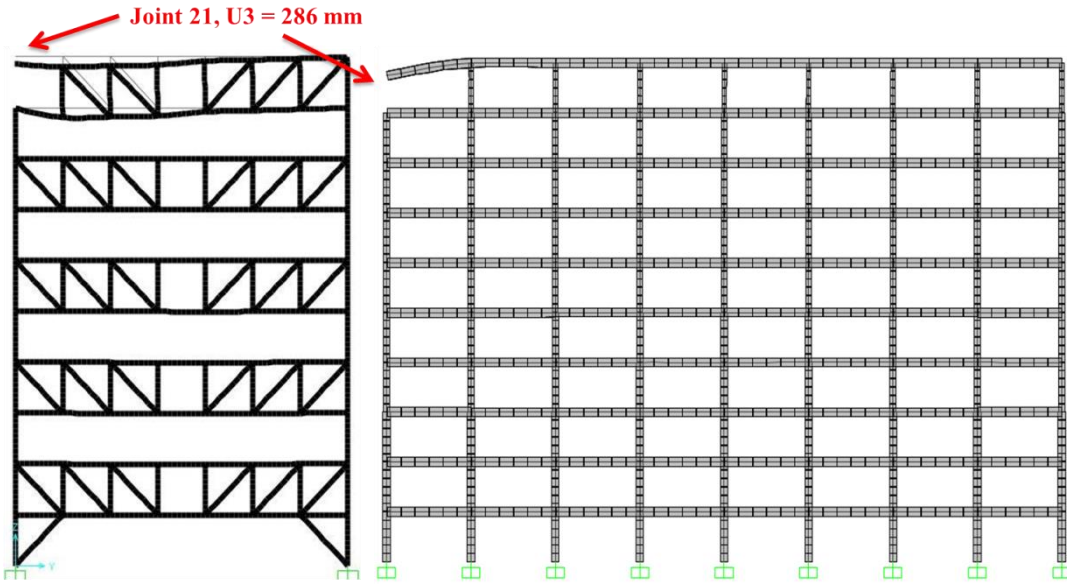


(c)

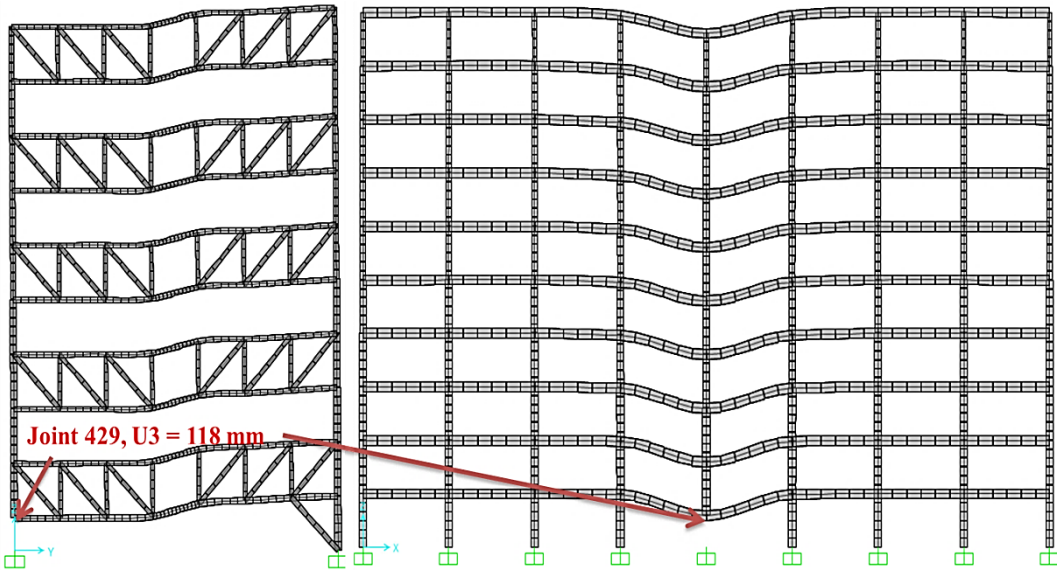


(d)

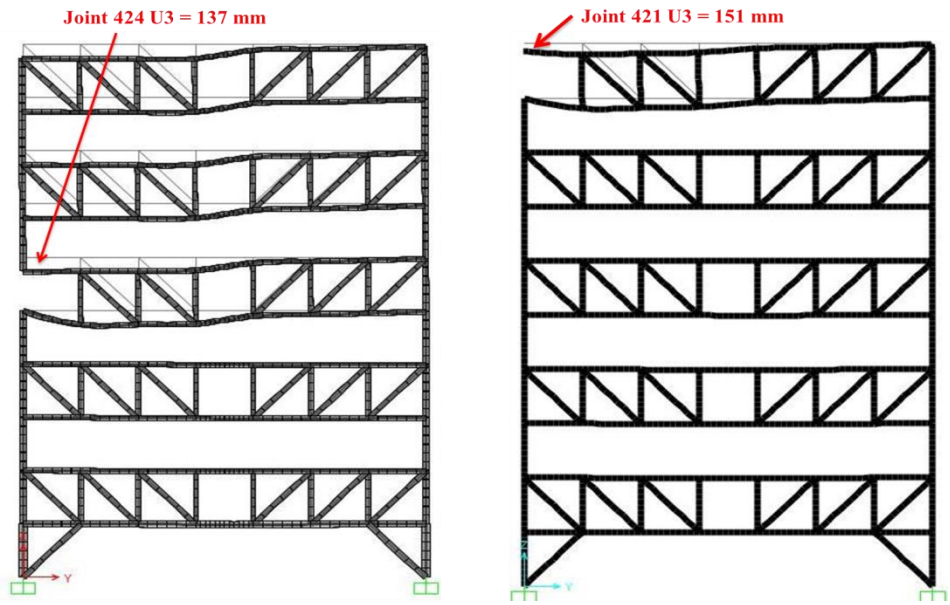


(e)

Figure 4.6: Column removal locations (5th frame) and their top joint settlement at Retrofitted Structure. (a): 1st frame ground floor - (b): 1st frame 6th floor -(c): 1st frame top floor- (d): 5th frame ground floor (e) 5th frame 6th floor

Table 4.8: Column properties of the Retrofitted structure after removing a column from first frame-ground floor

| section | Location | bf (in) | tf (in) | tw (in) | h (in) | Fye (ksi) | bf/2tf | h/tw | P (kip) | Pcl (kip) | P/Pcl | m-factors | DCR | Column Status |
|---|---|---|---|---|---|---|---|---|---|---|---|---|---|---|
| W14*605 | 1st floor-gridline A | 17.415 | 4.16 | 2.595 | 20.92 | 55 | 2.093 | 8.062 | 1529 | 9165.4 | 0.16682 | 8.000 | 0 | removed |
| W14*605 | 1st floor-gridline B | 17.415 | 4.16 | 2.595 | 20.92 | 55 | 2.093 | 8.062 | 2839 | 9165.4 | 0.30975 | 5.805 | 1.43 | Not Failed |
| W14*605 | 2nd floor-gridline A | 17.415 | 4.16 | 2.595 | 20.92 | 55 | 2.093 | 8.062 | 1497 | 9165.4 | 0.16333 | 8.000 | 0.69 | Not Failed |
| W14*605 | 2nd floor-gridline B | 17.415 | 4.16 | 2.595 | 20.92 | 55 | 2.093 | 8.062 | 2785 | 9165.4 | 0.30386 | 5.923 | 1.5 | Not Failed |
| W14*605 | 3rd floor-gridline A | 17.415 | 4.16 | 2.595 | 20.92 | 55 | 2.093 | 8.062 | 1376 | 9165.4 | 0.15013 | 8.000 | 0.5 | Not Failed |
| W14*605 | 3rd floor-gridline A | 17.415 | 4.16 | 2.595 | 20.92 | 55 | 2.093 | 8.062 | 2737 | 9165.4 | 0.29862 | 6.028 | 1.4 | Not Failed |
| w14*455 | 4th floor-gridline A | 16.835 | 3.21 | 2.015 | 19.02 | 55 | 2.622 | 9.439 | 1334 | 7010 | 0.1903 | 8.000 | 0.7 | Not Failed |
| w14*455 | 4th floor-gridline B | 16.835 | 3.21 | 2.015 | 19.02 | 55 | 2.622 | 9.439 | 1968 | 7010 | 0.28074 | 6.385 | 1.5 | Not Failed |
| W14*398 | 5th floor-gridline A | 16.59 | 2.845 | 1.77 | 18.29 | 55 | 2.916 | 10.333 | 1097 | 5907.3 | 0.1857 | 8.000 | 0.7 | Not Failed |
| W14*398 | 5th floor-gridline B | 16.59 | 2.845 | 1.77 | 18.29 | 55 | 2.916 | 10.333 | 1926 | 5907.3 | 0.32604 | 5.479 | 1.54 | Not Failed |
| W12*305 | 6th floor-gridline A | 13.235 | 2.705 | 1.625 | 16.32 | 55 | 2.446 | 10.043 | 986 | 4602 | 0.21425 | 7.715 | 0.96 | Not Failed |
| W12*305 | 6th floor-gridline B | 13.235 | 2.705 | 1.625 | 16.32 | 55 | 2.446 | 10.043 | 1402 | 4602 | 0.30465 | 5.907 | 1.68 | Not Failed |
| W12*305 | 7th floor-gridline A | 13.235 | 2.705 | 1.625 | 16.32 | 55 | 2.446 | 10.043 | 682 | 4602 | 0.1482 | 8.000 | 0.77 | Not Failed |
| W12*305 | 7th floor-gridline B | 13.235 | 2.705 | 1.625 | 16.32 | 55 | 2.446 | 10.043 | 1365 | 4602 | 0.29661 | 6.068 | 1.47 | Not Failed |
| W12*305 | 8th floor-gridline A | 13.235 | 2.705 | 1.625 | 16.32 | 55 | 2.446 | 10.043 | 639 | 4602 | 0.13885 | 8.000 | 0.84 | Not Failed |
| W12*305 | 8th floor-gridline B | 13.235 | 2.705 | 1.625 | 16.32 | 55 | 2.446 | 10.043 | 841 | 4602 | 0.18275 | 8.345 | 1.21 | Not Failed |
| W12*305 | 9th floor-gridline A | 13.235 | 2.705 | 1.625 | 16.32 | 55 | 2.446 | 10.043 | 333 | 4602 | 0.07236 | 10.553 | 0.7 | Not Failed |
| W12*305 | 9th floor-gridline B | 13.235 | 2.705 | 1.625 | 16.32 | 55 | 2.446 | 10.043 | 807 | 4602 | 0.17536 | 8.493 | 1.1 | Not Failed |
| W12*106 | 10th floor-gridline A | 13.235 | 2.705 | 1.625 | 16.32 | 55 | 2.446 | 10.043 | 293 | 1578 | 0.18568 | 8.000 | 1.74 | Not Failed |
| W12*106 | 10th floor-gridline B | 12.22 | 0.99 | 0.61 | 12.89 | 55 | 6.172 | 21.131 | 46 | 1578 | 0.02915 | 8.000 | 1.24 | Not Failed |

Table 4.9: Beam properties of the Retrofitted structure after removing a column from1ts frame-ground floor

| section | Location | h (in) | DCR (Mu/Mp) | Acceptance Criteria | Linear Static Result |
|---|---|---|---|---|---|
| W21*147 | moment frame-1st floor, left | 22.06 | 0.357 | 2.469 | Not Failed |
| W21*166 | moment frame-2nd floor,left | 22.48 | 0.332 | 2.777 | Not Failed |
| W21*166 | moment frame-3rd floor,left | 22.48 | 0.312 | 2.777 | Not Failed |
| W21*166 | moment frame-4th floor,left | 22.48 | 0.304 | 2.777 | Not Failed |
| W21*166 | moment frame-5th floor,left | 22.48 | 0.287 | 2.777 | Not Failed |
| W21*147 | moment frame-6th floor,left | 22.06 | 0.283 | 2.807 | Not Failed |
| W21*147 | moment frame-7th floor,left | 22.06 | 0.28 | 2.807 | Not Failed |
| W21*132 | moment frame-8th floor,left | 22.83 | 0.287 | 2.801 | Not Failed |
| W21*132 | moment frame-9th floor,left | 22.83 | 0.276 | 2.814 | Not Failed |
| W21*132 | moment frame-10th floor,left | 22.83 | 0.246 | 2.982 | Not Failed |
| W12*120 | staggered truss frame-1st floor | 13.12 | 0.189 | 4.333 | Not Failed |
| W10*106 | staggered truss frame-2nd floor | 12.89 | 0.194 | 3.230 | Not Failed |
| W10*112 | staggered truss frame-3rd floor | 11.36 | 0.149 | 4.694 | Not Failed |
| W10*112 | staggered truss frame-4th floor | 11.36 | 0.139 | 4.694 | Not Failed |
| W10*112 | staggered truss frame-5th floor | 11.36 | 0.144 | 4.640 | Not Failed |
| W10*88 | staggered truss frame-6th floor | 10.84 | 0.189 | 4.640 | Not Failed |
| W10*88 | staggered truss frame-7th floor | 10.84 | 0.186 | 4.666 | Not Failed |
| W10*88 | staggered truss frame-8th floor | 10.84 | 0.186 | 4.666 | Not Failed |
| W10*88 | staggered truss frame-9th floor | 10.84 | 0.141 | 4.732 | Not Failed |
| W10*88 | staggered truss frame-10th floor | 10.84 | 0.148 | 4.732 | Not Failed |

Table 4.10: Beam properties of the Retrofitted structure after removing a column from1st frame-6th floor

| section | Location | h (in) | DCR (Mu/Mp) | Acceptance Criteria | Linear Static Result |
|---|---|---|---|---|---|
| W21*166 | moment frame-5th floor,left | 22.48 | 0.231 | 2.777 | Not Failed |
| W21*147 | moment frame-6th floor,left | 22.06 | 2.6 | 2.807 | Not Failed |
| W21*147 | moment frame-7th floor,left | 22.06 | 2.77 | 2.807 | Not Failed |
| W21*132 | moment frame-8th floor,left | 22.83 | 2.79 | 2.801 | Not Failed |
| W21*132 | moment frame-9th floor,left | 22.83 | 2.46 | 2.814 | Not Failed |
| W21*132 | moment frame-10th floor,left | 22.83 | 1.54 | 2.982 | Not Failed |
| W10*112 | 1st staggered truss frame-5th floor | 11.36 | 2.92 | 4.640 | Not Failed |
| W10*88 | 1st staggered truss frame-6th floor | 10.84 | 1.16 | 4.640 | Not Failed |
| W10*88 | 1st staggered truss frame-7th floor | 10.84 | 1.56 | 4.666 | Not Failed |
| W10*88 | 1st staggered truss frame-8th floor | 10.84 | 1.44 | 4.666 | Not Failed |
| W10*88 | 1st ststaggered truss frame-9th floor | 10.84 | 1.26 | 4.732 | Not Failed |
| W10*88 | 1st staggered truss frame-10th floor | 10.84 | 1.14 | 4.732 | Not Failed |

Table 4.11: Beam and Column properties of the Retrofitted structure after removing a column from1st frame-top floor

| section | Location | h (in) | DCR (Mu/Mp) | Acceptance Criteria | Linear Static Result |
|---|---|---|---|---|---|
| Beam-W21*132 | moment frame-10th floor,left | 22.83 | 2.4 | 2.814 | Not Failed |
| Beam-W10*88 | staggered truss frame-10th floor | 10.84 | 1.76 | 4.730 | Not Failed |
| Beam-W10*88 | staggered truss frame-9th floor | 10.84 | 5.7 | 4.730 | Not Failed |
| Column-W12*106 | 10th floor,gridline B | 20.99 | 0.44 | 2.982 | Not Failed |

Table 4.12: Beam properties of the Retrofitted structure after removing a column from5th frame-1st floor

| section | Location | h (in) | DCR (Mu/Mp) | Acceptance Criteria | Linear Static Result |
|---|---|---|---|---|---|
| W21*147 | moment frame-1st floor, left | 21.62 | 2.64 | 2.770 | Not Failed |
| W21*147 | moment frame-1st floor, right | 21.62 | 2.64 | 2.770 | Not Failed |
| W21*147 | moment frame-2nd floor,left | 21.62 | 2.6 | 2.770 | Not Failed |
| W21*147 | moment frame-2nd floor,right | 21.62 | 2.6 | 2.770 | Not Failed |
| W21*147 | moment frame-3rd floor,left | 21.62 | 2.48 | 2.770 | Not Failed |
| W21*147 | moment frame-3rd floor,right | 21.62 | 2.48 | 2.770 | Not Failed |
| W21*147 | moment frame-4th floor,left | 21.62 | 2.36 | 2.770 | Not Failed |
| W21*147 | moment frame-4th floor,right | 21.62 | 2.36 | 2.770 | Not Failed |
| W21*147 | moment frame-5th floor,left | 21.62 | 2.14 | 2.770 | Not Failed |
| W21*147 | moment frame-5th floor,right | 21.62 | 2.14 | 2.770 | Not Failed |
| W21*132 | moment frame-6th floor,left | 22.83 | 2.1 | 2.814 | Not Failed |
| W21*132 | moment frame-6th floor,right | 22.83 | 2.1 | 2.814 | Not Failed |
| W21*132 | moment frame-7th floor,left | 22.83 | 2 | 2.814 | Not Failed |
| W21*132 | moment frame-7th floor,right | 22.83 | 2 | 2.814 | Not Failed |
| W21*132 | moment frame-8th floor,left | 22.83 | 2.05 | 2.814 | Not Failed |
| W21*132 | moment frame-8th floor,right | 22.83 | 2.05 | 2.814 | Not Failed |
| W21*132 | moment frame-9th floor,left | 22.83 | 1.95 | 2.814 | Not Failed |
| W21*132 | moment frame-9th floor,right | 22.83 | 1.95 | 2.814 | Not Failed |
| W21*132 | moment frame-10th floor,left | 22.83 | 1.72 | 2.814 | Not Failed |
| W21*132 | moment frame-10th floor,right | 22.83 | 1.7 | 2.814 | Not Failed |
| W12*152 | staggered truss frame-1st floor | 13.71 | 1.26 | 3.162 | Not Failed |
| W10*112 | staggered truss frame-2nd floor | 11.36 | 1.3 | 3.357 | Not Failed |
| W10*112 | staggered truss frame-3rd floor | 11.36 | 1.1 | 3.357 | Not Failed |
| W10*112 | staggered truss frame-4th floor | 11.36 | 1.11 | 3.357 | Not Failed |
| W10*112 | staggered truss frame-5th floor | 11.36 | 0.97 | 3.357 | Not Failed |
| W10*112 | staggered truss frame-6th floor | 11.36 | 1 | 3.357 | Not Failed |
| W10*112 | staggered truss frame-7th floor | 11.36 | 0.9 | 3.357 | Not Failed |
| W10*112 | staggered truss frame-8th floor | 11.36 | 0.922 | 3.357 | Not Failed |
| W10*88 | staggered truss frame-9th floor | 10.84 | 1.2 | 3.400 | Not Failed |
| W10*88 | staggered truss frame-10th floor | 10.84 | 1.23 | 3.400 | Not Failed |

Table 4.13: Column properties of the Retrofitted structure after removing a column from 5th frame- ground floor

| section | Location | bf (in) | tf (in) | tw (in) | h (in) | Fye (ksi) | bf/2tf | h/tw | P (kip) | Pcl (kip) | P/Pcl | m-factors | DCR | Column Status |
|---|---|---|---|---|---|---|---|---|---|---|---|---|---|---|
| W14*605 | 1st floor-left gridline | 17.4 | 4.16 | 2.6 | 21 | 55 | 2.093 | 8.06 | 2914 | 9165 | 0.32 | 5.641 | 1.35 | Not Failed |
| W14*605 | 1st floor-middle gridline | 17.4 | 4.16 | 2.6 | 21 | 55 | 2.093 | 8.06 | 2564 | 9165 | 0.28 | 6.405 | 0 | Removed |
| W14*605 | 1st floor-right gridline | 17.4 | 4.16 | 2.6 | 21 | 55 | 2.093 | 8.06 | 2914 | 9165 | 0.32 | 5.641 | 1.35 | Not Failed |
| W14*605 | 2nd floor-left gridline | 17.4 | 4.16 | 2.6 | 21 | 55 | 2.093 | 8.06 | 2860 | 9165 | 0.31 | 5.759 | 1.38 | Not Failed |
| W14*605 | 2nd floor-middle gridline | 17.4 | 4.16 | 2.6 | 21 | 55 | 2.093 | 8.06 | 2515 | 9165 | 0.27 | 6.512 | 0.1 | Not Failed |
| W14*605 | 2nd floor-right gridline | 17.4 | 4.16 | 2.6 | 21 | 55 | 2.093 | 8.06 | 2860 | 9165 | 0.31 | 5.759 | 1.4 | Not Failed |
| W14*605 | 3rd floor-left gridline | 17.4 | 4.16 | 2.6 | 21 | 55 | 2.093 | 8.06 | 2807 | 9165 | 0.31 | 5.875 | 1.3 | Not Failed |
| W14*605 | 3rd floor-middle gridline | 17.4 | 4.16 | 2.6 | 21 | 55 | 2.093 | 8.06 | 2364 | 9165 | 0.26 | 6.841 | 0.1 | Not Failed |
| W14*605 | 3rd floor-right gridline | 17.4 | 4.16 | 2.6 | 21 | 55 | 2.093 | 8.06 | 2808 | 9165 | 0.31 | 5.873 | 1.29 | Not Failed |
| W14*455 | 4th floor-left gridline | 16.8 | 3.21 | 2.02 | 19 | 55 | 2.622 | 9.44 | 2032 | 7010 | 0.29 | 6.203 | 1.36 | Not Failed |
| W14*455 | 4th floor-middle gridline | 16.8 | 3.21 | 2.02 | 19 | 55 | 2.622 | 9.44 | 2301 | 7010 | 0.33 | 5.435 | 0.154 | Not Failed |
| W14*455 | 4th floor-right gridline | 16.8 | 3.21 | 2.02 | 19 | 55 | 2.622 | 9.44 | 2032 | 7010 | 0.29 | 6.203 | 1.37 | Not Failed |
| W14*398 | 5th floor-left gridline | 16.6 | 2.85 | 1.77 | 18 | 55 | 2.916 | 10.3 | 1980 | 5907 | 0.34 | 5.296 | 1.5 | Not Failed |
| W14*398 | 5th floor-middle gridline | 16.6 | 2.85 | 1.77 | 18 | 55 | 2.916 | 10.3 | 1765 | 5907 | 0.3 | 6.024 | 0.11 | Not Failed |
| W14*398 | 5th floor-right gridline | 16.6 | 2.85 | 1.77 | 18 | 55 | 2.916 | 10.3 | 1980 | 5907 | 0.34 | 5.296 | 1.5 | Not Failed |
| W12*305 | 6th floor-left gridline | 13.2 | 2.71 | 1.63 | 16 | 55 | 2.446 | 10 | 1450 | 4602 | 0.32 | 5.698 | 1.52 | Not Failed |
| W12*305 | 6th floor-middle gridline | 13.2 | 2.71 | 1.63 | 16 | 55 | 2.446 | 10 | 1705 | 4602 | 0.37 | 4.590 | 0.4 | Not Failed |
| W12*305 | 6th floor-right gridline | 13.2 | 2.71 | 1.63 | 16 | 55 | 2.446 | 10 | 1450 | 4602 | 0.32 | 5.698 | 1.5 | Not Failed |
| W12*305 | 7th floor-left gridline | 13.2 | 2.71 | 1.63 | 16 | 55 | 2.446 | 10 | 1399 | 4602 | 0.3 | 5.920 | 1.43 | Not Failed |
| W12*305 | 7th floor-middle gridline | 13.2 | 2.71 | 1.63 | 16 | 55 | 2.446 | 10 | 1171 | 4602 | 0.25 | 6.911 | 0.123 | Not Failed |
| W12*305 | 7th floor-right gridline | 13.2 | 2.71 | 1.63 | 16 | 55 | 2.446 | 10 | 1399 | 4602 | 0.3 | 5.920 | 1.49 | Not Failed |
| W12*305 | 8th floor-left gridline | 13.2 | 2.71 | 1.63 | 16 | 55 | 2.446 | 10 | 870 | 4602 | 0.19 | 8.000 | 1.11 | Not Failed |
| W12*305 | 8th floor-middle gridline | 13.2 | 2.71 | 1.63 | 16 | 55 | 2.446 | 10 | 1114 | 4602 | 0.24 | 7.159 | 0.32 | Not Failed |
| W12*305 | 8th floor-right gridline | 13.2 | 2.71 | 1.63 | 16 | 55 | 2.446 | 10 | 870 | 4602 | 0.19 | 8.000 | 1.11 | Not Failed |
| W12*305 | 9th floor-left gridline | 13.2 | 2.71 | 1.63 | 16 | 55 | 2.446 | 10 | 821 | 4602 | 0.18 | 8.000 | 1.13 | Not Failed |
| W12*305 | 9th floor-middle gridline | 13.2 | 2.71 | 1.63 | 16 | 55 | 2.446 | 10 | 570 | 4602 | 0.12 | 8.000 | 0.1 | Not Failed |
| W12*305 | 9th floor-right gridline | 13.2 | 2.71 | 1.63 | 16 | 55 | 2.446 | 10 | 830 | 4602 | 0.18 | 8.000 | 1.127 | Not Failed |
| W12*106 | 10th floor-left gridline | 13.2 | 2.71 | 1.63 | 16 | 55 | 2.446 | 10 | 51 | 1578 | 0.03 | 8.000 | 1.44 | Not Failed |
| W12*106 | 10th floor-middle gridline | 13.2 | 2.71 | 1.63 | 16 | 55 | 2.446 | 10 | 525 | 1578 | 0.33 | 5.346 | 0.7 | Not Failed |
| W12*106 | 10th floor-right gridline | 12.2 | 0.99 | 0.61 | 13 | 55 | 6.172 | 21.1 | 51 | 1578 | 0.03 | 8.000 | 1.44 | Not Failed |

Table 4.14: Beam properties of the Retrofitted structure after removing a column from 5th frame- 6th floor

| section | Location | h (in) | DCR (Mu/Mp) | Acceptance Criteria | Linear Static Result |
|---|---|---|---|---|---|
| W21*147 | moment frame-5th floor,left | 21.83 | 0.29 | 2.770 | Not Failed |
| W21*132 | moment frame-5th floor,right | 21.83 | 0.29 | 2.800 | Not Failed |
| W21*132 | moment frame-6th floor,left | 21.83 | 2.57 | 2.800 | Not Failed |
| W21*132 | moment frame-6th floor,right | 21.83 | 2.58 | 2.800 | Not Failed |
| W21*132 | moment frame-7th floor,left | 21.83 | 2.52 | 2.800 | Not Failed |
| W21*132 | moment frame-7th floor,right | 21.83 | 2.52 | 2.800 | Not Failed |
| W21*132 | moment frame-8th floor,left | 21.83 | 2.48 | 2.800 | Not Failed |
| W21*132 | moment frame-8th floor,right | 21.83 | 2.48 | 2.800 | Not Failed |
| W21*132 | moment frame-9th floor,left | 21.83 | 2.36 | 2.800 | Not Failed |
| W21*132 | moment frame-9th floor,right | 21.83 | 2.36 | 2.800 | Not Failed |
| W21*132 | moment frame-10th floor,left | 21.83 | 2.1 | 2.800 | Not Failed |
| W21*132 | moment frame-10th floor,right | 21.83 | 2.1 | 2.800 | Not Failed |
| W10*112 | staggered truss frame-5th floor | 11.36 | 2.71 | 3.357 | Not Failed |
| W10*112 | staggered truss frame-6th floor | 11.36 | 1.25 | 3.357 | Not Failed |
| W10*112 | staggered truss frame-7th floor | 11.36 | 1.19 | 3.357 | Not Failed |
| W10*112 | staggered truss frame-8th floor | 11.36 | 1.15 | 3.357 | Not Failed |
| W10*88 | staggered truss frame-9th floor | 10.84 | 1.5 | 3.400 | Not Failed |
| W10*88 | staggered truss frame-10th floor | 10.84 | 1.5 | 3.400 | Not Failed |

Table 4.15: Column properties of the Retrofitted structure after removing a column from 5th frame- 6th floor

| section | Location | bf (in) | tf (in) | tw (in) | h (in) | Fye (ksi) | bf/2tf | h/tw | P (kip) | Pcl (kip) | P/Pcl | m-factors | DCR | Column Status |
|---|---|---|---|---|---|---|---|---|---|---|---|---|---|---|
| W12*305 | 6th floor-left gridline | 13.2 | 2.705 | 1.625 | 16.3 | 55 | 2.446 | 10.04 | 1450 | 4602 | 0.32 | 5.698 | 1.6 | Not Failed |
| W12*305 | 6th floor-middle gridline | 13.2 | 2.705 | 1.625 | 16.3 | 55 | 2.446 | 10.04 | 1705 | 4602 | 0.37 | 4.590 | 0 | Removed |
| W12*305 | 6th floor-right gridline | 13.2 | 2.705 | 1.625 | 16.3 | 55 | 2.446 | 10.04 | 1450 | 4602 | 0.32 | 5.698 | 1.6 | Not Failed |
| W12*305 | 7th floor-left gridline | 13.2 | 2.705 | 1.625 | 16.3 | 55 | 2.446 | 10.04 | 1399 | 4602 | 0.3 | 5.920 | 1.7 | Not Failed |
| W12*305 | 7th floor-middle gridline | 13.2 | 2.705 | 1.625 | 16.3 | 55 | 2.446 | 10.04 | 1171 | 4602 | 0.25 | 6.911 | 0.7 | Not Failed |
| W12*305 | 7th floor-right gridline | 13.2 | 2.705 | 1.625 | 16.3 | 55 | 2.446 | 10.04 | 1399 | 4602 | 0.3 | 5.920 | 1.7 | Not Failed |
| W12*305 | 8th floor-left gridline | 13.2 | 2.705 | 1.625 | 16.3 | 55 | 2.446 | 10.04 | 870 | 4602 | 0.19 | 8.000 | 1.24 | Not Failed |
| W12*305 | 8th floor-middle gridline | 13.2 | 2.705 | 1.625 | 16.3 | 55 | 2.446 | 10.04 | 1114 | 4602 | 0.24 | 7.159 | 0.13 | Not Failed |
| W12*305 | 8th floor-right gridline | 13.2 | 2.705 | 1.625 | 16.3 | 55 | 2.446 | 10.04 | 870 | 4602 | 0.19 | 8.000 | 1.24 | Not Failed |
| W12*305 | 9th floor-left gridline | 13.2 | 2.705 | 1.625 | 16.3 | 55 | 2.446 | 10.04 | 821 | 4602 | 0.18 | 8.000 | 1.25 | Not Failed |
| W12*305 | 9th floor-middle gridline | 13.2 | 2.705 | 1.625 | 16.3 | 55 | 2.446 | 10.04 | 570 | 4602 | 0.12 | 8.000 | 0.06 | Not Failed |
| W12*305 | 9th floor-right gridline | 13.2 | 2.705 | 1.625 | 16.3 | 55 | 2.446 | 10.04 | 830 | 4602 | 0.18 | 8.000 | 1.25 | Not Failed |
| W12*106 | 10th floor-left gridline | 13.2 | 2.705 | 1.625 | 16.3 | 55 | 2.446 | 10.04 | 51 | 1578 | 0.03 | 8.000 | 1.65 | Not Failed |
| W12*106 | 10th floor-middle gridline | 13.2 | 2.705 | 1.625 | 16.3 | 55 | 2.446 | 10.04 | 525 | 1578 | 0.33 | 5.346 | 0.6 | Not Failed |
| W12*106 | 10th floor-right gridline | 12.2 | 0.99 | 0.61 | 12.9 | 55 | 6.172 | 21.13 | 51 | 1578 | 0.03 | 8.000 | 1.62 | Not Failed |

Table 4.16: Beam and Column properties of the Retrofitted structure after removing a column from 5th frame- top floor

| section | Location | h (in) | DCR (Mu/Mp) | Acceptance Criteria | Linear Static Result |
|---|---|---|---|---|---|
| Beam-W21*132 | moment frame-10th floor,left | 22.83 | 2.57 | 2.814 | Not Failed |
| Beam-W21*132 | moment frame-10th floor,rigth | 22.83 | 2.57 | 2.814 | Not Failed |
| Beam-W10*88 | staggered truss frame-10th floor | 10.84 | 3.3 | 4.730 | Not Failed |
| Beam-W10*88 | staggered truss frame-9th floor | 10.84 | 1.96 | 4.730 | Not Failed |
| Column-W12*106 | 10th floor-left gridline | 20.99 | 1.17 | 2.982 | Not Failed |
| Column-W12*106 | 10th floor-middle gridline | 20.99 | 0 | 2.982 | Removed |
| Column-W12*106 | 10th floor-right gridline | 20.99 | 1.17 | 2.982 | Not Failed |

Tables 4.8 to 4.16, show the column and beam properties for Retrofitted Model after removing several columns. As previously mentioned, the new model was designed against failure mechanism due to column loss. LSA showed no failures in the new model and the structure remained stable after removing the columns. Therefore, for the new retrofitted model there is not any progressive collapse potential after removing a column from structural system.

## 4.6 Structural Response

### 4.6.1 Elastic Moment and Axial Load Distribution

In this section, structural response to the shocks resulted from bending moment and axial load increases will be investigated. The phase consists of comparing internal force diagrams in Moment frames and Staggered Truss frames before and after demolishing a column. The values of internal forces (bending moments and axial forces) are increased drastically in sections directly above the demolished column. For this study 12 column removal scenarios were studied in the Original and the Retrofitted model. However due to intense information resulted from all column removal scenarios, one scenario was selected to investigate the structural

response in full detail. The column removal location was selected from middle frame 6$^{th}$ floor.

#### 4.6.1.1 Bending Moment Distribution after a central column removal from 6$^{th}$ floor

Figures 4.7 to 4.10 show the bending moment distribution in both the original and the retrofitted model. The bending moment diagrams are illustrated at moment frames and Staggered Truss frames for two phases of before and after removing the column. In the moment frame direction, only the elements neighboring to the removed column was illustrated. The reason behind is that the changes in the forces led the sections to fail.

In the Original model (before removing the column), the 6$^{th}$ floor beams (beams above the column removal) had a maximum bending moment equal to $M_{max}$= -150 *kN.m* (Figure 4.7 left). After removing the column, the maximum bending moment in these beams increased to 3964 *kN.m* which shows a considerable increase in the bending moment in the moment frames (Figure 4.7- right). Unlike the beams above the removed column, beams located beneath the removal location showed minor changes in bending moments after removing of the column. In table 4.5 all beam properties for this level are monitored and it is shown that the beams have failed after absorbing the shock resulted from such a load increase. For upper beams, the percentage decreases only 2 floors above the removed column level. But based on Acceptance criteria and the DCR ratios calculated and shown in table 4.5 and 4.6 all beams and some columns have failed.

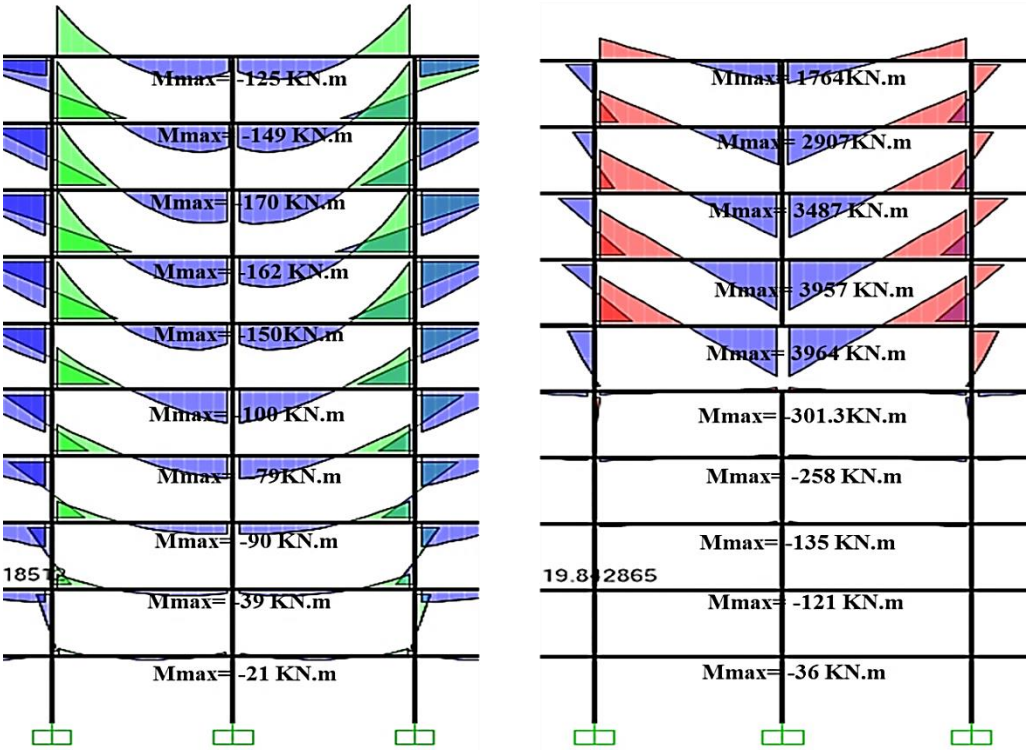


Figure 4.7: Elastic Bending Moment Distribution in Moment frame in the Original Model (left: before removing the column - right: after removing the column)

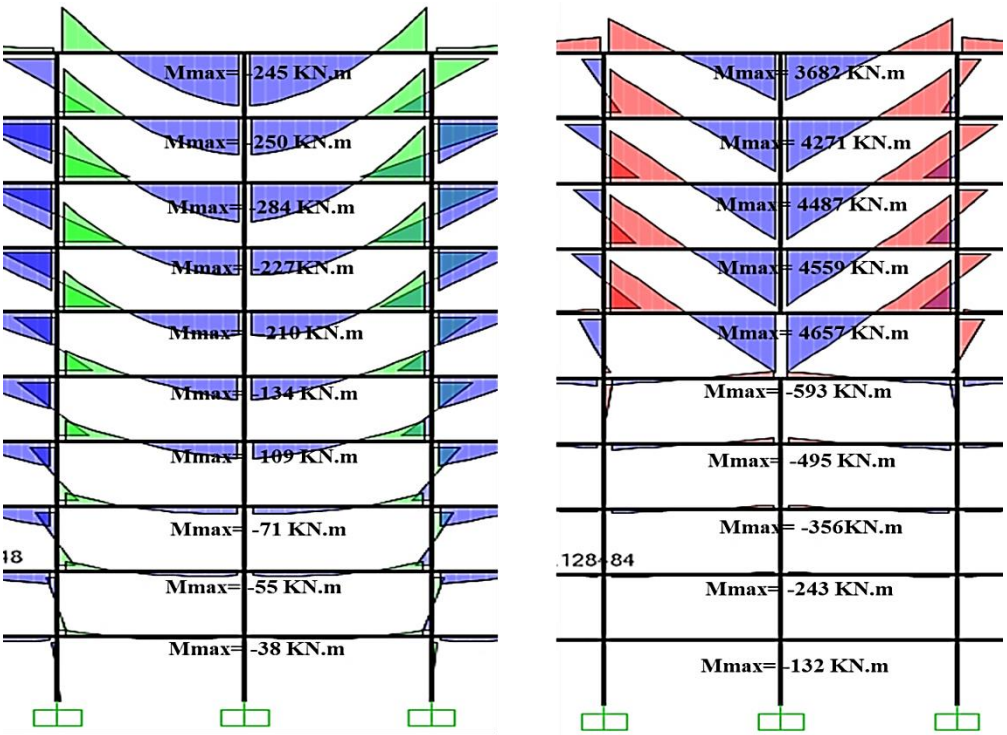


Figure 4.8: Elastic Bending Moment Distribution in Moment frame in the Retrofitted Model (left: before removing the column - right: after removing the column

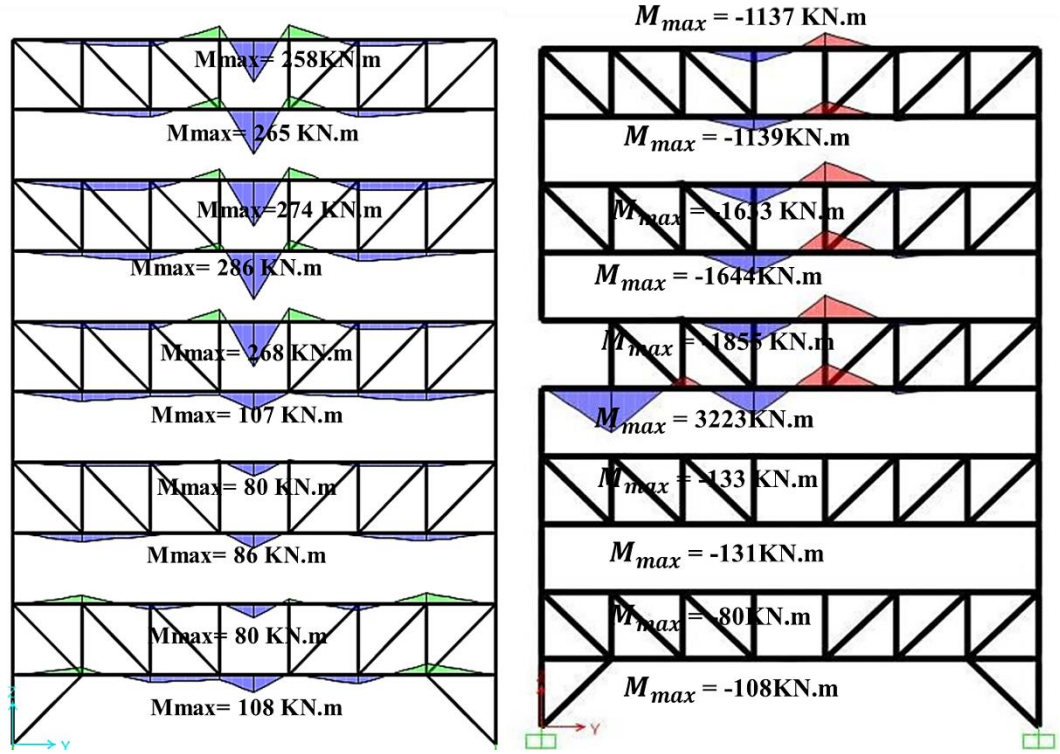


Figure 4.9: Elastic Bending Moment Distribution in Staggered Truss frame in the Original Model (left: before removing the column - right: after removing the column)

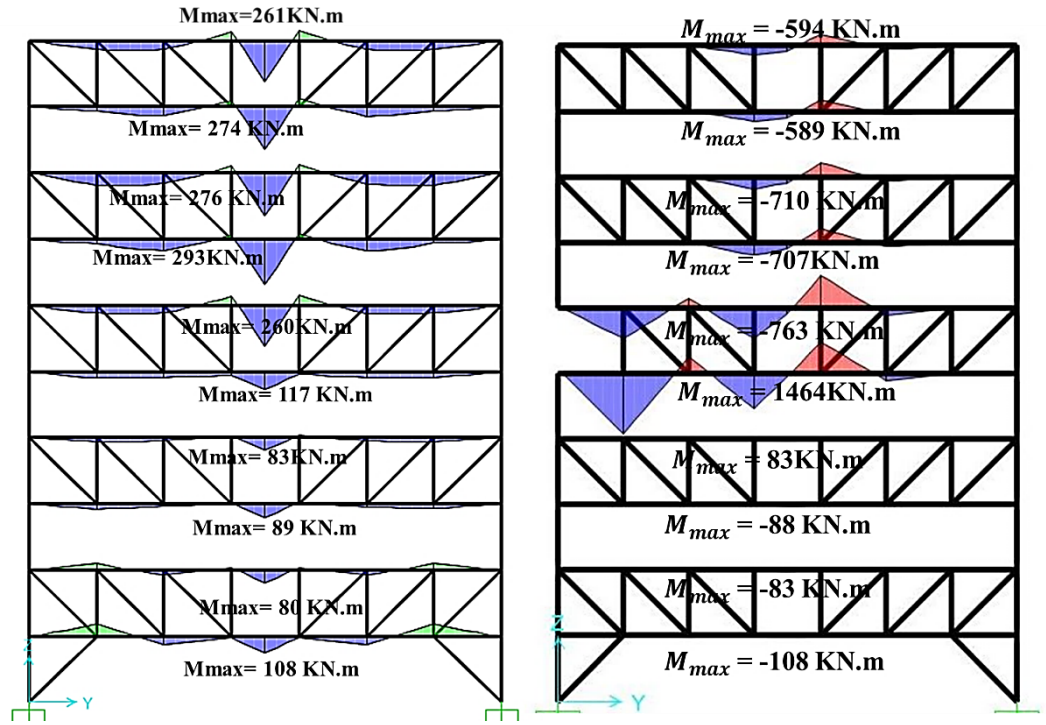


Figure 4.10: Elastic Bending Moment Distribution in Staggered Truss frame in the Retrofitted Model (left: before removing the column - right: after removing the column)

Similarly, truss chords faced the same bending moment increase occurrence for beams neighboring the removal location. For instance in the 5$^{th}$ floor chord which is located directly below the column, the $\boldsymbol{M_{max}}$ increased to 3223 *kN.m* from its previous value 107 *kN.m*. The 6th floor chord directly above the removed column had even a considerable amount of increase (Figure 4.9) from 268 *kN.m* to -1855 *kN*.m, although it was less than the below chord.

For the Retrofitted model, the bending moments in moment frame direction are bigger in comparison to the Original model. Despite these bigger forces, the beams and chords have not failed due to stronger cross- sections. In the Staggered Truss direction, the bending moments are almost the same with the Original model before removing the column. By contrast, after removing the column they were bigger in the Original model. For instance, the 5$^{th}$ floor chord in the Original model has $\boldsymbol{M_{max}}$ = 3223 *kN.m* whereas the same chord in the Retrofitted model has $\boldsymbol{M_{max}}$ = 1464 *kN.m*. The main reason for this load decrease in the second model is that, after strengthening the Spandrels in the moment frame direction they were able to withstand more against distributed loads after removal of the column. In this case the majority of the redundant loads will be transmitted toward moment frame instead of the trusses. Therefore the moment frame beams are a priority concern for Progressive collapse Design rather than the truss chords in spite of their shorter lengths.

Except the truss located between 5$^{th}$ and 6$^{th}$ floors, in all models the lower truss chords have bigger maximum bending moment. This can lead to a higher yield potential for those chords. To evaluate the yield position of a chord, the maximum

bending moment ($\boldsymbol{M_{max}}$) should be compared to the Ultimate Moment Capacity ($M_p$) [27].

Where $\mathbf{M_p = F_Y \cdot Z}$ (4.7)

$M_p$: Ultimate Moment Capacity (Plastic Moment)

Z: Plastic Modulus

$F_Y$: Yield Strength

Regarding equation 4.7, the Table 4.17 was built to investigate the yield happening process in the truss chords after removing the column. It can be seen that all maximum moments in chords were bigger than their calculated ultimate capacity. In this case the section had to be replaced by a stronger one in order to increase the resistance capacity of the zone close to bearing elements loses. However, in some cases the software analysis showed yield for some chords with $M_{max} < M_p$. In these cases, it could be concluded that, the section has been yielded before reaching its ultimate capacity due to local buckling of flange or web. The AISC 14 guideline [8] suggests using longitudinal stiffeners on the flange of-

Table 4.17: Yielded chords in the Original Model after removing the column from the middle frame 6th floor

| **Section** | **Location** | **Fy** (Yield Strength) kN/m² | **Z** (Plastic Modulus) m³ | **M**max (kN.m) | **Mp=Fy.Z** (kN.m) | **Condition** | **Replaced Section in the Retrofitted Model** |
|---|---|---|---|---|---|---|---|
| W10*88 | Original Model-5th floor Chord | 344738 | 1.85E-03 | 3223 | 638.45 | Yielded | W10*112 |
| W10*88 | Original Model-6th floor Chord | 344738 | 1.85E-03 | 1855 | 638.45 | Yielded | W10*112 |
| W10*77 | Original Model-7th floor Chord | 344738 | 1.60E-03 | 1644 | 551.24 | Yielded | W10*112 |
| W10*77 | Original Model-8th floor Chord | 344738 | 1.60E-03 | 1634 | 551.24 | Yielded | W10*112 |
| W10*49 | Original Model-9th floor Chord | 344738 | 9.90E-04 | 1139 | 341.22 | Yielded | W10*88 |
| W10*49 | Original Model-10th floor Chord | 344738 | 9.90E-04 | 1137 | 341.22 | Yielded | W10*88 |

chords to reinforce them against local buckling. This would prevent from uneconomical section upgrades when the yielded section has not reached to its ultimate capacity.

#### 4.6.1.2 Axial Load Transfer Mechanism in Trusses and Columns After a Central Column Removal From 6$^{th}$ Floor

The axial loads in the columns close to the removed column increased rapidly after the column removal. However, the axial loads were decreased for the columns above the removed column location. For instance the axial load of the 7$^{th}$ floor column above the removed column (6$^{th}$ floor) was -13313 *kN*. After removal of the column, the axial load decreased to -2015 *kN* which is a considerable decrease. This indicates that after removing the 6$^{th}$ floor column, there was not any element to transfer the axial load to the lower elements and therefore the columns above the removal grade are suspended over by their attached beams.

Figures 4.11 and 4.12, shows the axial load distribution in truss diagonals before and after removing the column. By dividing the Staggered Truss frame into 4 zones, it was noticed that different load distributions have occurred after that the column was cut off.

In both structures, the diagonals at zone 1 are in tension and verticals are in compression. The axial load in these members has decreased after removing the column. By contrast the axial load at zone 2 in truss members was increased and both the diagonals and verticals had bigger axial load values after removing the column. Zone 3 and 4 had reverse conditions where the axial load in zone 3 was increased and in zone 4 was decreased after the corner column removal.

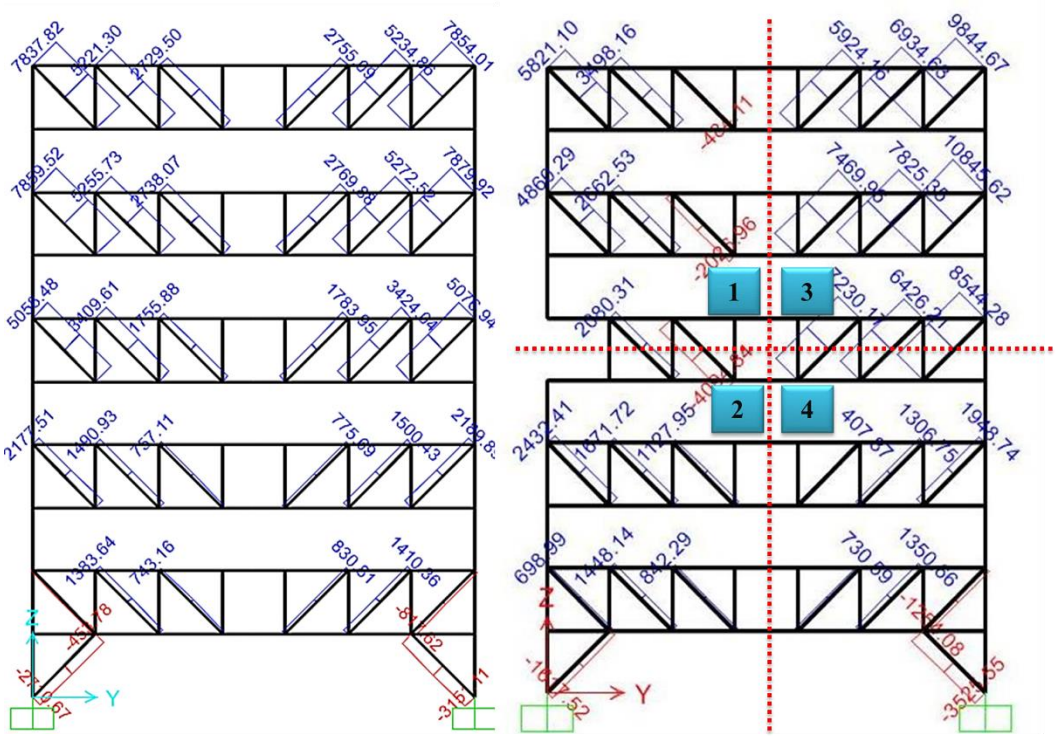


Figure 4.11: Axial load distribution in the Original Structure

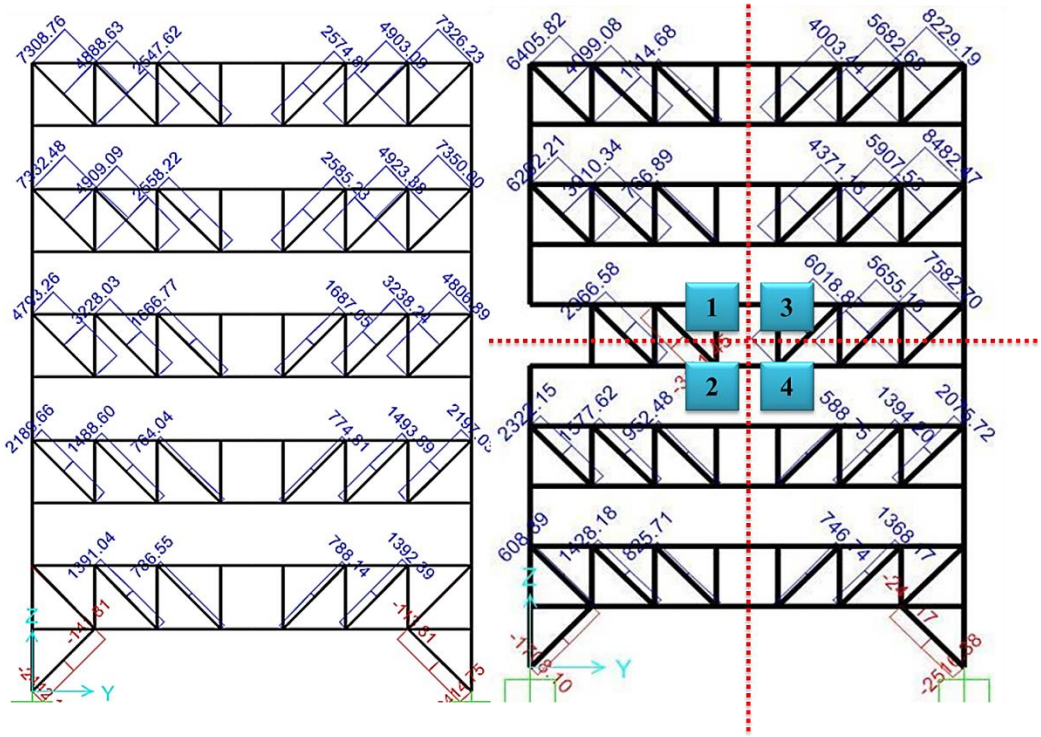


Figure 4.12: Axial load distribution in the Retrofitted Structure

This shows that the force flow was from zones 1 and 4 to zones 2 and 3. It could be seen that the ground floor braces are in compression and even the first diagonal at first floor level close to these brace is in compression. But this diagonal had tensile force after removing the column.

### 4.6.2 Truss Behavior and Deformation

For the normal beams, deflection is mainly caused by bending and the effect of axial and shear forces can be neglected. However, the shear deformation of trusses resulting from the axial load deformation of web members cannot be neglected [21]. After removing a column, the vertical displacements of the points located directly above the removed column and at the top floor were observed and are illustrated in Table 4.18.

Table 4.18: Vertical Displacements of the Retrofitted model

| Column Removal Location | U3 at Top Point of the Removed Column (mm) | U3 at Top Floor (mm) |
|---|---|---|
| First Frame-First Floor | -135 | -141 |
| First Frame-Sixth Floor | -175.5 | -178 |
| First Frame-Top Floor | -286 | -286 |
| Fifth Frame-First Floor | -118 | -126 |
| Fifth Frame-Sixth Floor | -137 | -140 |
| Fifth Frame-Top Floor | -151 | -151 |

It is obvious that, the vertical deflection *U3* increases at higher levels and the overall deflection of the corner frame is bigger than that of the middle frame. The reason for bigger deflections at higher levels and at corner frame is that, there are less structural elements involved in progressive collapse resistance at these levels.

Figure 4.13 compares the deflection of truss located between 5th and 6th floor in both structures. The vertical deflections in the original truss are much greater than that in the retrofitted model. In the retrofitted model, the greatest deflections are occurred between 6th and 7th floor truss members where the vierendeel opening is located. Therefore the maximum deflection normally happens around the vierendeel openings and the linear static analysis showed that this zone has the most vulnerability potential in staggered truss systems against vertical and lateral deflections.

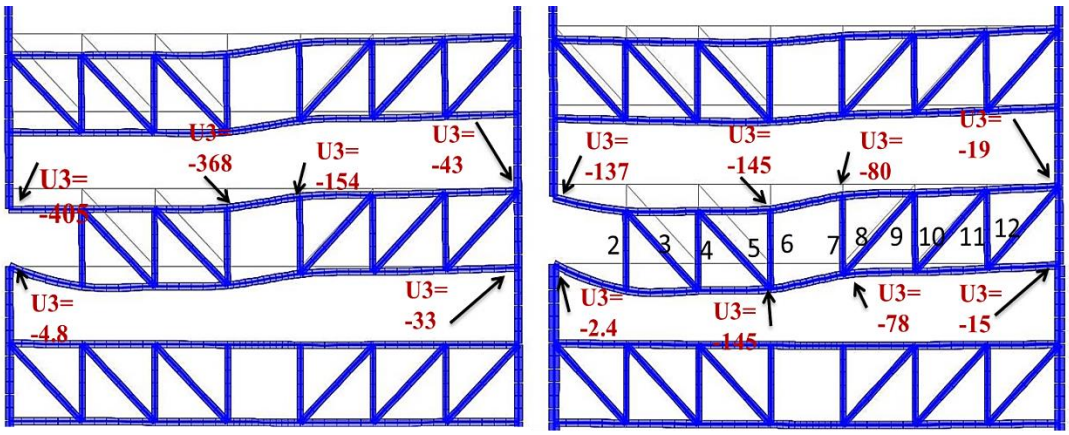


*Original Structure*

*Retrofitted Structure*

Figure 4.13: Cross section of 5th frame in both structures with middle truss deflections presented

Because the chords are continues members, they transmit the bending moments [8] and these bending moments are the main reason for chord deflection. The typical staggered–truss geometry is that of a Pratt truss with diagonal members intentionally arranged to be in tension when gravity loads are applied [8]. These truss members connect up and bottom chords and make the whole system very stiff against axial loads affecting them. The truss members will not get the axial

loads until the chords start to deform. When for example the upper chord deflects, it transmits the axial load to the diagonals and verticals, therefore the main load carrying members in these trusses are continues chords. This can be considered as the main reason of different axial load distributions in the 4 zones of staggered truss frame described in previous section.

The axial load in truss members at zone 1 of the Original structure are more than Retrofitted structure (Figure 4.13). In the first structure, the *W10×88* section was used as truss chord section whereas in the second structure it is upgraded to *W10×112*. The bigger deflection of *W10×88* section in comparison with the *W10×112*, leads to more axial load transmission through diagonals and verticals at this zone for the Original structure, therefore they have bigger axial loads.

The truss member number 12 has the greatest axial load among truss members before removing the column. After removing the column, the member number 12 had the greatest axial load. Therefore the truss member number 12 is the most critical truss member before and after removing the column. Considering the force flows in the trusses, for designing the truss members against both the axial loads and the progressive collapse resistance, they should have the same dimensions equal to the most critical member. In the Original model, none of the truss members were yielded after removing different columns. The main reason is that, the sections for these members were selected based on the most critical load situation in truss members and none of them have reached to its ultimate capacity.

# Chapter 5

# NONLINEAR DYNAMIC TIME HISTORY PROCEDURE IN PROGRESSIVE COLLAPSE CASE STUDY

## 5.1 Introduction

In this chapter the whole process which should be used to perform a Nonlinear Dynamic Analysis for progressive collapse potential in a structure in general will be introduced. This includes geometric and material nonlinearity considerations both in theoretical concept and its application in SAP2000 software. This chapter can also be used as an introduction to the next chapter (chapter 6).It describes, how a designer can use SAP2000 loading options to perform a Time-History Analysis against progressive collapse. To qualify a building's performance due to a sudden removal of one or more structural members, progressive collapse analysis is used. The sudden removal usually takes place in a short period of time, with high local strain rates [22]. After the key element has been removed, for example a column, the structure begins to deflect dynamically while the strain rates are almost similar to an earthquake. Figure 5.1 shows a typical column removal scenario in a simple frame which is under a constant distributed gravity load. As shown in Figure 5.1 (a), the frame has three columns and when the center column is in place, it exerts an upward load on the above beam. This upward load is the column resistance against the gravity load. However, after removing the

center column, this load will be replaced by a downward load resulting from distributed gravity load as shown in figure 5.1(b).

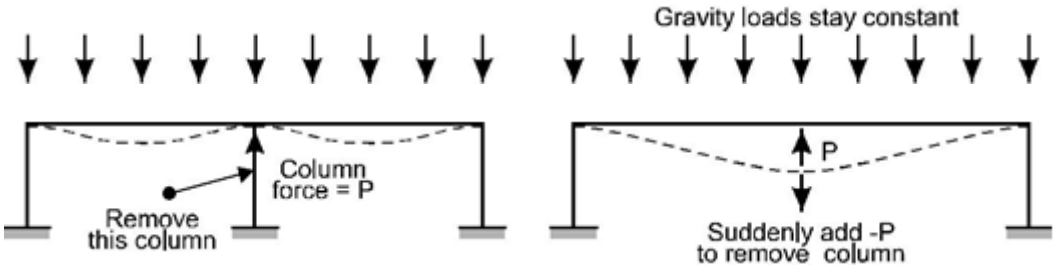


Figure 5.1: Progressive Collapse Behaviors

(a) Frame in normal state. (b) Sudden Column Removal

There are four methods to assess the progressive collapse in a building: Linear Static Procedure (LSP), Nonlinear Static Procedure (NSP), Linear Dynamic Procedure (LDP) and Nonlinear Dynamic Procedure (NDP). Among these methods the linear static procedure is the simplest and the most economical way to analyze a progressive collapse. But in many cases a linear static procedure cannot estimate the maximum deflections resulting from a structural removal case and a nonlinear analysis seems to be essential. UFC 2013 [2] proposes two methods for designing against the progressive collapse:

1- Tie Force Method: In this approach, the structure components are assumed to mechanically tie together. There are three horizontal ties that must be delivered: longitudinal, transverse and peripheral [2]. The vertical ties are essential in bearing walls plus columns.
2- Alternate Path Method: This method uses structural analysis in both linear and nonlinear conditions. Actually this method follows the LRFD [4] philosophy and ASCE 7 load factors. The procedure follows the general approach in ASCE 41 [7] with modifications to accommodate the

particular issues associated with progressive collapse. The gridlines generally recommend this method. In this approach, the structure will be designed in such a way that if one component fails, alternate paths exist for the loads to prevent total collapse [18].

In nonlinear cases the maximum deflection depends on load-deflection curve. This maximum displacement depends on the nonlinear behavior of the structure and how the structure will absorb the distributed energy produced from a column removal.

The amount of energy that can be absorbed by the structure depends on its yield strength, strain hardening behavior and ductile capacity, and on whether there are any catenary effects [23]. Ductility, defined as the ratio of ultimate displacement to yield displacement. The ductility ratio increases when the corner columns are removed. Also the ductility ratio decrease when the number of stories increases [23].

If nonlinear analysis for progressive collapse is required, both material nonlinear aspects and structural geometry nonlinearity aspects should be considered. The strength, initial stiffness, strain hardening and interaction effects such as P-M interaction in columns are importance when nonlinear analyses are carried out. In earthquake analysis, the lateral load resisting system is of most concern and floor diaphragms are considered as secondary systems. By contrast in a progressive collapse analysis, the gravity load and gravity load resisting systems including slabs are of most concern and earthquake resisting components are not as important as perpendicular load resisting components. Therefore the importance

of structural slabs in a nonlinear progressive collapse is inevitable. It may also be necessary to model nonlinear composite action between slabs and beams [23, 24]. This is very difficult to accomplish in earthquake analysis, because the shape of hysteric loops due to cyclic loading should be considered. But these are less important in collapse analysis. Because in this case we just need the maximum deflection which occurs at one cycle of vertical motion and cyclic deformation effects are less important [2].

## 5.2 Catenary and Membrane Effects

The definition of catenary goes to a cable or a chain which is hanged from its both ends. This especially happens in suspended bridges where strong cables are hanging from piers. The cable transfers the gravity loads to the ending columns and simultaneously holds them and increases their stiffness. Therefore catenary effect means that the member takes the u shape of a deformed cable. In some cases of progressive collapse analysis with SAP2000 software, significant deformations could be seen in structural elements above removed column. This made the analysis trend more time consuming and the results were critical. That means, incidentally, that SAP2000 had predicted collapse for the analysis model. But that does not necessarily mean that the actual structure will collapse, or that an analysis of the same structure with a different computer program will predict collapse. The reason is that this type of analysis is very sensitive to the assumed strengths and ductile capacities of the structural components, and to how the designer accounts for the Catenary Effect. If a series of models with progressively increasing strength were analyzed, it could be found that there is one strength where the analysis predicts collapse and a slightly larger strength where the analysis predicts little damage. The reason behind is due to the energy

considerations and catenary effects in a structure. Catenary effect relates to large displacements in the model and to investigate its effect, in this way the model can be analyzed with different strengths. This important issue has direct influence on slab/shell design of the model, because concrete slabs develop membrane and catenary actions. Therefore, the slab designing section is complex and each kind of slabs will result in different findings. One way to design a slab is to use a one-way shell type element, which is more accurate but more complex [24].

## 5.3 Analytical Modeling

To analyze and assess a structure with alternate path method, a 3D model should be established. Two dimensional models are not permitted due to lack of accuracy to predict membrane and catenary effects [2]. Note that UFC 2013 [2] categorizes the structural members to Deformation-Controlled and Force-Controlled members.

a. Deformation Controlled Actions: when the primary and secondary elements have surpassed the deformation capacities more than the full calculated deformation demands, then they will be measured as Deformation Controlled Members [2].
b. Force-Controlled Actions: Force controlled actions in all primary and secondary elements would be assessed based on equation 5.1 :

$$\boldsymbol{\Phi Q_{CL} \geq Q_{UF}} \tag{5.1}$$

where,

$Q_{UF}$= Force-Controlled action from nonlinear dynamic model.

$Q_{CL}$= Lower-bound strength of a component.

Φ = Strength reduction factor should be calculated from ASCE 41, chapter 5 through 8 [4].

The model will first be tested for perpendicular loads and will be designed against earthquake loads according to the relevant codes. In this study, as discussed in chapter 3, the UBC 97 code was used for designing against earthquake. In this case the model will resemble a true conventional building. After designing the model, sudden component removal scenarios could be done either with a linear or with a nonlinear procedure. But the fundamental difference between these two methods is that, in nonlinear dynamic method the inelastic behavior and geometric nonlinearities are taken into account. Therefore while modeling the prototype with SAP2000; it is necessary to define steel and concrete nonlinear specifications including steel section's yield stress and ultimate stress. In this study yield stress of steel sections $F_y$ = 345 $N/mm^2$ and tensile stress $F_u$ = 450 $N/mm^2$ were used. All steel and concrete stress strain data have been described in chapter 3.

The most important aspect of a nonlinear analysis is the plastic hinge definitions. All plastic hinge calculations for columns, truss members and braces were discussed in chapter 3. In SAP2000, the plastic hinge behavior is defined by a piece-wise linear moment-plastic rotation relationship [24]. Figures 5.2-(a) and 5.2- (b) show plastic hinge diagrams of a beam and a truss member respectively. As illustrated in Figure 5.2 (a), in a beam the actual path follows the skeleton path. Unlike the beams in columns, the actual path usually deviates from skeleton path. This could be deduced because of the normal force on the moment-plastic rotation relationship.

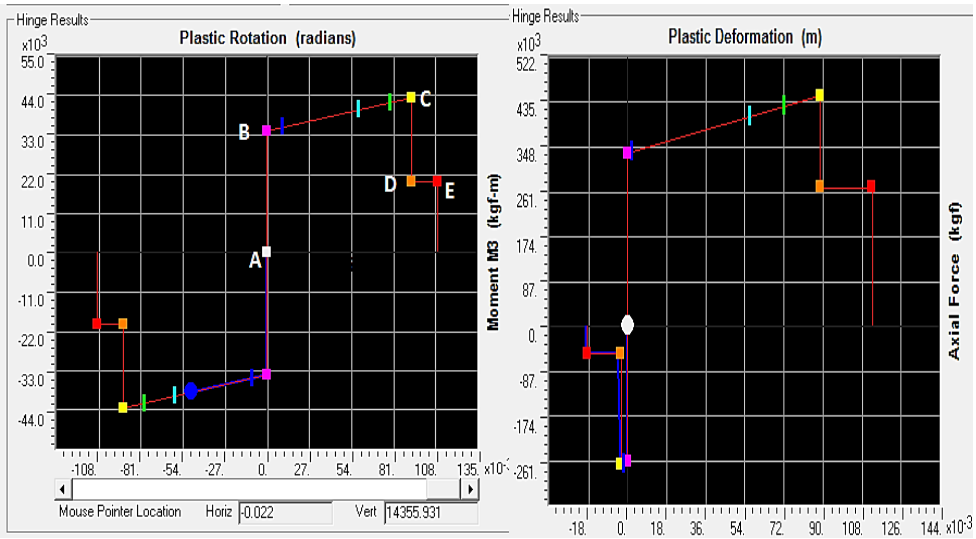


(a) Beam plastic hinge diagram (b) Truss member plastic hinge diagram

Figure 5.2: Plastic hinge definition in a beam and a truss member

Point B in figure 5.2 (a) is represents the yield moment while the point C represents the ultimate moment point and the corresponding plastic rotation. For columns the moment-plastic rotation relationship depends also on the normal force and this interaction could be activated in SAP2000 [25].

## 5.4 P- Δ Effects

To perform a Nonlinear Dynamic Progressive Collapse (PRC), both material and geometric nonlinearity should be taken into account. The P- Δ Effect was considered as a geometric nonlinearity. UFC 2013 [2] indicates that, "all overall vertical and lateral stability as well as local stability must be considered". To include P- Δ analysis to SAP2000, in Time History load definition page the P- Δ should be selected from "Geometric Nonlinearity Parameters" section. Unified Facilities Criteria (UFC 2013) also allows using P- Δ plus large displacements; however in this study only the first option was adapted to all the analytical models.

## 5.5 Nonlinear Dynamic Loading Procedure

The analysis should start from zero second and the gravity loads needed to apply monotonically and proportionally increase for the entire model. After the equilibrium was reached, the column should be removed in a time period not more than one tenth of the period related with the structural response mode for the vertical motion of the bays overhead the detached column, as found from analytical model with the column detached [2].

UFC 2013 [2] proposes the equation 5.2 to be applied as a nonlinear dynamic load to the structure. Note that this equation is similar to the nonlinear static load case proposed by UFC 2013 with the dynamic increase factor missing.

$$G_{ND} = 1.2\,D + (0.5\,L \text{ or } 0.2\,S) \quad (5.2)$$

where $G_{ND}$ = Gravity loads for Nonlinear Dynamic Analysis

D = Dead load including facade loads (lb/ft2 or kN/m2)

L = Live load (lb/ft2 or kN/m2)

S = Snow load (lb/ft2 or kN/m2).

The loading method of UFC 2013 is essentially unchanged from the 2005 UFC. It uses the ASCE 7 extraordinary event load combination with the exception that the lateral load has been removed. The reason is that, in alternate path analysis, the impairment is restricted to the column or deletion position and the lateral load resisting system is assumed to remain intact. However the UFC 2013, recommends influencing the wind effect by a 0.2 coefficient [2]. After removing a column, the lateral stability is highly unlikely to be destabilized. For progressive collapse, the main elements should withstand in contradiction of the gravity loads

throughout the removal period and during this time it would be rare if an earthquake happens. Therefore, the UFC 2013 prefers to not affect the lateral loading for PRC (progressive collapse) analysis.

## 5.6 Acceptance Criteria for Structural Steel

The nonlinear acceptance criteria for Life Safety stage for columns and Collapse Prevention stage for beams are chosen from ASCE 41 chapter 5 tables for all primary and secondary components. The UFC 2013 [2] suggests Collapse Prevention and Life Safety for beams and columns respectively as their acceptance criteria. These components are considered as deformation controlled components. But if the $\boldsymbol{P/P_{CL}}$ ratio becomes bigger than 0.5 for columns, they will be considered as force controlled components in SAP2000. In this case, the column is under high axial load influence. If the $\boldsymbol{P/P_{CL} \leq 0.5}$, the interaction equation shall be used with the moment measured as deformation controlled and the axial load as force controlled. These nonlinear criteria are shown in table 5.1, which are adopted from tables 5.5, 5.6, and 5.7 of ASCE 41 [7].

The UFC 2013 allows Life Safety acceptance criteria for columns and Collapse Prevention acceptance criteria for beams and braces [2].For Strength Capacities, the material over-strength factors (Ω) are chosen from AISC LRFD [4] code. The material over-strength factor is equal to 1.3 for steel structures and strength reduction factor is equal to 0.9 [4]. On the contrary, for shear effects, the yield is not allowed and zero ductility was assumed.

Table 5.1: Modeling Parameters and Acceptance Criteria for Nonlinear Modeling of Steel Frame Connections [12]

| Connection Type | Nonlinear Modeling Parameters(1) | | | Nonlinear Acceptance Criteria | |
|---|---|---|---|---|---|
| | Plastic Rotation Angle, radians | | Residual Strength Ratio | Plastic Rotation Angle, radians | |
| | a | b | c | Primary(2) | Secondary(2) |
| **Fully Restrained Moment Connections** | | | | | |
| Improved WUF with Bolted Web | 0.021 - 0.0003d | 0.050 - 0.0006d | 0.2 | 0.021 - 0.0003d | 0.050 - 0.0006d |
| Reduced Beam Section (RBS) | 0.050 - 0.0003d | 0.070 - 0.0003d | 0.2 | 0.050 - 0.0003d | 0.070 - 0.0003d |
| WUF | 0.0284 - 0.0004d | 0.043 - 0.0006d | 0.2 | 0.0284 - 0.0004d | 0.043 - 0.0006d |
| Side Plate® | 0.089 - 0.0005d(3) | 0.169 - 0.0001d | 0.6 | 0.089 - 0.0005d | 0.169 - 0.0001d |
| **Partially Restrained Moment Connections (Relatively S** | | | | | |
| Double Split Tee | | | | | |
| a. Shear in Bolt | 0.036 | 0.048 | 0.2 | 0.03 | 0.040 |
| b. Tension in Bolt | 0.016 | 0.024 | 0.8 | 0.013 | 0.020 |
| c. Tension in Tee | 0.012 | 0.018 | 0.8 | 0.010 | 0.015 |
| d. Flexure in Tee | 0.042 | 0.084 | 0.2 | 0.035 | 0.070 |
| **Partially Restrained Simple Connections (Flexible)** | | | | | |
| Double Angles | | | | | |
| a. Shear in Bolt | $0.0502 - 0.0015d_{bg}$(4) | $0.072 - 0.0022d_{bg}$ | 0.2 | $0.0502 - 0.0015d_{bg}$ | $0.0503 - 0.0011d_{bg}$ |
| b. Tension in Bolt | $0.0502 - 0.0015d_{bg}$ | $0.072 - 0.0022d_{bg}$ | 0.2 | $0.0502 - 0.0015d_{bg}$ | $0.0503 - 0.0011d_{bg}$ |
| c. Flexure in Angles | $0.1125 - 0.0027d_{bg}$ | $0.150 - 0.0036d_{bg}$ | 0.4 | $0.1125 - 0.0027d_{bg}$ | $0.150 - 0.0036d_{bg}$ |
| Simple Shear Tab | $0.0502 - 0.0015d_{bg}$ | 0.1125 - | 0.2 | $0.0502 - 0.0015d_{bg}$ | $0.1125 - 0.0027d_{bg}$ |

## 5.7 Nonlinear Dynamic Procedure

The Nonlinear Dynamic analysis for Progressive Collapse is a quite complex method and requires sophisticated analysis procedures and software to be accomplished. This method is usually avoided due to its analytical complexity.

Additionally, evaluation and validation of the results can be very time consuming and expensive. Moreover, the second problem comes after the kind of software which had to be used. To overcome such a complex method, the finite element software should be equipped to define nonlinear loadings. This can be done by considering the staged construction analysis with removing a structural component in a specific period. The Nonlinear SAP2000 version 17 was chosen because; this software is generally able to perform a combined load analysis. Even the UFC 2013 [2] uses this software throughout all structural steel examples analysis done in this code.

The Nonlinear Dynamic procedure was carried out in 7 steps and all details with relevant figures are presented hereby.

### 5.7.1 Building a Finite Element Computer Model

This model was fully described in chapter 3 of this study. The structure was designed according to the AISC LRFD [4] regulations and load combinations for gravity and lateral loadings. All primary structural sections including columns, beams, truss members and braces were optimally designed with P-M ratios close to 0.95. In this case the impact of progressive collapse on a structure which is designed based on conventional lateral and perpendicular load resisting systems will be more obvious. The model used in this approach is a 10 story steel building with 2 Moment Frames in left and right of the structure (X direction) and 8 Staggered Truss Systems (STS) in transverse (Y) direction. Figures 5.3, 5.4, 5.5 show architectural geometry details; detailed information was presented in chapter 3 of this thesis.

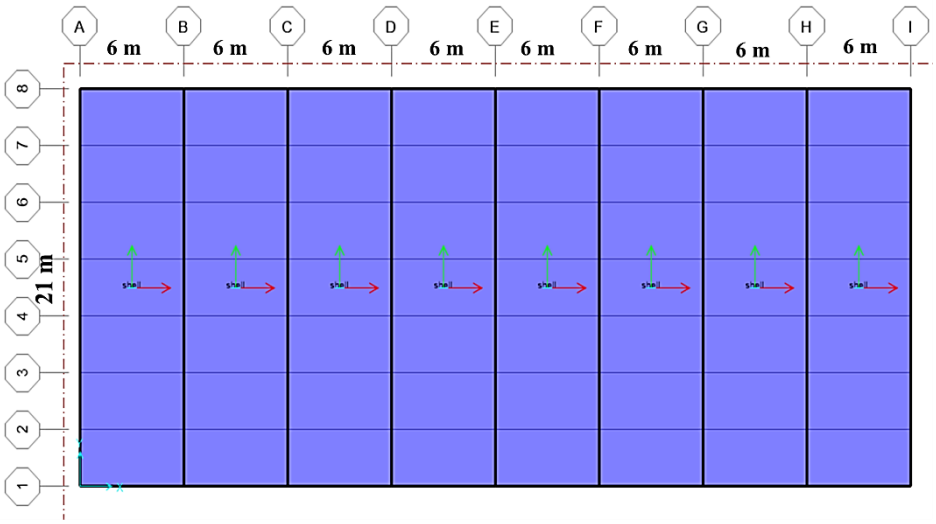


Figure 5.3: Plan view of the Model

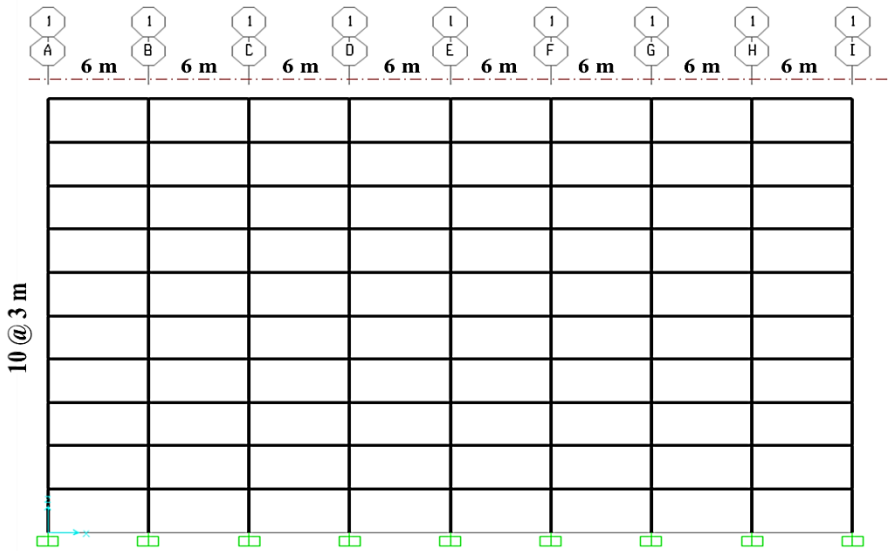


Figure 5.4: Side view of the building (Moment Frame System)

### 5.7.2 Nonlinear Dynamic Analysis Cases

The nonlinear dynamic technique needs numerous analysis cases for each column exclusion. These analysis cases are to define forces coming from any section detached. Before removing a structural element like a column, the force equilibrium has to be reached, however after removing a column the equilibrium will change throughout the structure.

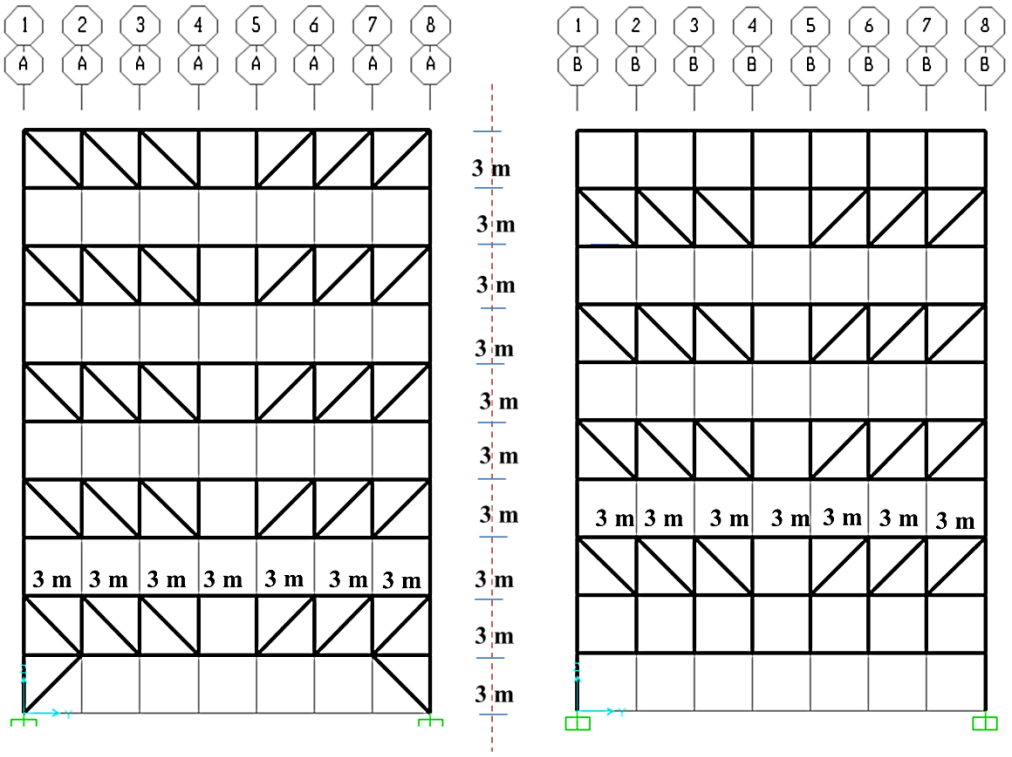


Figure 5.5: Staggered Truss Fames (STS) in row (a) and row (b)

Before removing a column, the force diagrams and structural deflections should be determined from the undamaged structure. This involves the static analysis of undamaged structure. The Nonlinear Static load case shall be added to the designing load cases and equation 4.2 is used for its load combination case (Figure 5.6). Load Application Control for Nonlinear Static Analysis, was chosen as a FULL LOAD in *U3* direction at the center of gravity of the top floor (Figure 5.6). Because we only need the final stage, of deflection therefore the final state option is only selected. SAP2000 design techniques may be used to estimate whether columns are deformation or force controlled [2]. For each analysis case a design combination also had to be defined to evaluate the structural stability before starting the Progressive Collapse. Figure 5.7 shows the bending moment, $M_3$, diagram due to the Nonlinear Static load case.

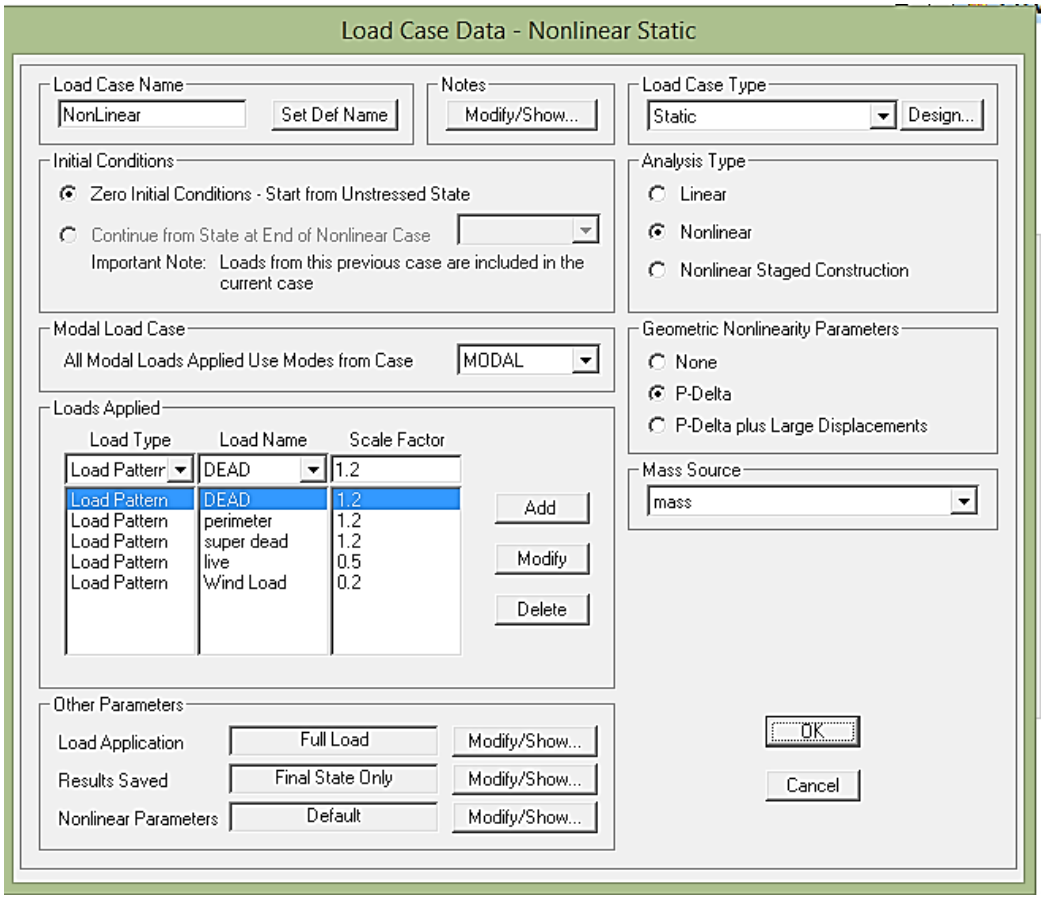


Figure 5.6: Nonlinear Static Load Case using Equation 5.2 Parameters

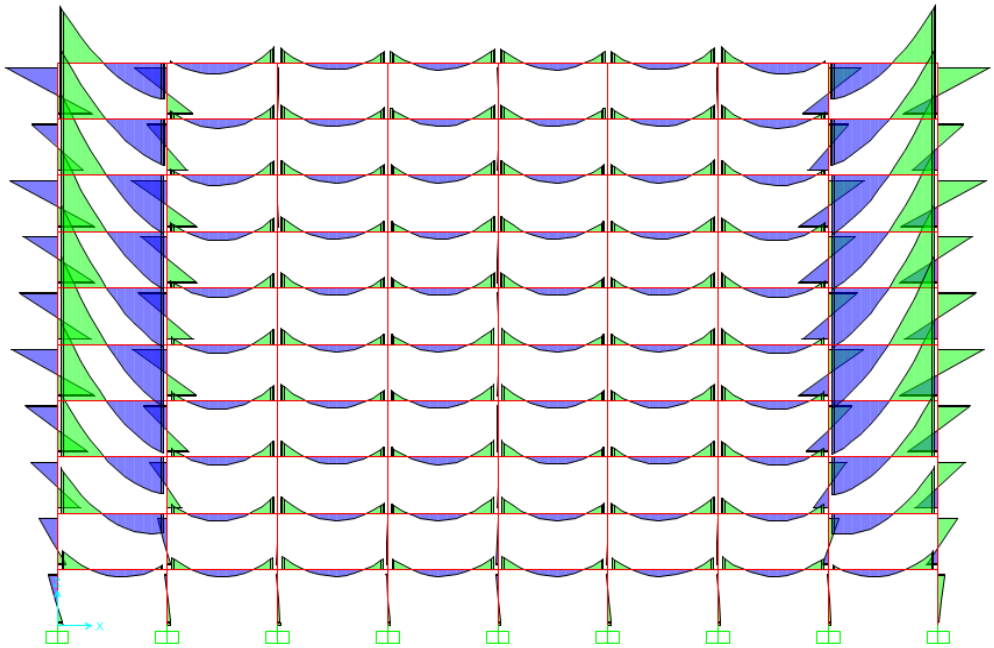

Figure 5.7: Moment diagram for Nonlinear Static Load case

### 5.7.3 Column Removal and Initial Load Case

For each column removal, the column is removed in the structural prototype and the internal forces found from the equilibrium model are applied to the structure as a load case to the joint or joints at each column joint. These static nonlinear analysis cases are used as the preliminary conditions for the column eliminations.

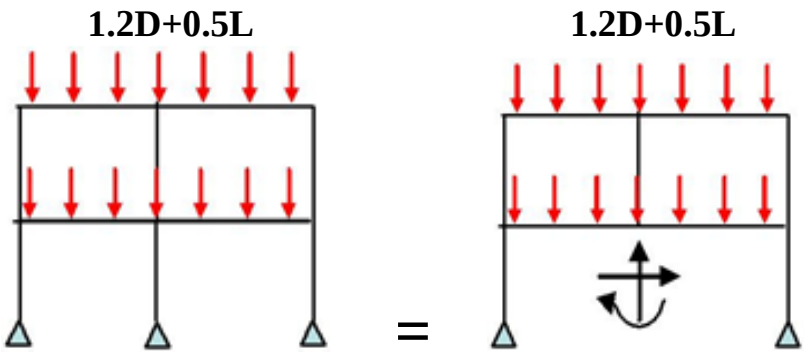


Figure 5.8: Column replaced with Opposite Direction Loads

The column end forces are applied to both end joints of the removed column. Figure 5.8 shows a simple column removal scenario, of a 2 span, 2 story frame. In this frame the middle column was removed in an instantaneous period of time and its internal loads have applied in an opposite direction to the top end of the column. To expand this method more, we should refer to Newton's third law "When one body exerts a force on a second body, the second body simultaneously exerts a force equal in magnitude and opposite in direction on the first body ".

As shown in Figure 5.8, the applied upward load represents the columns resistance against the oncoming gravity loads from top columns, beams and floor. For a middle column two kinds of load cases are defined. In Figure 5.9, the Opposite load case represents the column resistance against perpendicular loads coming from upper components. However in the equivalent load case, the load is

transmitted to the floor below by the column that had to be removed [23]. These load cases eventually will be added to the Nonlinear Static Load Case.

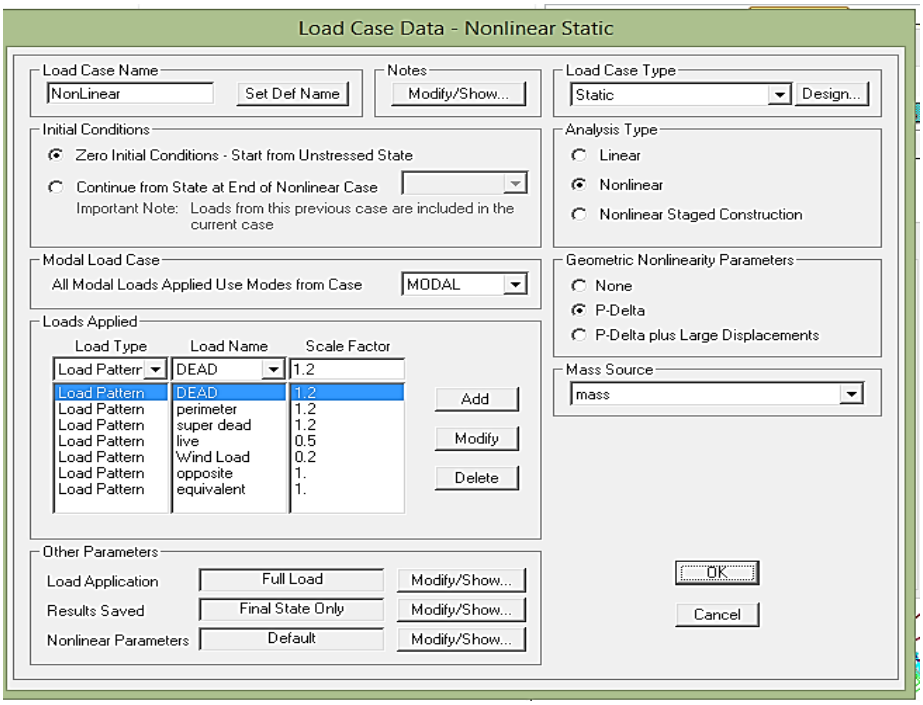


Figure 5.9: Nonlinear Static Load Case as the Initial Condition Load, with Column end Loads applied

The Nonlinear Static Load Case is the initial load case for the Nonlinear Dynamic Analysis. To sum up, the column had to be removed from the model and the calculated reactions are applied to the column joints. These reactions will be used in a new nonlinear static load case as an initial load case for Time History Analysis. For instance, the $6^{th}$ floor column in row E was removed and then its axial load-bending moments and Shear forces were applied to the model without the column as shown in Figure 5.10.

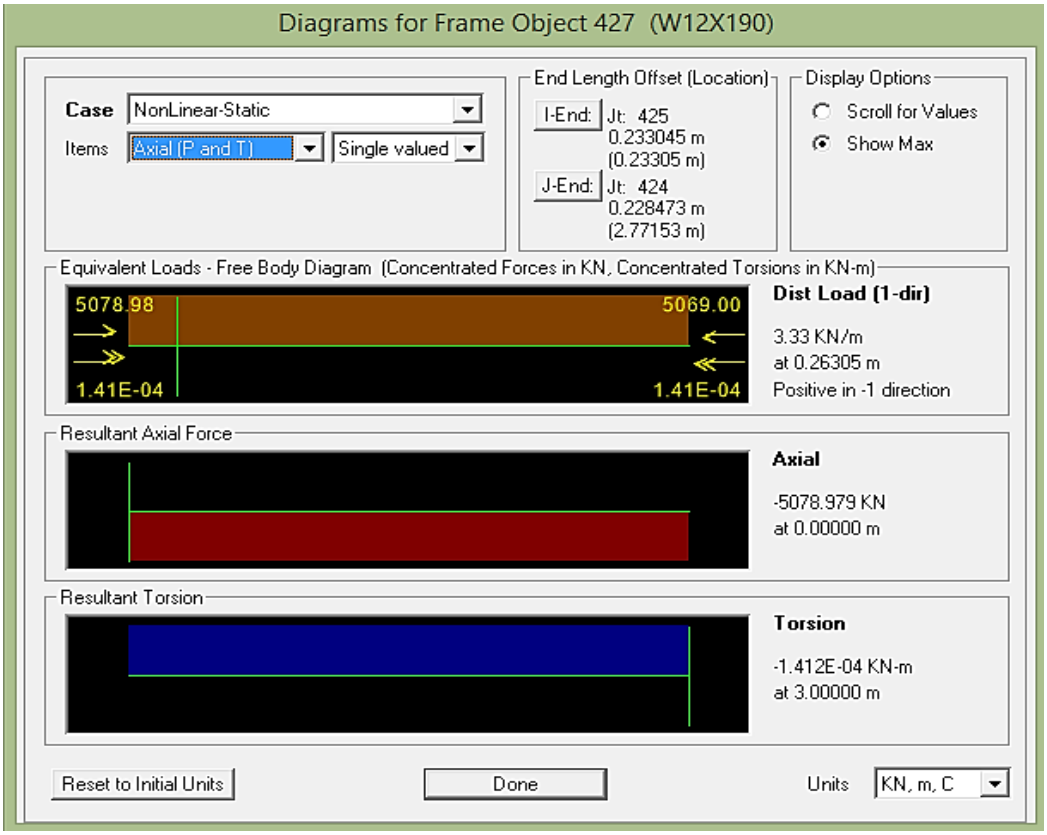


Figure 5.10: Axial load of the 6th floor middle column under Nonlinear Static load case

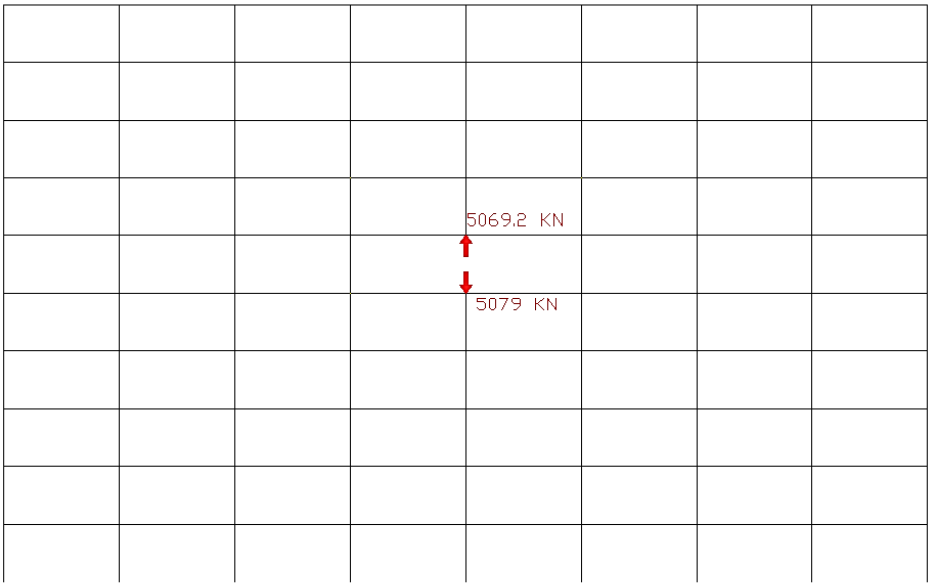


Figure 5.11: Applied Opposite and Equivalent Axial loads to the joints of removed column

According to Figure 5.11, the E-1 column in the 6$^{th}$ floor has the axial loads of 5079 *kN* and 5069.2 *kN* at bottom joint and top joint respectively. A new model was developed and the same loads were applied to the new model with the column missing as shown in Figure 5.10. These extracted internal forces are externally applied to the analytical model and stabilize the structure. Progressive collapse starts with suddenly removing these external forces in a short period of time. After running both models, the obtained $M_3$ moment diagrams were compared together (Figure 5.13) to evaluate the accuracy of the procedure.

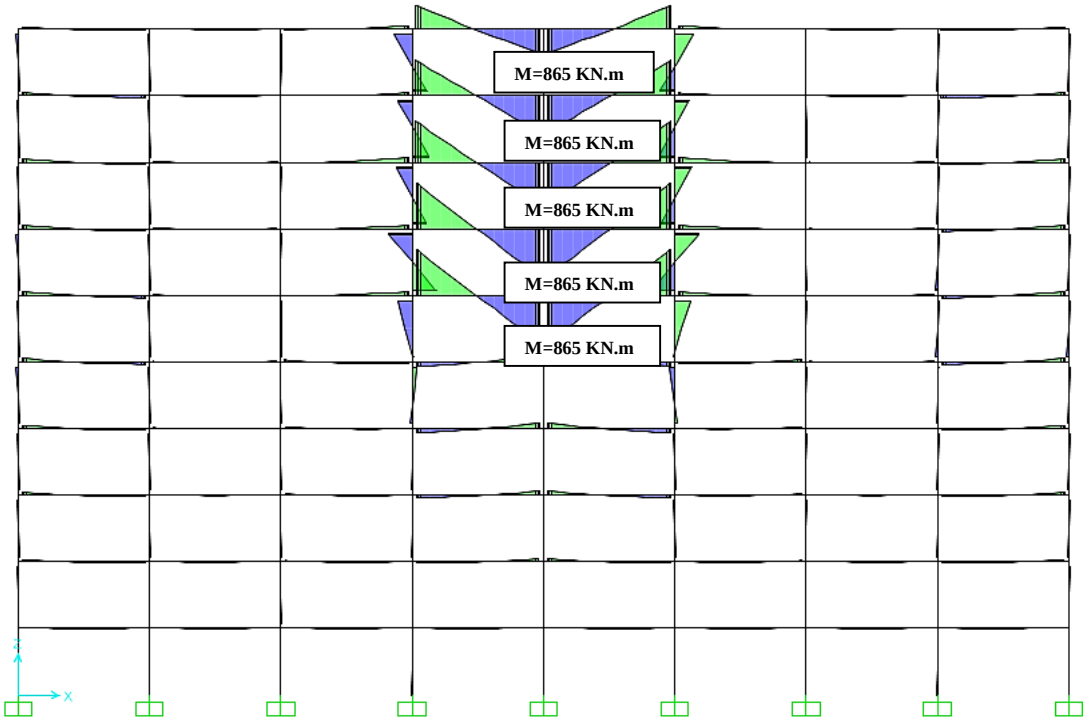


Figure 5.12: Calculated Bending Moment Diagram due to Nonlinear Static load case with internal loads missing

Figure 5.12 shows the bending moments at the center of the frame. In this case the opposite and equivalent external loads are not yet applied to the structure. The magnitude of the moments in comparison to the other beams is considerably

greater. As discussed earlier, the nonlinear static load case is the initial condition for Time History Analysis. This means that at time zero of time history load case the forces and deflections had to be equal to the nonlinear static load case. To reach equilibrium at time zero, the designer has to carefully compare the analytical model with missing column with the original model. These two models are supposed to show similar internal force reactions for the Nonlinear Static load case. Figure 5.13 (b) shows the bending diagram to a column removal at E-1 gridline. In this figure the bending moments of both the original model and the model with missing column are presented. It is clear that both models have almost similar bending moment diagrams for Nonlinear Static load case.

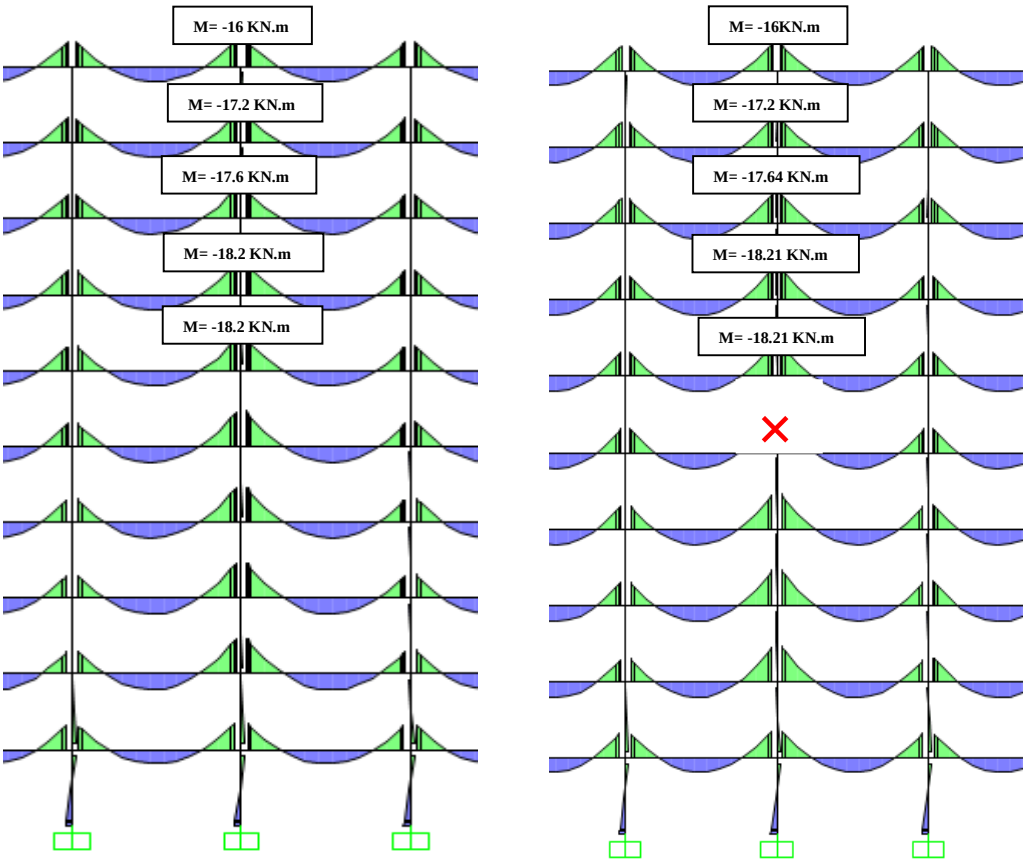


(a) (b)

Figure 5.13: Bending Moment Diagrams for (a) Original model (b) Model with missing column

The bending moments for beams above removed column showed a drastic increase in a model without successor external forces when it was compared to the original model (Figure 5.12). Whereas in Figure (5.13-a) and (5.13-b), the bending moments are approximately the same. This proves the accuracy of the process of removing a column from structure and replacing with its internal forces in order to represent the column attendance. These successor loads will be removed from structure in a very short time during Time History Analysis.

### 5.7.4 Time History Analysis

When the structure was in equilibrium, the dynamic analysis performed using "Nonlinear Direct Integration Time History" option in SAP2000 (Figure 5.14). The Newmark method of integration and default values of Gamma and Beta parameters were selected from SAP2000 menu. To expand the Time History case, the column under this load case should be removed by ramping down the column reactions under a very short time which is the natural period of response of the structure.

To find this period, a Modal Analysis was carried out and the dominating mode of vibration was selected visually based on the location of the column removal.

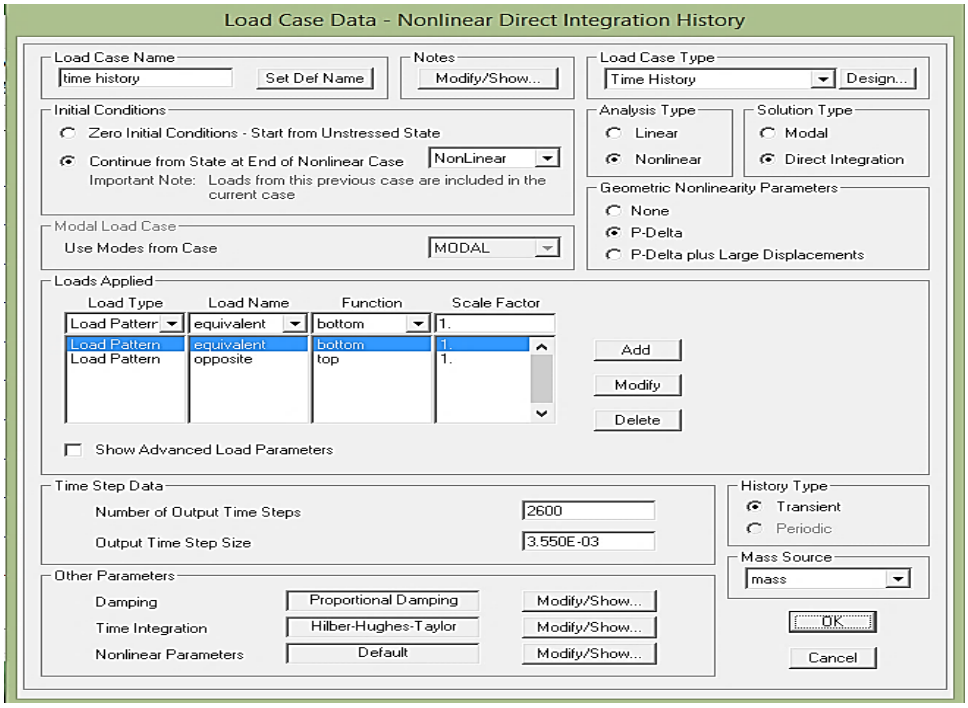


Figure 5.14: Nonlinear Direct Time History Load Case

In this research, the column was first removed and after performing a modal analysis, the corresponding period to the components directly above the removed column was selected as column removal period. This period was divided by 200 to calculate the column removal time step. The output time step sizes for time History analysis, was calculated as 1/200 of the above mentioned natural Period. The time history load case continues from the state at the end of nonlinear static analysis load case where P- Δ effect was also included [2]. The analysis will carry on until the maximum dislocation is achieved or one cycle of vertical motion occurs at the column exclusion position [2]. The opposite and equivalent external loads were added to the Time History load case with a scale factor of one. By these definitions, Time History Analysis will start from Nonlinear Static load case and will remove column internal loads in a short period of time considering the structural natural period.

# Chapter 6

# PLASTIC ANALYSES OF STRUCTURAL ROBUSTNESS AGAINST DISPROPORTIONATE COLLAPSE DUE TO COLUMN REMOVALS

## 6.1 Introduction

This chapter focuses on failure mechanism of Staggered Truss Systems and their Elastic- Perfectly Plastic behavior mainly under gravity loads when a column is removed. The internal forces including the axial forces will spread to the neighboring elements in a structural system under column removal scenario. As a result, the bending moments, axial force and shear forces in these elements increase dramatically. Surrounding beams in particular take a big portion of these forces and some of the beams will fail, because the total load due to a column removal has exceeded their ultimate capacity. Column removal scenarios will be done in two manners. In the first stage, one column would be removed from the structural system according to UFC 2013. In the second stage, 2 neighboring columns will be removed to find out the ultimate damage duo to column removal scenarios. In each stage after removing the elements based on the method discussed in chapter 4, the structure behavior will be assessed. This chapter includes comparison of the Hinge formations, Ductility, and Response of the Structure in each column removal scenarios. Since this chapter investigate the non-linear behavior of the proposed structure in Chapter 3, both material and geometric nonlinearities are taken into account. These involved introducing the

plastic hinges for all structural members following ASCE 41 [7] guidelines. Plastic hinges are considered as geometric nonlinearity however, for material nonlinearity, the stress-strain property and material capacities play significant role. Furthermore, Damping is an important factor for both material and geometric nonlinearity. Normally in progressive collapse analysis unlike the earthquake analysis, small damping amount should be considered. Graham Powell [24] describes that "In earthquake analysis, substantial energy dissipation can occur through miscellaneous mechanisms that are not considered directly in the analysis model. This dissipation is usually accounted for by assuming viscous damping. However, whereas earthquake response involves many cycles of vibration, progressive response analysis requires essentially only one half cycle, until the maximum deflection is reached. During this half cycle the effect of viscous damping is small and it is reasonable to ignore it." Therefore, in all column removal analysis conditions, a damping ratio of 1% was selected.

As the structure is equipped with Trusses in transvers direction, the impact of column removal on these trusses had to be analyzed. Because the story height trusses are main framing systems in this direction, it is vital to assess the behavior when the axial load increases suddenly through their members. In this work, the structure was designed in two methods. In the first structure, economically optimized sections were designed with Demand over Capacity ratios close to 0.95. In the second structure most of the spandrel beams in the moment frame direction were enhanced to reinforce the structure against progressive collapse potential. As shown in Table 6.1, W21 sections were replaced in the second structure. The truss members did not change in the second structure, since they performed well

against the progressive collapse but some chords were upgraded to converge with the analysis (Table 6.2).

Table 6.1: Spandrel Beams Changed in the Retrofitted Model

| Level | Spans | Framing System | Original Section | Retrofitted Section |
|---|---|---|---|---|
| 1 | AB-HI | Moment Frame | W18*40 | W21*44 |
| 1 | BC-CD-DE-EF-FH | Moment Frame | W18*35 | W21*44 |
| 2 | AB-HI | Moment Frame | W18*76 | W21*83 |
| 2 | BC-CD-DE-EF-FH | Moment Frame | W18*65 | W21*62 |
| 3 | AB-HI | Moment Frame | W18*76 | W21*83 |
| 3 | BC-CD-DE-EF-FH | Moment Frame | W18*65 | W21*62 |
| 4 | AB-HI | Moment Frame | W18*76 | W21*83 |
| 4 | BC-CD-DE-EF-FH | Moment Frame | W18*65 | W21*62 |
| 5 | AB-HI | Moment Frame | W18*76 | W21*83 |
| 5 | BC-CD-DE-EF-FH | Moment Frame | W18*65 | W21*62 |
| 6 | AB-HI | Moment Frame | W18*71 | W21*68 |
| 6 | BC-CD-DE-EF-FH | Moment Frame | W18*50 | W21*57 |
| 7 | AB-HI | Moment Frame | W18*60 | W21*57 |
| 7 | BC-CD-DE-EF-FH | Moment Frame | W18*50 | W21*57 |
| 8 | AB-HI | Moment Frame | W18*50 | W21*57 |
| 8 | BC-CD-DE-EF-FH | Moment Frame | W18*46 | W21*57 |
| 9 | AB-HI | Moment Frame | W18*46 | W21*83 |
| 9 | BC-CD-DE-EF-FH | Moment Frame | W18*40 | W21*83 |
| 10 | All | Moment Frame | W16*31 | W21*83 |

Table 6.2: Chords Changed in the Retrofitted Model

| Original Section | Levels | | | | | | | | | | Frame Gridline Position | | | | | | | | | Retrofitted Section |
|---|---|---|---|---|---|---|---|---|---|---|---|---|---|---|---|---|---|---|---|---|
| | 1 | 2 | 3 | 4 | 5 | 6 | 7 | 8 | 9 | 10 | A | B | C | D | E | F | G | H | I | |
| w10*45 | | | | | | | | | √ | √ | √ | | | | | | | | | w10*68 |
| w10*49 | | | | | | | | √ | √ | √ | | √ | √ | √ | √ | | √ | | √ | w10*68 |
| w10*54 | | | | | | | | √ | √ | √ | | | | √ | | √ | √ | | √ | w10*68 |
| w10*60 | | | | | | | | √ | √ | √ | √ | | | | | √ | | √ | | w10*68 |
| W10*68 | | | | | | √ | | | | | √ | | | | | | | | | W10*88 |
| W10*77 | | | | | √ | | | | | | √ | | | | | | | | | W10*88 |
| W10*88 | | | | | | √ | | | | | | | | √ | | | | | | W10*100 |
| W10*88 | | | | | √ | | | | | | | | | √ | | | | | | W10*100 |

## 6.2 Ground Floor Column Removal Scenarios

### 6.2.1 Inelastic Deformation Locations at Ground Level

In this context, one column will be removed in a short period of time equal to 1/20 of the vertical mode relating to elements directly above removed column. Figure 6.2 shows the location of removed columns at ground floor level. The neighboring diagonal connected to the removed column was also removed from the structures to simulate a true explosion or impact scenario.

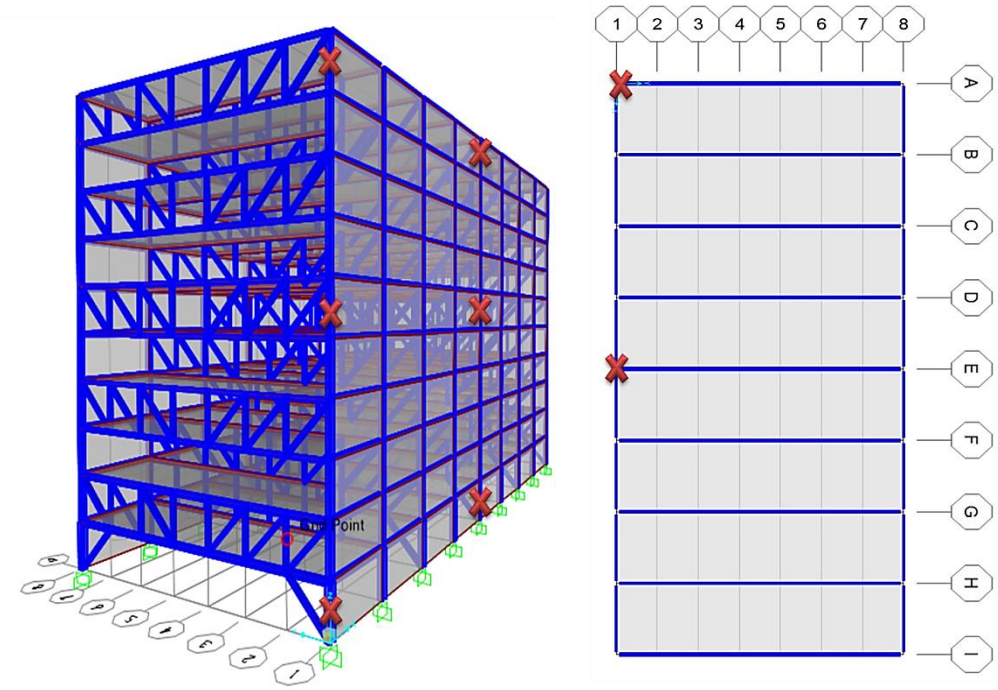


Figure 6.1: column removal locations, plan and side view

Firstly, the columns located at corner and middle gridlines were removed from the structure. Details of the column removal were discussed in detail in Chapter 5 of the thesis. After the removal of the corner column at the ground floor, a non-linear dynamic analysis was carried out. The results from the analysis showed a vertical deflection equal to $U_3$=-131 *mm* (in Z direction) at joint 21 (above the removed column location shown in Figure 6.3-a). When the column from center of the

structure was removed, the vertical displacement in Z direction reached 118 *mm* at the joint 429 above the column removal location (Figure 6.3-b).

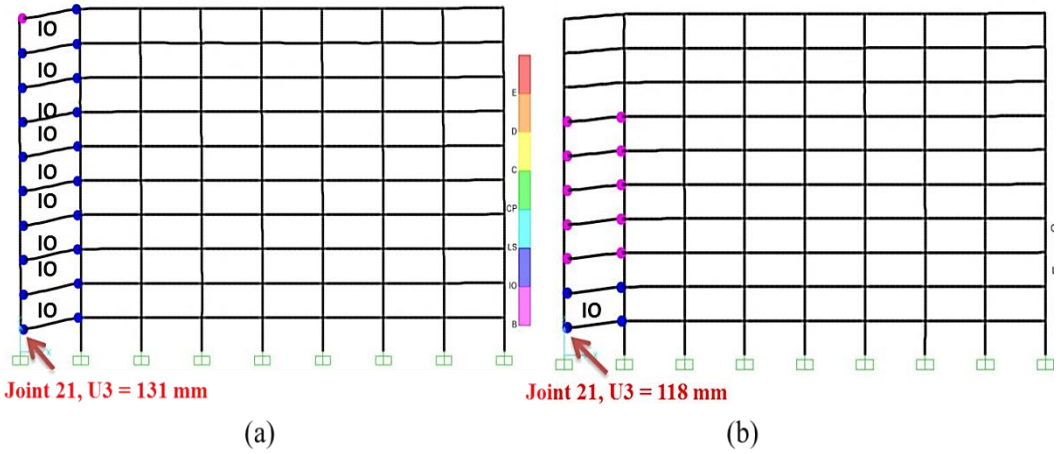


Figure 6.2: Inelastic Deformation after removing the ground floor corner column was removed for (a) Original structure and (b) Retrofitted structure

The plastic hinges formation for both the models were located in acceptance criteria zone. All plastic hinges in middle column case were in Immediate Occupancy (IO) range at moment frame direction. The displacements are smaller in Retrofitted Model as stronger sections were allocated in this model.

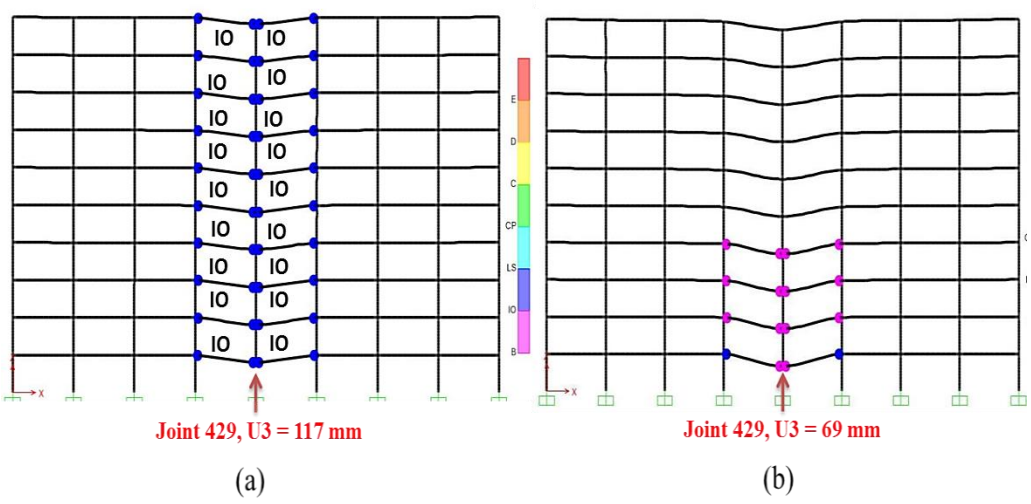


Figure 6.3: Inelastic deformation when the ground floor middle column was removed for the (a) Original structure, and (b) Retrofitted structure

The formation of the plastic hinges in direction, were mostly at Chords. The UFC 2013 [2] allows defining plastic hinges wherever a failure mechanism is probable. When the chords where assessed under different load cases, it was observed that mostly, maximum bending moments were located around the vertical truss member connection. It is true that in a truss no bending moments exist around member connections. However, because the chords are continuous long beams, the bending moments are inevitable through the length of the chords. Taking this into the account, 6 plastic hinges were introduced to chords at each connection location with verticals as maximum bending moments were developed these points. The chord connections to the columns at the beginning and endings were exempted from hinge definitions since these connections are hinged connection. It was seen that most plastic hinges on chords were formed around vierendeel panels. These panels were left empty to open an access corridor.

The plastic hinges occurred at $9^{th}$ and $10^{th}$ floor chords in Original model but no plastic hinge occurred in retrofitted model with upgraded chords. These chords were upgraded because they failed to withstand against progressive collapse.

The retrofitted structure showed less vertical displacement at all locations compared to the original model. However, both structures remained stable after a column was removed at ground floor level. This could be interpreted: although structures have interred into plastic behaviors after a column being removed, but no failure mechanism took place at this stage. The results from the analysis showed that the original structure was well designed to robust and maintain

stability after absorbing the shock coming from a ground level column removal in all locations.

### 6.2.2 Concrete Deck Effect

According to the AISC 14 design guideline for staggered truss Systems [8], in a staggered truss building, the diaphragms function significantly differs when compared with diaphragms in other building types. This is to the fact that they receive the lateral loads from the staggered trusses and transfers them from truss to truss. The design issues in a hollow-core diaphragm are stiffness, strength and ductility, as well as the design of the connections required to unload the lateral forces from the diaphragm to the lateral-resisting elements. In this study the concrete slabs were assumed to be totally rigid as the analysis of flexible diaphragms is more complex. This thesis focuses mostly on the inelastic behavior of the steel sections and therefore during the analysis, elastic behavior was assumed for the slab decks. This assumption remains acceptable as long as the diaphragm lateral and vertical deformations are limited.

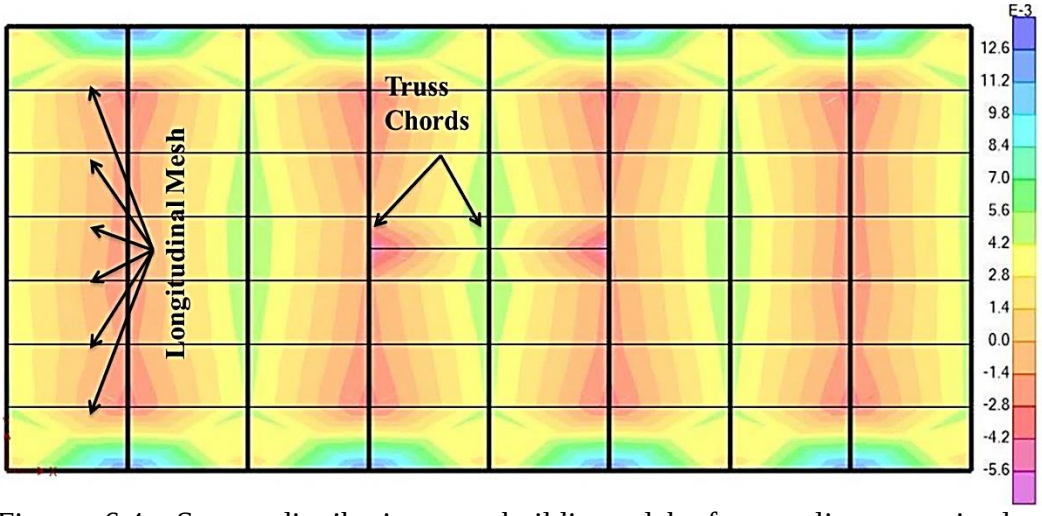


Figure 6.4: Stress distribution on building slab for nonlinear static load combination ($N/mm^2$)

To model a slab in SAP2000, different element types including Shell elements, membrane elements and plate elements can be used. Shell type elements have both in-plane and out-of-plane stiffness which convey both shear and moments. By default, shells transfer load two-way only at meshed joint locations. Membrane elements have in-plane stiffness only, and transfer shear load (not moments) as one-way uniform distributed load to beams. Plate elements have the out-of-plane stiffness only. A thick shell element includes transverse shear effects. In most applications including concrete slabs, mat foundations, walls or steel tanks/vessels, thin shell elements are more appropriate. Membrane element is used to model shear walls if the designer wants to avoid wall's out-of-plane stiffness, and when the load transfer from wall to floor is shear load only without moments. Membrane is also used to model floors which distribute shear load one-way without taking credit for the floor stiffness to resist moments from gravity loads. Therefore in this thesis, it was decided to use thin shell element type (thickness=20 cm) for slabs and the shells were meshed in longitudinal direction to let the system represents a One-Way Concrete floor slab system. By using this method the major bending moments and gravity loads will be transmitted to Truss Chords. This was shown in Figure 6.4 which illustrates the stress distribution over the floor. It is clear that the maximum stress distribution is mainly around Chords and near Column joints.

As discussed earlier, it is vital to prevent floors from entering an inelastic zone, which makes the study incredibly complex. To achieve this, the stiffness modifiers option to reduce the slab stiffness in each direction was used. These modifications will allow the slabs to transmit a portion of bending moments

affecting slabs directly to Spandrel Beams and Truss Chords. The concrete slab and the steel beams are acting as a composite T beam at those areas where the slab is sitting on beams. The flange of this T beam consists of concrete and the web is steel. During the analyses, slabs with default modifiers in SAP2000 which is equal to 1, showed extra stiffness and the structure did not collapse where a big damage was expected after a column removal. Therefore it was decided to reduce slab modifiers to let the flange of the T beam transmit the loads to the web.

To evaluate this technique, the designed model was compared to at least 5 previous studies. The first one is a study done by *JINKO KIM, JOON LEE* (Inelastic Behavior of Staggered Truss Systems) [19]. The second one is a journal paper by *Seweryn Kokot* (Static and dynamic analysis of a reinforced concrete flat slab frame building for progressive collapse) [25]. And the third one the ASCE journal paper published by *Shalva Marjanishvili* and *Elizabeth Agnew* (Comparison of Various Procedures for Progressive Collapse Analysis) [26]. All these studies used analytical models designed and investigated by software. These models were redesigned by SAP2000 following their material and structural definitions and by allocating the above mentioned slab design procedure. Finally all plastic deformations like plastic hinge locations and structural deformations and force distribution in beams and columns were compared to their models. The results converged and showed close similarities, and this proves that the process chosen is correct. Moreover the data were compared to 2 researches done on Staggered Truss Systems with presence of the slab effects. The first one is the *Changkun Chen* publication (Simplified Model for Fire Resistance Analysis on Steel Staggered Truss System under Lateral Force) [9] and the second one is a

journal paper by the same author (Comparative experimental investigation on steel staggered truss constructed with different joints in fire) [27]. Finally it was seen that, slab modifications should be different for each column removal cases, because the stiffness and the behavior of the structure is different for different column removal scenarios.

## 6.3 6th Floor Column Removal Scenarios

### 6.3.1 Inelastic Deformation Locations at Corner

In the second step, to simulate progressive collapse occurrence at middle levels of the structure, the columns of 6$^{th}$ floor were removed. UFC 2013 [4] suggests the removal of a column at this level to evaluate the progressive collapse probability.

A 329 mm of vertical settlement at joint 16 was seeing when the corner column was detached in the original structure. The results from the non-linear dynamic analysis showed that at time 0.09 seconds, first plastic hinges are formed at 9$^{th}$ and 10$^{th}$ floor chords. The first plastic hinges on Spandrel beams at moment frame direction activated later at time 0.125 second at 7$^{th}$ floor beams. The plastic hinges emerged on all truss chords above or equal the removed column level as shown in Figure 6.5. At 9$^{th}$ and 10$^{th}$ floor maximum deformation took place around Vierendeel panel opening (at the center of the chord), therefore the plastic hinges activated in D state which is beyond the acceptance criteria (CP). Here the chords have failed but at 7$^{th}$ and 8$^{th}$ floor the plastic hinges are in green color which represents for Collapse Prevention Level and consequently they did not fail. While removing the column at 6$^{th}$ floor, because the diagonal is attached to the column, it was removed simultaneously (Figure 6.5)

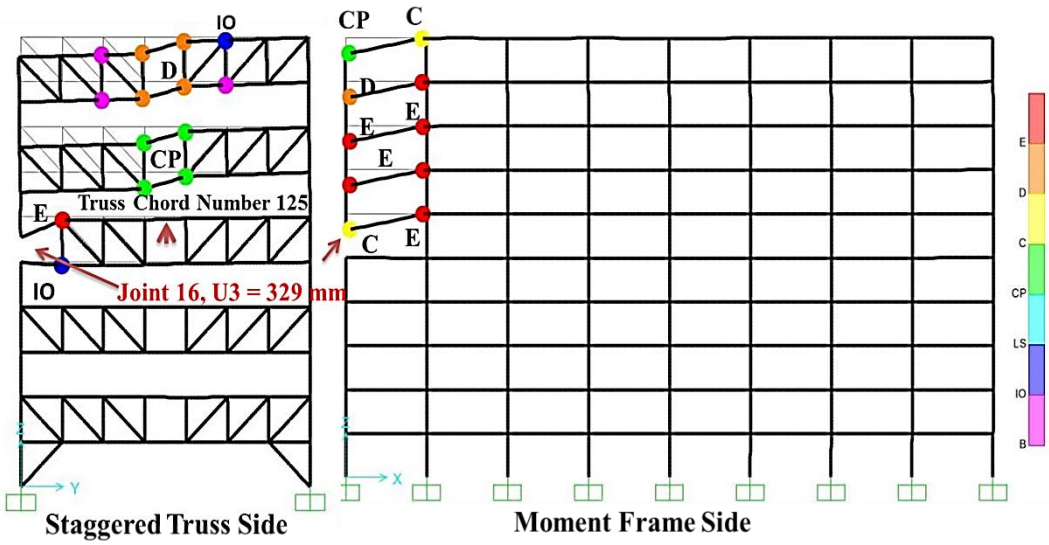


Figure 6.5: Inelastic Deformation of the Original Structure when the Corner Column removed at 6th Floor

This can be described as the impact of an explosion or an accident which leads to removal of both column and attached diagonal member. By referring to Figure 6.5, it is clear that the truss located between 5$^{th}$ and 6$^{th}$ floor (column removal location) shows a different behavior from the higher trusses. Here, because of lack of a diagonal, the above column transfers the axial load directly to the chord and the spandrel beam attached at their joint. As a consequence, a plastic hinge in "E" state (Failure) was formed 3 meters to the right side of the chord directly above the truss vertical member. The maximum vertical deflection of the chords will not always occur at the mid-span of the section and sometimes like the 6$^{th}$ floor chord maximum vertical deflection can happen at a different location. The nonlinear analysis showed that, spandrel beams at Moment frame direction were all failed after the column was removed. The vertical displacement of joint 21 of the original model in ground floor column removal scenario was131 mm whereas 6 floors above this joint, the displacement of joint 16 after removal of 6$^{th}$ floor column reached to 329 mm. This proves that, the deflection due to a column

removal increases when it happens at higher levels. The main reason is that, as progressive collapse happens in higher levels less structural elements would be involved to carry the redundant loads.

After redesigning the model, shown in tables 6.1 and 6.2, the inelastic behavior of the structure was investigated repeating the same process. In this case the plastic hinges activated in both directions were under Collapse Prevention State. (UFC 2013 [2] defines Collapse Prevention level as the acceptance boundary for beams Figure 6.6).

The results from analysis indicated that, the original structure's robustness could not prevent the collapse potential of the structure when a column was removed from corner of the building at middle level. After enhancing the structure by replacing the weaker sections with stronger ones (Chords and Spandrels) the building did not failed due to removal of the columns, although it was interred in to the inelastic behavior.

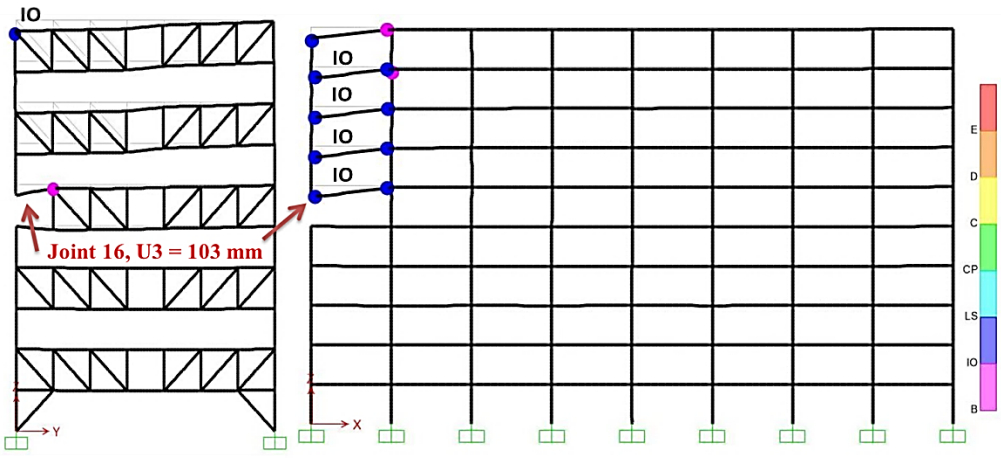


Figure 6.6: Inelastic Deformation of the Retrofitted Structure when the Corner Column removed at 6th Floor

To avoid the collapse of the structure due to a column removal scenario at 6th floor, all spandrel beams at moment frame direction in the original structure were replaced by stronger sections in retrofitted structure. The truss members did not change, because plastic hinges resulting from axial load increases were in primary stages. The details of all changed sections are given in Tables 6.1 and 6.2. Multiple Time-History analyses were carried out to find optimum sections capable to resist against progressive collapse.

Results showed that the progressive collapse design changes the design trend. In the original model the spandrel beam sections of *W18×40* and *W16×31*, were used at 9th and 10th stories respectively. Comparing these with the beams at lower floors (*W18×50*-*W18×60*-*W18×65*-*W18×71* and *W18×76*), they were categorized as the weakest beams. Surprisingly in the Retrofitted model upper floors needed stronger sections to resist against a progressive collapse scenario. In the retrofitted model, the *W21×83* sections were used in order to develop big plastic rotations resulting from increased bending moments in moment frame direction. This section was the strongest when compared with sections at lower stories (*W21×44*-*W21×57* and *W21×62*).

### 6.3.2 Inelastic Deformations at 5th Frame (Middle of the Building)

Both the original and retrofitted structures had bigger deformations at this location when compared with ground floor column removal scenario. However, the inelastic deformations were smaller (*U3*=258*mm*) than the 6th floor corner column removal scenario (see Figure. 6.7 and 6.8). First plastic hinges formed at time 0.115*s* in 6th floor's Spandrels at both ends. At this time no plastic hinges were formed at staggered truss frames but few moments later at a very close time of

0.13*s* the first plastic hinge formed on 6th floor chord at 3 meters distance from joint 424. It was observed that this point is very critical point on the chords connected to the top of the removed column location.

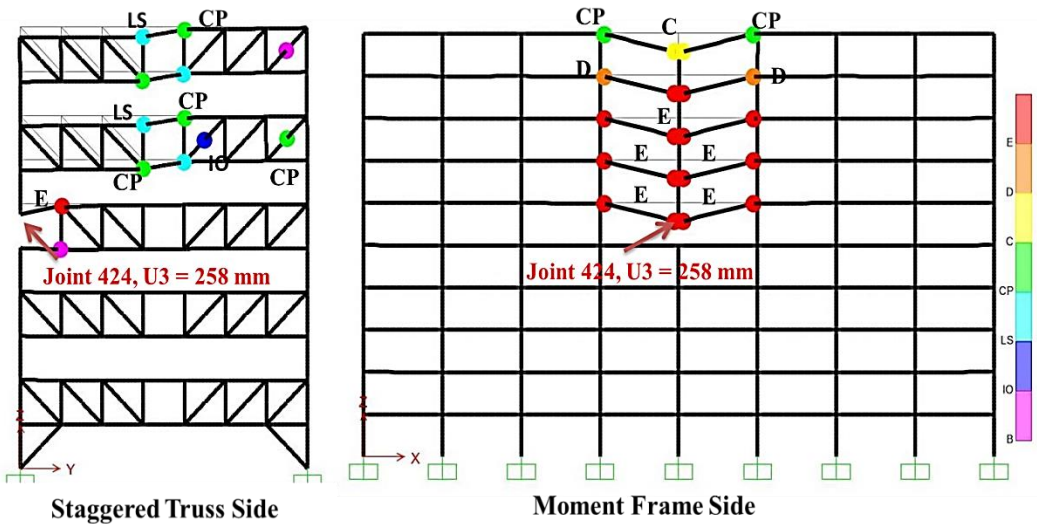


Figure 6.7: Inelastic Deformation of the Original Structure when the Middle Column removed at 6th Floor

Figure 6.8 shows the von-misses stress distribution of the truss located between 5th and 6th floors with missing corner column and its attached diagonal. The finite element analysis done by ABAQUS software [28] showed the same plastic hinges developed close to the first vertical truss member. The same result was also achieved for the non-linear dynamic analysis when SAP 2000 software was used. Figure 6.7 shows the formation of the plastic hinge from SAP 2000 Package.

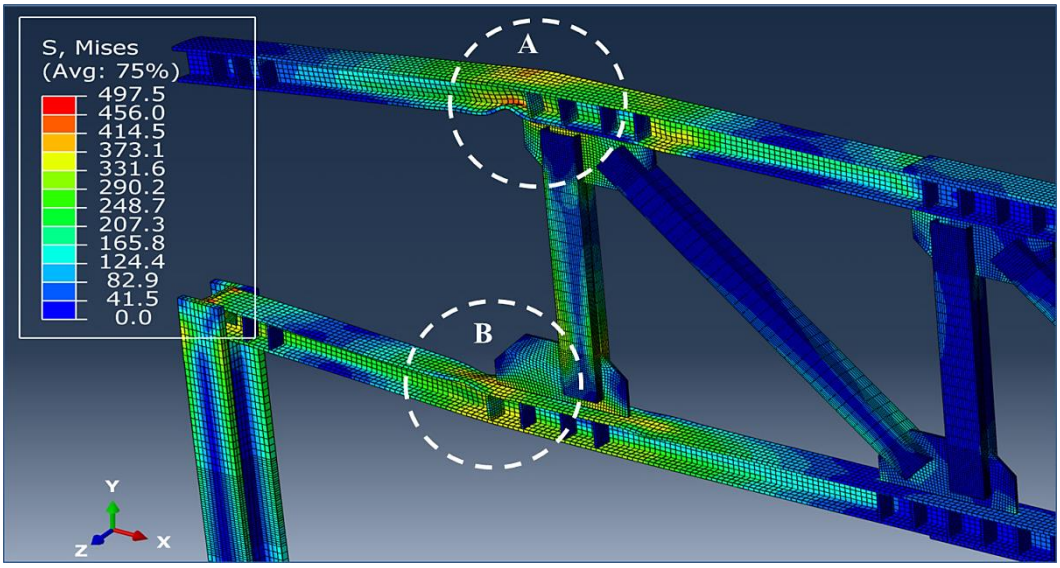

Figure 6.8: Finite Element Model of the Truss with missing Left Column and Attached Diagonal

Zones A and B (shown in Figure 6.8) are zoomed and illustrated in Figures 6.9, and 6.10 where, these are the locations of plastic hinge formation. The 258 mm deflection of the upper chord of this truss due to the axial load coming from upper columns has led the W10×88 section to yield and enter to the plastic zone. The stress at bottom flange as shown in Figure 6.9 has reached to 500 *MPa* which is much higher than the yield stress ($F_Y$ = 345 *MPa)* of the steel material used in the structure. Figure 6.10 clearly shows that the web of upper chords is yielded due to its high stress concentration.

Therefore after removing the column from $5^{th}$ frame- $6^{th}$ floor, the vertical deflection of the end of chord will lead to a plastic hinge formation on most parts

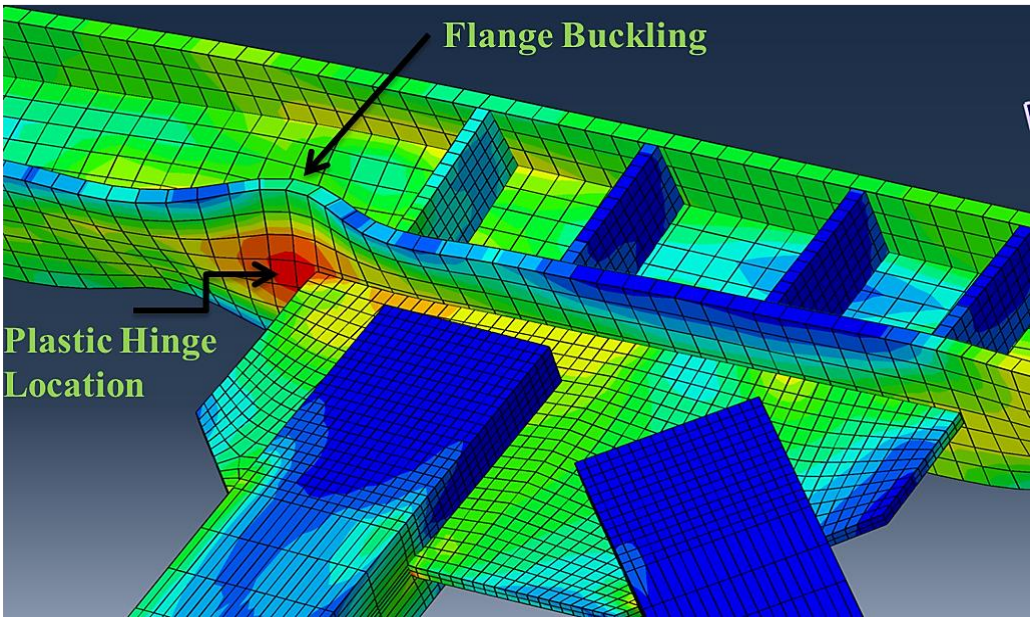

Figure 6.9: Plastic hinge Location at the Bottom Flange of the Top Chord

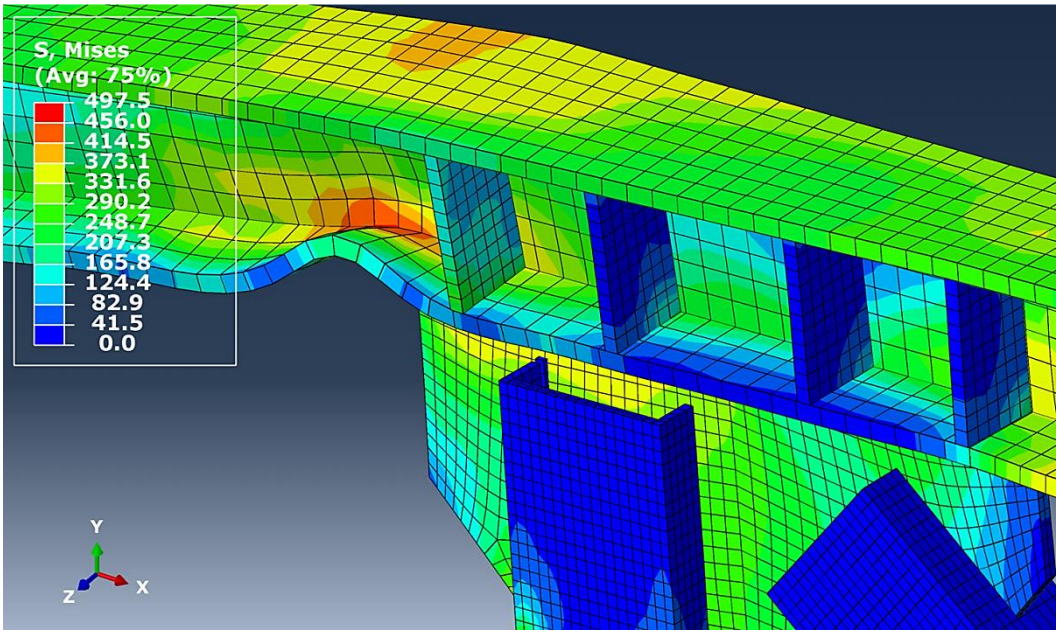

Figure 6.10: Plastic Hinge at Top Flange and the Web of the Top chord

of the chord at a distance equal to 3 meters from the Column removal location where even the bottom flange is suffering from a grate local buckling. It is clear that the chord will not be able to maintain its robustness after the sudden removal of adjacent column and diagonal and will fail at this point.

At the end of Nonlinear Direct Integration Time History analysis, the beams at moment frame direction were failed due to absorbing the axial load transferred to them following the removal of the column. Except the 6$^{th}$ frame chords, the remaining truss chords stayed under acceptance criteria after formation of the inelastic zone. The same results were not achieved when both the 9$^{th}$ and 10$^{th}$ floor trusses collapsed after removing the corner column. Therefore trusses are less vulnerable at central parts of the building which means that at corners, truss chords are more involved in resisting against the inelastic progressive collapse. Figures 6.6 and 6.7 reveal that, the maximum inelastic deformation occurs around vierendeel panels especially at corner column removal scenario (Figure 6.6). This leads to formation of a weak story and subsequently to a total collapse.

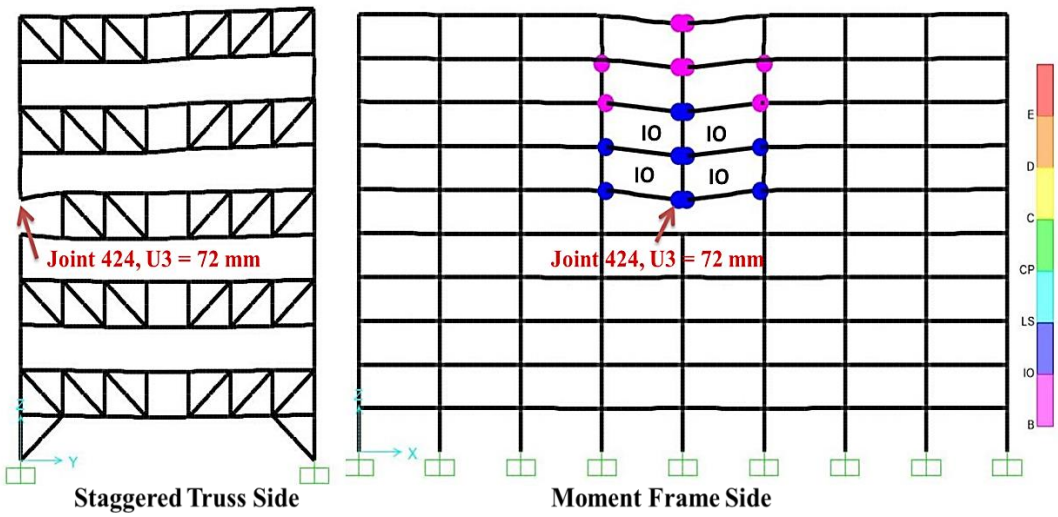


Figure 6.11: Inelastic Deformation of the Retrofitted Structure when the Middle Column removed at 6$^{th}$ Floor

Some reinforcing schemes for a staggered truss can be applied at Vierendeel panels and at the location of plastic hinge formation on 6$^{th}$ floor chords. As discussed by *Che*n and *Zhang* [27], that the potential progressive collapse of the whole structure might be aroused due to local buckling and joint fracture in the

case that the STS was constructed with welded joints. If a truss chord collapse happens as it was in sections 6.2.1 and 6.2.2, the destruction of the truss may lead to the collapse of the two stories supported by the single truss. Thus the load carried by the two stories would be applied to the lower floor all of a sudden. In this way the serious domino effect of the collapse might be formed, and the danger of the STS system under column removal condition might be very real. The AISC 14 guideline [8] proposed the application of stiffener plates around Vierendeel panels to increase the stiffness and strength of trusses. This is very economical especially for $6^{th}$ floor chord which has inelastic deformation only at one point close to the column connection. If adequate reinforcements attribute on such areas, beams plastic hinge will be below the acceptance criteria, there would not be any need for expensive section changes. To evaluate the effect of using stiffeners instead of changing the section dimensions, a finite element model of the truss located between $9^{th}$ and $10^{th}$ floors with equal loading conditions was made using ABAQUS software. From figure 6.12-a, it is clear that the stress of the chord around the vierendeel panel is more than yield stress ($F_y = 344\ Mpa$). To prevent the local buckling of the chord, in the second model a plate on the top flange of the top chord plus vertical stiffeners was adopted. In the second model, the maximum stress around vierendeel panel did not exceed from *317 Mpa* which is under the yield stress. Moreover, the local buckling of the chord as it was seen in the Figure 6.12-a, stopped as a result of applying stiffeners. It can be concluded that, using stiffeners for the top chords will eliminate plastic potential hinge formation around the critical zones of staggered truss systems like vierendeel panels.

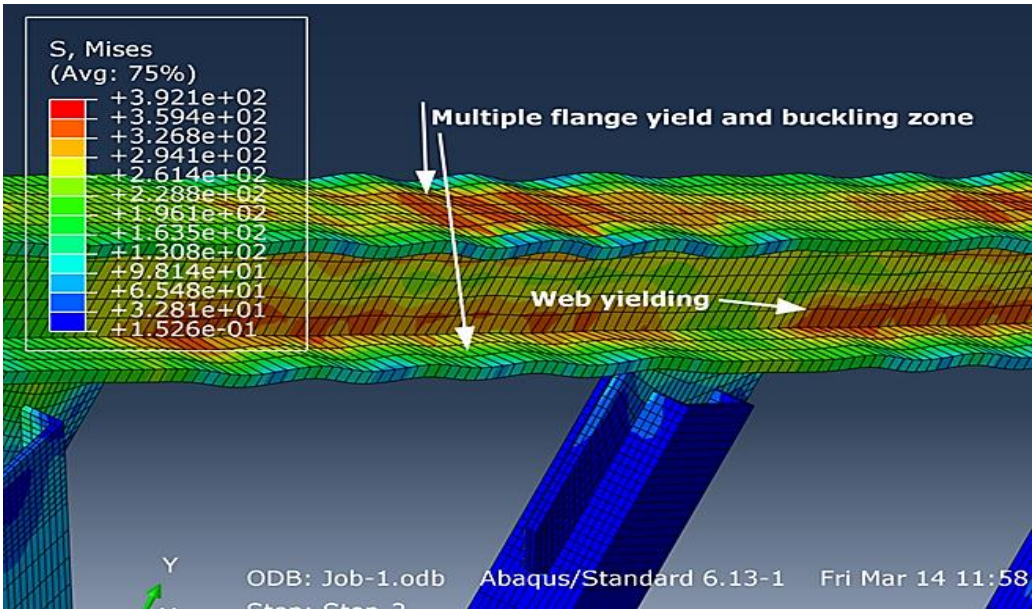


(a)

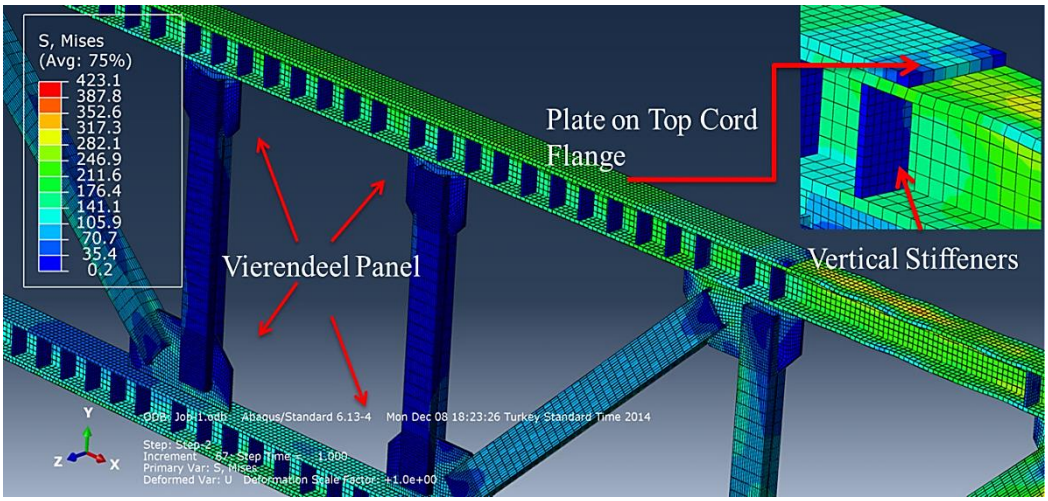


(b)

Figure 6.12: Deformed shaped of the truss located between 9th and 10th floors. (a): before applying stiffeners,(b): after applying stiffeners

Figure 6.11 shows the same column removal for the retrofitted model. As discussed in the section 6.1, after that inelastic failure observed in the original model due to column removals, few sections were replaced with bigger sections to withstand against progressive collapse. In the retrofitted model, a vertical displacement equal to $U_3$=72 *mm* was recorded at point 424. Plastic hinges were developed in the spandrel beams at moment frame direction and the plastic hinges

were under Immediate Occupancy level therefore no failure happened at this stage. At the Transverse direction where Staggered Trusses are located, plastic hinges did not formed. This means that for the retrofitted structure, when the column was removed from $5^{th}$ and $6^{th}$ floor level location, the retrofitted structure was still in elastic range and inelastic behavior was not observed.

### 6.3.3 Comparison of the Plastic Rotation ($\Theta_p$) for $6^{th}$ Floor Column Removals

Tables 6.3 and 6.4 show the beam hinge properties for both the Original and the retrofitted structure. Comparing the Hinge development for both models indicated that the inelastic rotations led to a progressive collapse of the first model. Whereas in the second model with retrofitted sections, the structure remains stable against the inelastic deflections.

In both cases, big plastic rotations could be seen in the original model in some moment frame and staggered truss frame beams. These plastic rotations are very small in the retrofitted model. For the corner column removal scenario (Table 6.3), the retrofitted structure showed higher bending moments in spandrel beams and chords when compared to the original structure. This means that after strengthening the model, elements absorbed more forces with smaller rotations.

Table 6.3: Hinge Properties and Plastic Rotation for Case 6rh Floor Corner Column Removal (Both Original and Retrofitted Models)

| TABLE 6.3 | | | ORIGINAL STRUCTURE | | | | RETROFITTED STRUCTURE | | | |
|---|---|---|---|---|---|---|---|---|---|---|
| **Beam Location** | **Relative Distance** | **Absolute Distance** | **Section** | **M3** | **R3-Plastic Rotation** | **Hinge Status** | **Section** | **M3** | **R3-Plastic Rotation** | **Hinge Status** |
| | **Unitless** | **m** | | **KN-m** | **Radians** | | | **KN-m** | **Radians** | |
| staggered truss 10th floor | 0.429 | 9.009 | W10*45 | 33.158 | 0.0722 | **D (Collapsed)** | W10*68 | 241.26 | 0 | A to IO |
| staggered truss 10th floor | 0.715 | 15.015 | W10*45 | 29.837 | 0.0042 | **IO** | W10*68 | 54.819 | 0 | A to IO |
| staggered truss 10th floor | 0.286 | 6.006 | W10*45 | -29.8 | -0.004 | **A to IO** | W10*68 | -42.911 | 0 | A to IO |
| staggered truss 10th floor | 0.572 | 12.012 | W10*45 | -33.162 | -0.073 | **D (Collapsed)** | W10*68 | -243.37 | 0 | A to IO |
| staggered truss 9th floor | 0.286 | 6.006 | W10*45 | 29.775 | 0.003 | **A to IO** | W10*68 | 43.226 | 0 | A to IO |
| staggered truss 9th floor | 0.572 | 12.012 | W10*45 | 33.156 | 0.0717 | **D (Collapsed)** | W10*68 | 255.28 | 0 | A to IO |
| staggered truss 9th floor | 0.429 | 9.009 | W10*45 | -33.158 | -0.071 | **D (Collapsed)** | W10*68 | -240.17 | 0 | A to IO |
| staggered truss 9th floor | 0.715 | 15.015 | W10*45 | -29.822 | -0.004 | **IO** | W10*68 | -46.551 | 0 | A to IO |
| staggered truss 8th floor | 0.429 | 9.009 | W10*60 | 501.96 | 0.045 | **CP** | W10*68 | 266.58 | 0 | A to IO |
| staggered truss 8th floor | 0.572 | 12.012 | W10*60 | -502.87 | -0.046 | **CP** | W10*68 | -269.22 | 0 | A to IO |
| staggered truss 7th floor | 0.572 | 12.012 | W10*68 | 576.15 | 0.0469 | **CP** | W10*68 | 281.36 | 0 | A to IO |
| staggered truss 7th floor | 0.429 | 9.009 | W10*68 | -575.14 | -0.046 | **CP** | W10*68 | -265.79 | 0 | A to IO |
| staggered truss 6th floor | 0.143 | 3.003 | W10*68 | -593.06 | -0.104 | **E-(Collapsed)** | W10*88 | -702.92 | -5E-04 | A to IO |
| staggered truss 5th floor | 0.858 | 18.018 | W10*77 | 613.41 | 0.0061 | **D (Collapsed)** | W10*88 | 513.39 | 0 | A to IO |
| moment frame 10th floor | 0.05 | 0.3 | W16*31 | 375.8 | 0.0636 | **CP** | W21*83 | 1067.9 | 0 | IO |
| moment frame 10th floor | 0.95 | 5.7 | W16*31 | -375.82 | -0.064 | **C (Collapsed)** | W21*83 | -1225.7 | -0.002 | A to IO |
| moment frame 9th floor | 0.05 | 0.3 | W18*46 | 630.97 | 0.0562 | **D (Collapsed)** | W21*83 | 1240.7 | 0.0047 | IO |
| moment frame 9th floor | 0.95 | 5.7 | W18*46 | -630.8 | -0.056 | **D (Collapsed)** | W21*83 | -1244.1 | -0.005 | IO |
| moment frame 8th floor | 0.05 | 0.3 | W18*50 | 702.14 | 0.0554 | **E (Collapsed)** | W21*57 | 826.65 | 0.008 | IO |
| moment frame 8th floor | 0.95 | 5.7 | W18*50 | -702.78 | -0.055 | **E (Collapsed)** | W21*57 | -829.58 | -0.009 | IO |
| moment frame 7th floor | 0.05 | 0.3 | W18*60 | 855.19 | 0.0548 | **E (Collapsed)** | W21*57 | 833.74 | 0.0103 | IO |
| moment frame 7th floor | 0.95 | 5.7 | W18*60 | -854.73 | -0.055 | **E (Collapsed)** | W21*57 | -833.26 | -0.01 | IO |
| moment frame 6th floor | 0.05 | 0.3 | W18*71 | 1009 | 0.0544 | **E (Collapsed)** | W21*68 | 1014.1 | 0.005 | IO |
| moment frame 6th floor | 0.95 | 5.7 | W18*71 | -1008.3 | -0.054 | **E (Collapsed)** | W21*68 | -1029.2 | -0.009 | IO |

Table 6.4: Hinge Properties and Plastic Rotation for Case 6rh Floor 5th frame Column Removal (Both Original and Retrofitted Models)

| TABLE 6.4 | | | ORIGINAL STRUCTURE | | | | RETROFITTED STRUCTURE | | | |
|---|---|---|---|---|---|---|---|---|---|---|
| **Beam Location** | **Relative Distance** | **Absolute Distance** | **Section** | **M3** | **R3-Plastic Rotatio** | **Hinge Status** | **Section** | **M3** | **R3-Plastic Rotation** | **Hinge Status** |
| | **Unitless** | **m** | | **KN-m** | **Radians** | | | **KN-m** | **Radians** | |
| staggered truss 10th floor | 0.429 | 9.009 | W10*49 | 394.37 | 0.0281 | **LS to CP** | W10*68 | 176.51 | 0 | A to IO |
| staggered truss 10th floor | 0.572 | 12.01 | W10*49 | -403.75 | -0.042 | **CP** | W10*68 | -193.42 | 0 | A to IO |
| staggered truss 9th floor | 0.429 | 9.009 | W10*49 | 402.79 | 0.0405 | **CP** | W10*68 | -169.52 | 0 | A to IO |
| staggered truss 9th floor | 0.572 | 12.01 | W10*49 | -395.3 | -0.029 | **LS to CP** | W10*68 | 196.77 | 0 | A to IO |
| staggered truss 8th floor | 0.429 | 9.009 | W10*77 | 641.66 | 0.0309 | **LS to CP** | W10*77 | 210.46 | 0 | A to IO |
| staggered truss 8th floor | 0.572 | 12.01 | W10*77 | -653.83 | -0.042 | **CP** | W10*77 | -230.33 | 0 | A to IO |
| staggered truss7th floor | 0.572 | 12.01 | W10*77 | 653.52 | 0.0413 | **CP** | W10*77 | 235.04 | 0 | A to IO |
| staggered truss 7th floor | 0.429 | 9.009 | W10*77 | -642.68 | -0.032 | **LS to CP** | W10*77 | -202.17 | 0 | A to IO |
| staggered truss 6th floor | 0.143 | 3.003 | W10*88 | -786.46 | -0.102 | **E (Collapsed)** | W10*10( | -583.96 | 0 | A to IO |
| moment frame 10th floor-left | 0.95 | 5.7 | W16*31 | 375.76 | 0.0636 | **C (Collapsed)** | W21*83 | 1223.3 | 0.0011 | A to IO |
| moment frame 10th floor-left | 0.05 | 0.3 | W16*31 | -374.54 | -0.039 | **CP** | W21*83 | -1046 | 0 | A to IO |
| moment frame 10th floor-rigth | 0.05 | 0.3 | W16*31 | 375.75 | 0.0636 | **C (Collapsed)** | W21*83 | 1223.3 | 0.0011 | A to IO |
| moment frame 10th floor-rigth | 0.95 | 5.7 | W16*31 | -374.6 | -0.039 | **CP** | W21*83 | -1046.1 | 0 | A to IO |
| moment frame9th floor-left | 0.95 | 5.7 | W18*40 | 701.75 | 0.0554 | **D (Collapsed)** | W21*83 | -17.097 | 0 | A to IO |
| moment frame 9th floor-left | 0.05 | 0.3 | W18*40 | -701.89 | -0.055 | **E (Collapsed)** | W21*83 | 1227 | 0.0019 | A to IO |
| moment frame 9th floor-rigth | 0.95 | 5.7 | W18*40 | 701.88 | 0.0554 | **D (Collapsed)** | W21*83 | -1212.9 | 0 | A to IO |
| moment frame 9th floor-rigth | 0.05 | 0.3 | W18*40 | -701.92 | -0.055 | **E (Collapsed)** | W21*83 | 1227 | 0.0019 | A to IO |
| moment frame 8th floor-left | 0.95 | 5.7 | W18*46 | 631.08 | 0.0559 | **E (Collapsed)** | W21*57 | 810.61 | 0.0029 | IO |
| moment frame 8th floor-left | 0.05 | 0.3 | W18*46 | -631.26 | -0.056 | **E (Collapsed)** | W21*57 | -807.37 | -0.002 | A to IO |
| moment frame 8th floor-rigth | 0.95 | 5.7 | W18*46 | 545.12 | 0.0566 | **E (Collapsed)** | W21*57 | -807.4 | -0.002 | A to IO |
| moment frame 8th floor-rigth | 0.05 | 0.3 | W18*46 | -545.53 | -0.057 | **E (Collapsed)** | W21*57 | 810.65 | 0.0029 | IO |
| moment frame 7th floor-left | 0.05 | 0.3 | W18*50 | 545.2 | 0.0566 | **E (Collapsed)** | W21*57 | -810.06 | -0.003 | IO |
| moment frame 7th floor-left | 0.95 | 5.7 | W18*50 | -545.61 | -0.057 | **E (Collapsed)** | W21*57 | 812.12 | 0.0034 | IO |
| moment frame 7th floor-rigth | 0.05 | 0.3 | W18*50 | 702.05 | 0.0554 | **E (Collapsed)** | W21*57 | 812.15 | 0.0034 | IO |
| moment frame 7th floor-rigth | 0.95 | 5.7 | W18*50 | -702.08 | -0.055 | **E (Collapsed)** | W21*57 | -810.09 | -0.003 | IO |
| moment frame 6th floor-left | 0.05 | 0.3 | W18*50 | 702.08 | 0.0554 | **E (Collapsed)** | W21*57 | -810.43 | -0.003 | IO |
| moment frame 6th floor-left | 0.95 | 5.7 | W18*50 | -701.89 | -0.055 | **E (Collapsed)** | W21*57 | 813.72 | 0.0039 | IO |
| moment frame 6th floor-rigth | 0.05 | 0.3 | W18*50 | 630.93 | 0.0559 | **E (Collapsed)** | W21*57 | 813.72 | 0.0039 | IO |
| moment frame 6th floor-rigth | 0.95 | 5.7 | W18*50 | -630.52 | -0.056 | **E (Collapsed)** | W21*57 | -810.44 | -0.003 | IO |

When the column was removed in 5th frame, the bending moments in the chords were decreased dramatically, whereas increase in the bending moments was observed in the spandrels after strengthening the model. Therefore after increasing the moment frame beams stiffness, they will parcicipate in structural rebustness more than truss chords at this stage. This is an indication that trusses are more involved in structural robustness at outer frames wherase the moment frame beams (spandrels) are more active to absorb the redundant bending moments resulting from removing a column from central frames.

Taking the hinge properties into account, Figures 6.13 and 6.14 and 6.15 show the results of a beam plastic hinge and Moment-Rotation property at truss chord Number 125 (Figure 6.5) in the original structure. The plastic hinge was formed at a distance of 3 meters from the column.

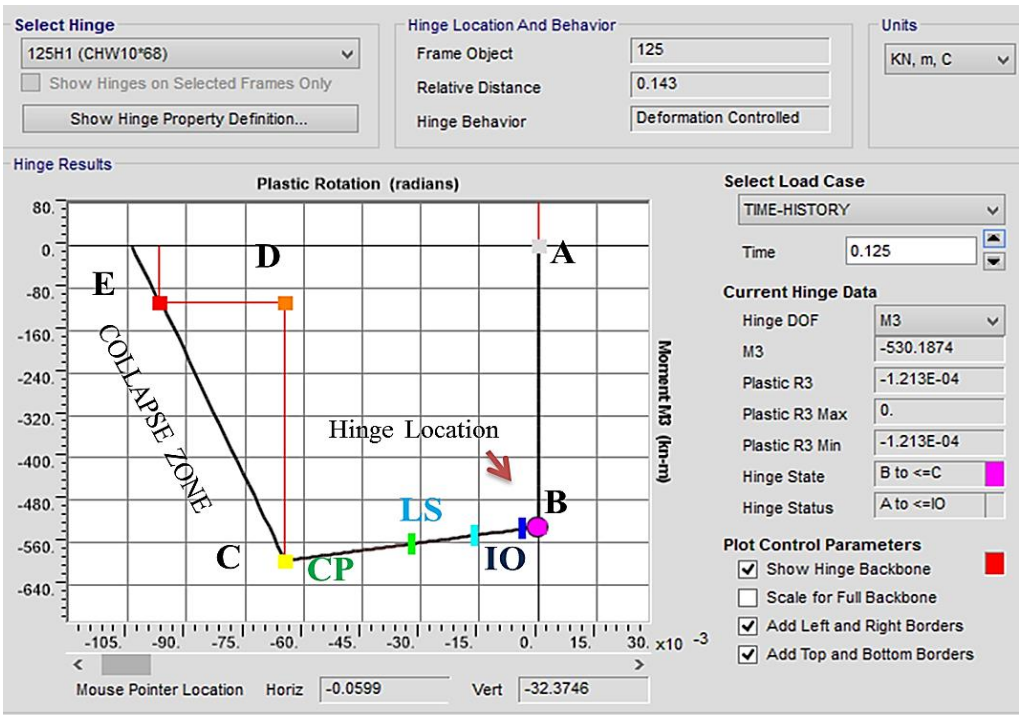

Figure 6.13: Moment-Rotation Table of Truss Chord Number 125 at T=0.12s in the Original model (distance from column connection=3m)

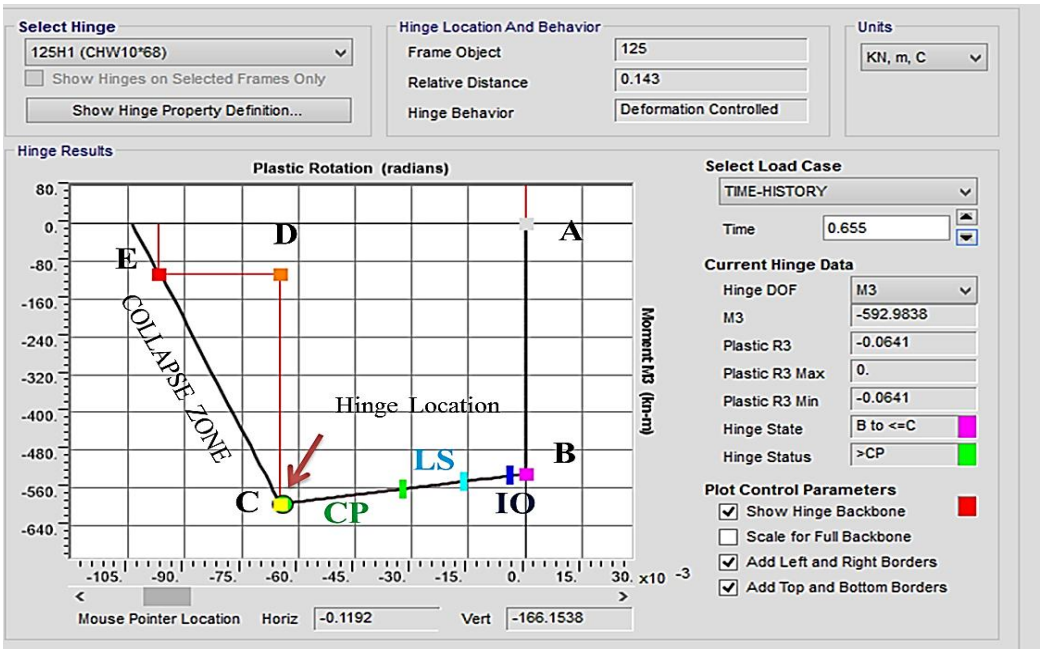


Figure 6.14: Moment-Rotation Table of Truss Chord Number 125at T=0.655s in the Original model (distance from column connection = 3m)

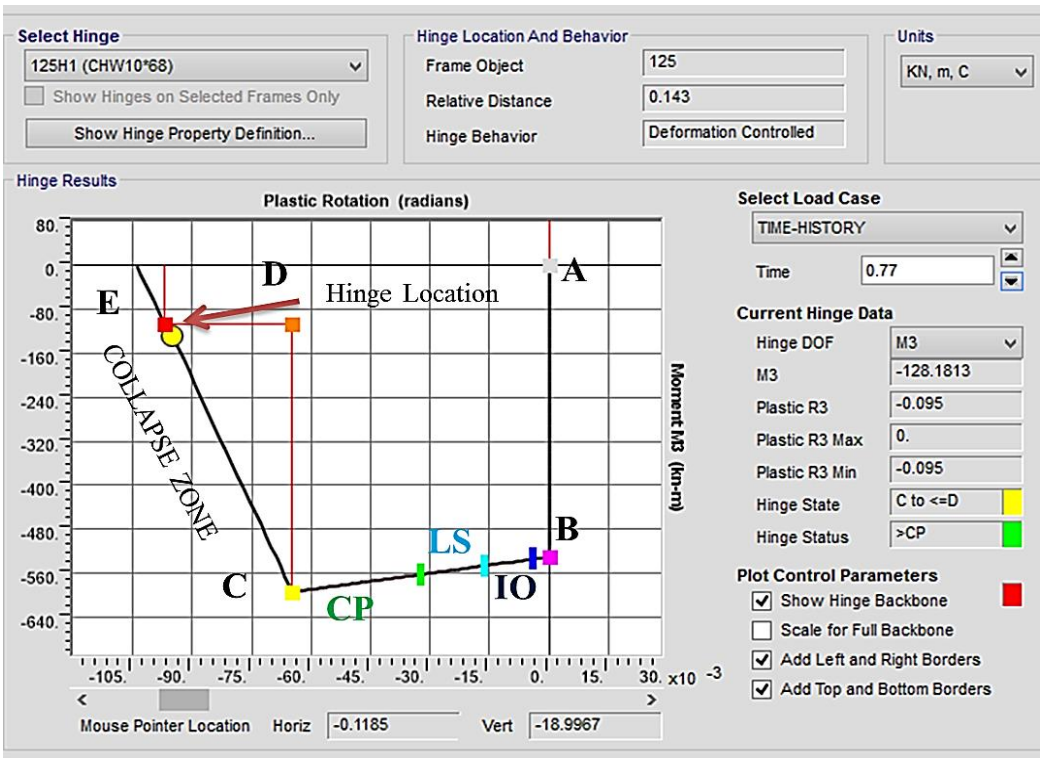


Figure 6.15: Moment-Rotation Table of Truss Chord Number 125 at T=0.77s in the Original model (distance from column connection = 3m)

By following these figures, some details about the behavior of the hinges can be produced:

- The Skeleton Path of the plastic hinge indicates Moment-Rotation data of the hinge. On this skeleton the pink point refers to the first yield and the moment relating to this point is the yield moment. This point is shown by B letter. Between points B and C, Strain Harding occurs. On this line, the first point which is in blue color refers to the Immediate Occupancy (IO) stage and the second and third points with the cyan and green colors belong to the Life Safety (LS) and Collapse Prevention (CP) stages respectively. Point C which is the limit border and defined by the UFC 2013 is the Collapse happening point. All the plastic hinges are supposed to take place before this point otherwise they will be categorized as failed hinges.
- The red line shown in Figure 6.13 is the Actual Path of the beam plastic hinge. It is obvious that this path which belongs to the *W10×68* (the beam number 125 in the original structure) does not exactly coincide with its Skeleton path after point C (Collapse).
- Figure 6.13, shows the status of the plastic hinge developed on the $6^{th}$ floor chord number 125 in the Original Model with *W10×68* section at time *T=0.12s*. At this time the hinge is before the IO stage (point B) which is defined by ***Yielding Moment***. At this stage the chord has a bending moment equal to $M_3$= 512.2 *kN.m* and the plastic rotation is as small as $\Theta_p$ = 0.0001213 Radians.
- Figure 6.14 shows the plastic hinge formation at time *T= 0.655 sec*. At this time the plastic hinge has reached to the end border of CP (Collapse

Prevention) stage (point C) point C defined as ***Ultimate Moment*** and corresponding Plastic Rotation. At this stage, the bending moment, $M_{3,}$ increased to 592.98 *kN.m* where the plastic rotation is equal to $\Theta_p$=0.0641 Radians. Therefore the plastic hinge is moving on BC line from *T1= 0.12 s to T2 = 0.655* s. This line belongs to the ***Strain Hardening*** Zone where the stress increases with increasing the Plastic Deformation. It was observed that the bending moment was increased from 512.2 *kN.m,* to 592.98 *kN.m* whereas; in the same time the plastic rotation was increased approximately by 528 times (from 0.0001213 radians to 0.0641 radians). At this time the beam is still stable and the $M_3$= 592.98 *kN.m* is the ultimate moment capacity of the beam before fracture happens. Any increases in loads affecting the truss chord can lead to a bigger plastic rotation and consequently to inelastic failure of the chord.

- If the time-history analysis continues after time 0.655s, the beam starts entering to the failure zone (CD and DE lines). The chords actual path coincides with its skeleton path from yield stress point until the end of CP stage. But these paths do not coincide (Figure 6.15) as plastic hinge enters to the collapse zone. It is clear that these paths are different for each beam and column plastic hinge properties. For a beam plastic hinge, the actual path follows exactly the skeleton path, while for a column plastic hinge; the actual path usually deviates from the skeleton path because of the influence of the normal force on the moment-plastic rotation relationship [25]. Figure 6.16 shows the plastic hinges belonging to a column from Row B at top and the beam attached to it at top corner floor. The actual path and skeleton path of both elements are illustrated in the Figure (6.16).

It can be seen in Figure 6.16 (b) that the plastic hinge of the column is in the IO stage and the actual path deviate from skeleton path around Immediate Occupancy zone. Similarly, the plastic hinge actual path of the beam attached to the column deviate from skeleton path at a zone between LS (Life Safety) and CP (Collapse Prevention) stages. (Figure 6.16).

At the final Stage (figure 6.15), the bending moment was dropped to $M_3$= 128.18 *kN.m* whereas the plastic hinge was reached to 0.095 Radians. In this zone a neck forms where the local cross-sectional area becomes significantly smaller than the original. The ratio of the tensile force to the true cross-sectional area at the narrowest region of the neck is called the true stress. The ratio of the tensile force to the original cross-sectional area is called the engineering stress. If the stress–strain curve is plotted in terms of true stress and true strain the stress will continue to rise until failure. Eventually the neck becomes unstable and the member fractures.

If the specimen is subjected to progressively increasing tensile force it reaches the ultimate tensile stress and then necking and elongation occur rapidly until fracture. If the specimen is subjected to progressively increasing length it is possible to observe the progressive necking and elongation, and to measure the decreasing tensile force in the specimen. Therefore the beam plastic hinge path located beyond point C is where the W10×68 chord starts to Necking and reaching to the failure point.

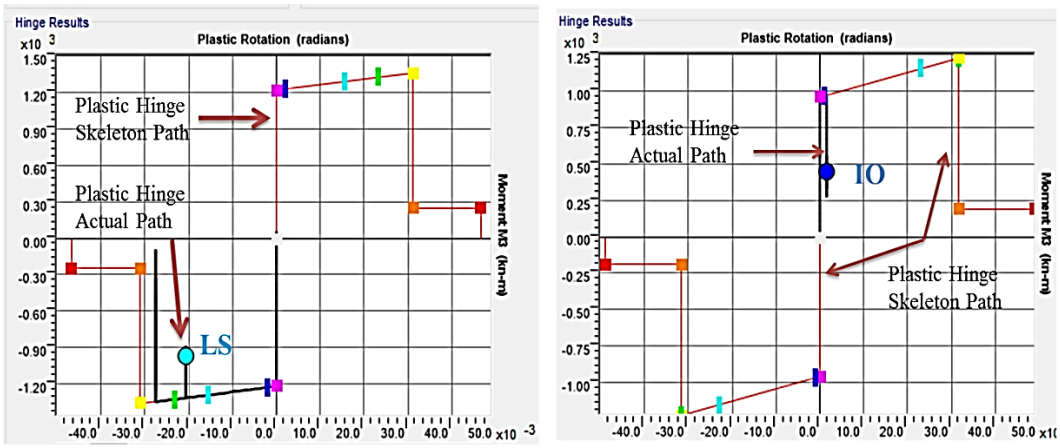


(a) (b)

Figure 6.16: Plastic Hinge Paths, (a) Beam attached to the Corner, 9th floor column in the original structure – (b) Row B frame, top floor column in the original structure

The UK guidance for design against disproportionate collapse (Review of International Research on Structural Robustness and Disproportionate Collapse) [29], categorizes the structural analysis into three forms. First category refers to using a linear elastic material model for design and to examine the over-stressing of members. The second category is the elastic-perfectly plastic material response. This method must be applied when the minor levels of plasticity and significant load shedding to alternative load paths occurs.

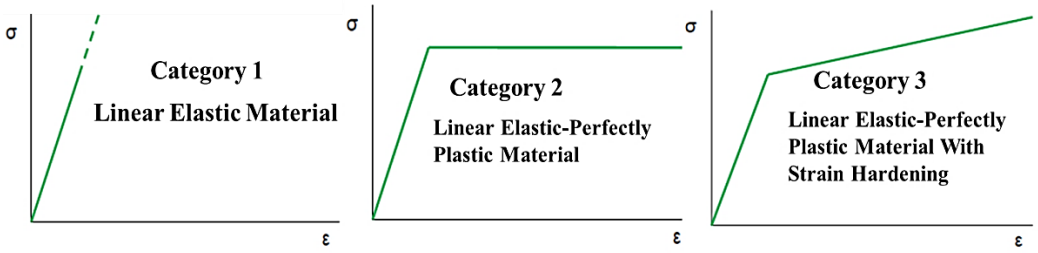


Figure 6.17: Different Material Properties for Robustness Design

And finally the last category is about the circumstances where the modeling of strain hardening is desirable in the plastic phase (Figure 6.17). This method is more precise than the second one as in this case the effect of material strain hardening and gaining the resistance after the shock of losing the structural element will be considered. Table 5.6 of ASCE 41 guideline was used to determine the plastic hinges properties for all column and beam elements and truss members. Consequently the behavior of the plastic hinges is similar to those hinge properties shown in Figures 6.13, 6.14 and 6.15. Based on the above descriptions, the inclined portion (BC) of the defined plastic hinges represents the strain hardening part of the material nonlinearity and therefore in this context the nonlinear dynamic analysis part would be coinciding with category 3 of the UK guidance for design against disproportionate collapse.

## 6.4 Top Floor Columns Were Removed

To calculate the building's maximum inelastic deformation, the UFC 2013 [2] suggests removing a column from Top Floor. As discussed earlier, at higher levels, less structural elements are involved to resist against progressive collapse and therefore the maximum settlement of the beams surrounding the column removal zone will occur.

Figures 6.18 to 6.21 show the inelastic deformations of the top floor column removal scenarios. When the vertical displacement of the joint above the column removals are compared with the lower story column removal scenarios discussed at sections 6.2 and 6.3, it can be concluded that maximum deflections took place at top floor beams. Because of the big deflections and less structural members

involved above the removed column, the plastic hinges were activated on some columns which are shown in Figures 6.18 to 6.21.

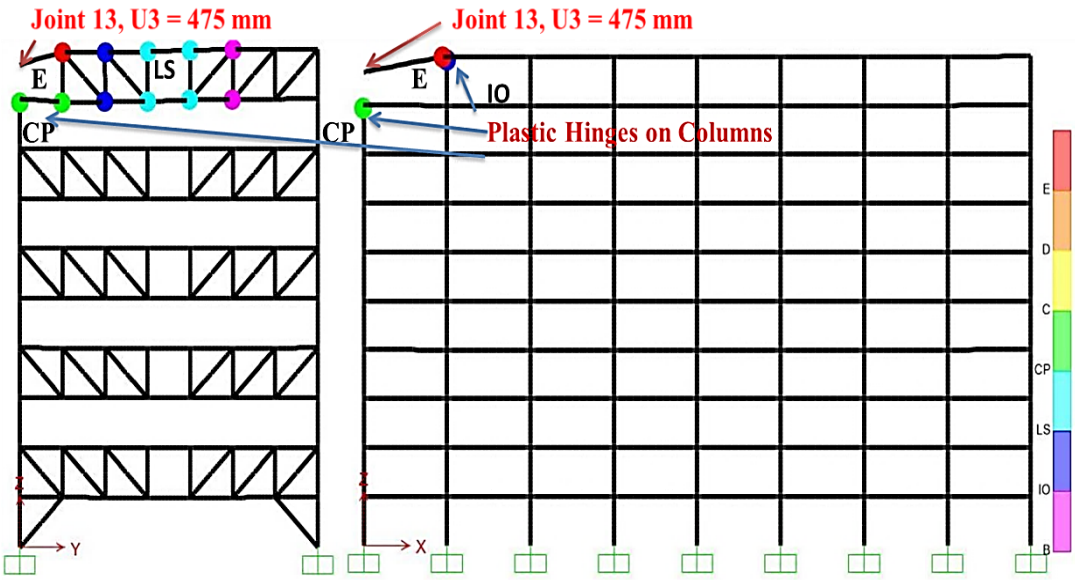


Figure 6.18: Inelastic Deformations at First Frame Top Floor in the Original Model

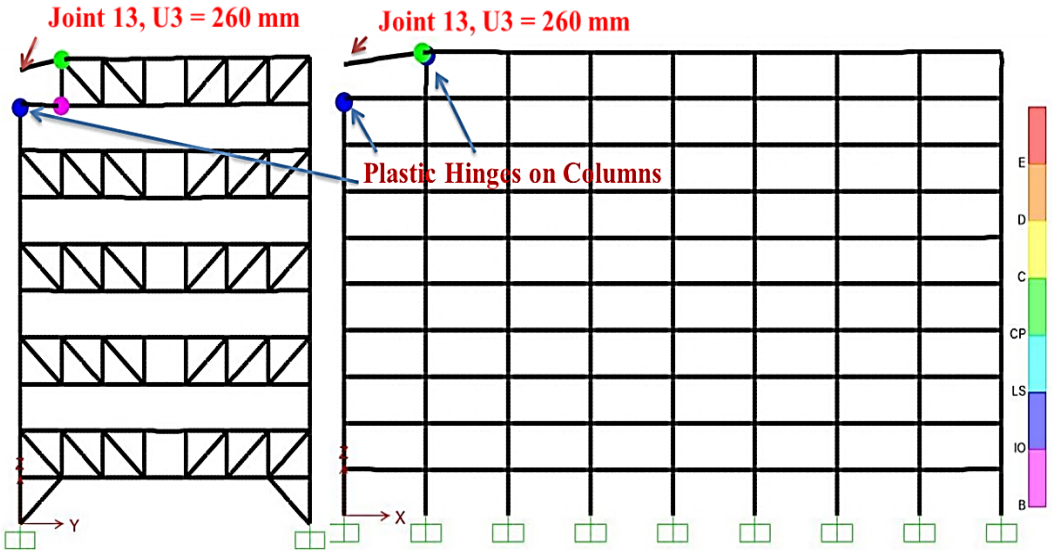


Figure 6.19: Inelastic Deformations at First Frame Top Floor in the Retrofitted Model

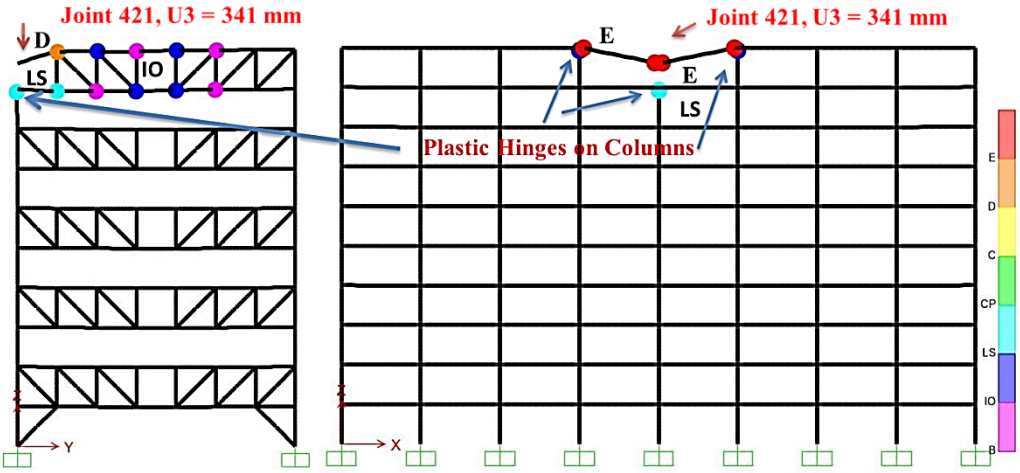


Figure 6.20: Inelastic Deformations at 5th Frame Top Floor in the Original Model

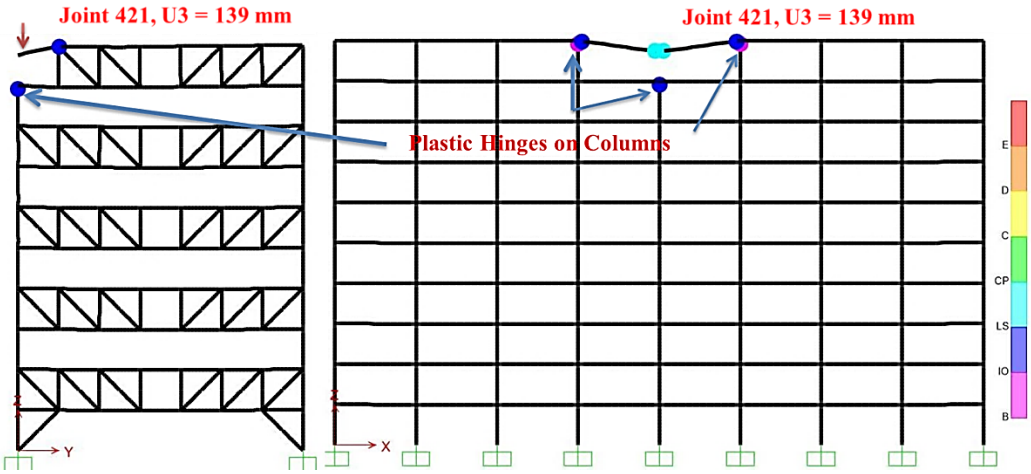


Figure 6.21: Inelastic Deformations at 5th Frame Top Floor in the Retrofitted Model

Figure 6.18 shows the removal corner column at top floor in the original model. The results from nonlinear time history analysis for 6 seconds, indicates the formation of plastic hinges on 9$^{th}$ floor chord and on 10$^{th}$ floor spandrel and chord. It is evident from Figure 6.18 that the top chord showed failure because of a plastic hinge formation near the first diagonal and vertical connection to the chord. Generally bending moments are close to zero at these points but consider Figure 6.18; it is obvious that five plastic hinges were formed at truss members (diagonal, vertical and the chord) connection joint. The main reason is that the

truss chords are working like continuous beams and whole truss system is acting as a huge beam with a length equal to 21 meters and depth of 3 meters. In figures 6.19, 6.20 and 6.21 the plastic hinge activations on columns for other member removals are clearly illustrated.

Figure 6.22 (a and b) shows the maximum bending moments for the nonlinear static load case and time history load case respectively. As discussed in Chapter 4, the nonlinear static load case consists of load combination as $1.2 \times DL + 0.5 \times LL + 0.2 \times WL$ and the column is not removed when this load case is applied. Hence the column will be removed during time-history analysis afterwards. It is obvious from Figure 6.22 that, the maximum bending moments took place at mid-spans between each couple of verticals, while after removal of the column and application of the time-history analysis, the maximum bending moments happened almost at vertical connection points at the $10^{th}$ and $9^{th}$ story chords. As during plastic hinge definition for beams, the bending moment $M_3$ was considered; therefore these big changes in bending moments in chords are the main reason of plastic hinge formations.

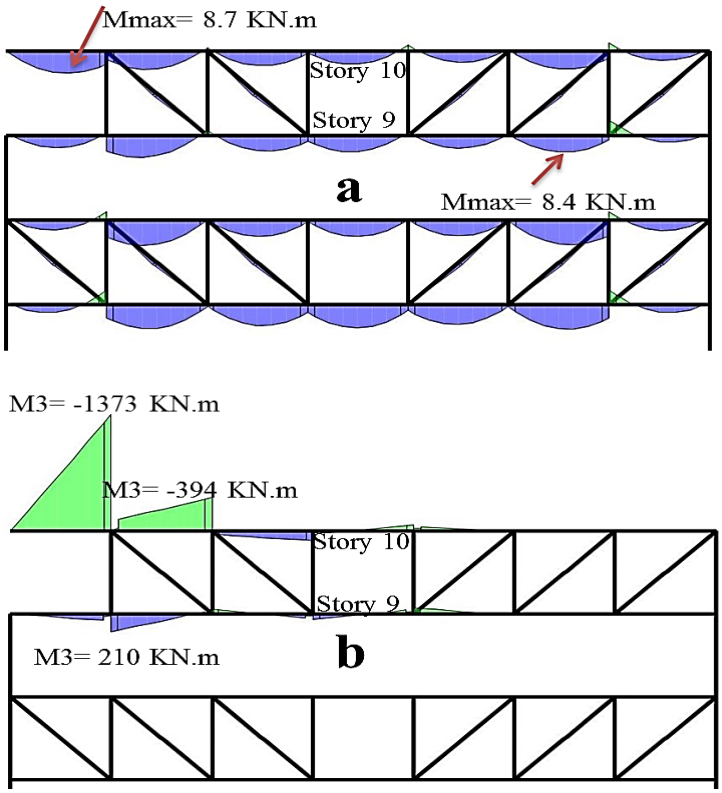


Figure 6.22: Maximum Bending Moment for chords at 10 and 9 stories. (a) Nonlinear Static Load Case (b) Nonlinear Dynamic Time-History Load Case

Unlike the column removals at 6th floor and ground floor, at this stage few plastic hinges were developed on the columns. Figure 6.18 shows the formation of a plastic hinge which is located in a column at first frame 9th floor. The hinge is at a distance of $0.05 \times L$ (L is the Length of the column) and is in CP level. The second plastic hinge has emerged on the same position of the 2nd frame top floor column (see Figure 6.18). The first column is located beneath the removed column of the first frame at the top floor. It was observed that the plastic hinge formations on the columns are mostly due to the increase in the axial load, *P*. Figure 6.23 shows the plastic hinge properties of $W12 \times 106$ column section at 9th floor. The lower bound strength ($P_{CL}$) for $W12 \times 106$ section was calculated according to Chapter 3 and is shown in Table 3.4. The lower bound strength was equal to $P_{CL}$ =1578.4 Kips or 7019 KN (7633.149× 0.9198).

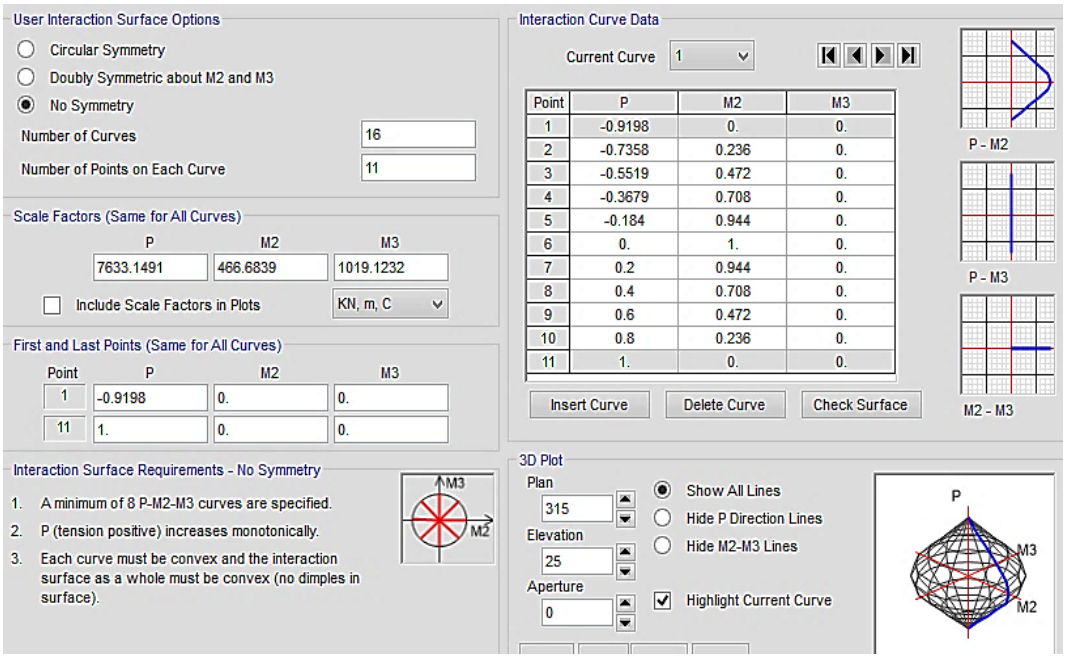


Figure 6.23: Column hinge Properties for W12x106 sections

Based on AISC-LRFD Manual of Steel Construction [4], the interaction of compression and flexure in beam-columns with singly and doubly symmetric cross sections is governed by Equations 6-1 and 6-2, repeated here for convenience:

For $\frac{\boldsymbol{P_u}}{\boldsymbol{\varphi P_n}} \geq 0.2$:

$$\frac{\boldsymbol{P_u}}{\boldsymbol{\varphi P_n}} + \frac{8}{9}\left(\frac{\boldsymbol{M_{ux}}}{\boldsymbol{\varphi_b \times M_{nx}}} + \frac{\boldsymbol{M_{uy}}}{\boldsymbol{\varphi_b \times M_{ny}}}\right) \leq 1 \qquad (6.1)$$

For $\frac{\boldsymbol{P_u}}{\boldsymbol{\varphi P_n}} \leq 0.2$:

$$\frac{\boldsymbol{P_u}}{\boldsymbol{2\varphi P_n}} + \frac{8}{9}\left(\frac{\boldsymbol{M_{ux}}}{\boldsymbol{\varphi_b \times M_{nx}}} + \frac{\boldsymbol{M_{uy}}}{\boldsymbol{\varphi_b \times M_{ny}}}\right) \leq 1 \qquad (6.2)$$

Where

$P_u$ = required tensile strength; i.e., the total factored tensile force, kips

$\phi P_n$ = design tensile strength, $\phi_t P_n$, kips

$\phi$ = resistance factor for tension, $\phi_t$ = 0.90

$P_n$ = nominal tensile strength, kips or *kN*

$M_u$ = required flexural strength; i.e., the moment due to the total factored load, kip-in or kip-ft or KN-m. (Subscript *x* or *y* denotes the axis about which bending occurs.)

$\phi_b M_n$ = design flexural strength, kip-in. or kip-ft or *kN-m*

$\phi_b$ = resistance factor for flexure = 0.90

$M_n$ = nominal flexural strength, kip-in. or kip-ft or *kN-m*.

The results from the time-history analysis for the case of the upper column removed showed that the maximum axial load in the 9th floor column became *Pu* = 1864 *kN* while the axial capacity $P_{CL}$ = 7019 *kN*. Therefore the $\frac{P_u}{\varphi P_n}$ will become 0.295. This indicates that the plastic hinge formation on top of the column is not due to the axial load strength of the column.

The major bending moment ($M_3$) in X direction is equal to -64 *kN* and the calculated flexural capacity of the $W12 \times 106$ section is equal to 1019 *kN-m* as shown in Figure 6.23. Therefore the minor axis bending moment ($M_2$) in Y direction pushes the section to yield and behave in plastic manner. Figure 6.24 shows the bending moment of the column about the weak axis which is equal to 739 *kN* at time 0.335 sec. According to Figure 6.23, the flexural capacity of the section is equal to 467 *kN*.

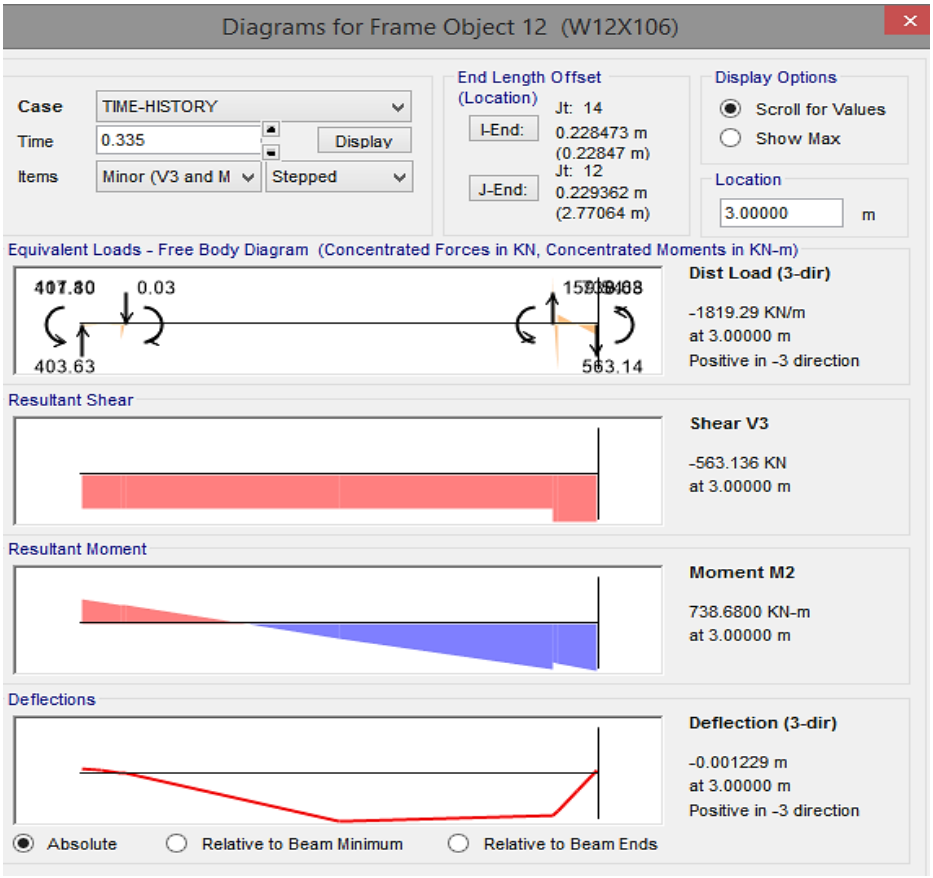


Figure 6.24: Nominal Bending Moment of the 9th Floor Column along Weak Axis (M2)

Consequently it was shown that the ratio of the $\frac{M_{ux}}{\varphi_b \times M_{nx}}$ (Equation 6.1) which was equal to 1.79 ($\frac{M_{ux}}{\varphi_b \times M_{nx}} = \frac{739}{0.9 \times 467} = 1.76$) will result to a plastic hinge formation on top of the column as discussed before. The chords had to be attached to the web of columns [8] because the spandrels will be connected to the flange of the column in moment frame direction. The development of a higher moment about the minor axis is due to the 9$^{th}$ floor chord attached to the web of column. After removing the 10$^{th}$ floor column, the axial load of this column will be transmitted from upper chord truss to the lower chord truss by diagonals and verticals. This will increase the shear force of the 9$^{th}$ floor chord and finally the

weak axis moment ($M_2$) will cause eccentricity at truss chord's connection with the column.

## 6.5 Dynamic Response and Vertical Displacements

The sudden removal of a load bearing elements from the structure causes immediate redistribution of gravity loads to the neighboring beams and columns. Since the removal of the column is sudden therefore, the loads will trigger a shock on the structure. The nonlinear dynamic analysis results indicate that maximum deflections happen at higher levels and if a column being removed from a corner frame, in most of times the deflection will be bigger in comparison with the same column removal level from middle frames. Therefore at the corners of the building there might be a higher failure capacity due to bearing element loses than the central areas. When the nonlinear dynamic analysis are compared to the linear static analysis, it is observed that the structure analyzed using nonlinear dynamic method shows smaller bending moments, smaller axial forces and smaller vertical deflections in the surrounding elements. To be more precise, the maximum elastic deflection obtained in Chapter 5 (linear static analyses) belongs to the corner frame at top floor where the joint above the column removal location had a vertical settlement of $U_3$ = -704 *mm*. When the non-linear dynamic analysis were performed, the vertical displacement of $U_3$ = -475 *mm* was recorded at the same location. Previous research done by other people using earlier versions of the GSA and the UFC to compare the linear static and nonlinear dynamic progressive collapse analysis, in most cases found that the dynamic analysis results to higher levels of the vertical deflections. Kokot and Anthoine [25] carried out static and dynamic analysis to a flat plate structure for the potential progressive collapse. The authors used the GSA 2003 and the UFC 2005 Guidelines for their analysis.

In their research they have found that in most cases the nonlinear dynamic analyses result in bigger deflections in the model structures. The conservative load increases offered by the UFC 2013 [2] and the GSA 2013 [14], are the main reason why the linear static analyses results led to bigger deflections in this research. *Jinkoo Kim* and *Taewan Kim* did a research on "Assessment of progressive collapse-resisting capacity of steel moment frames [18]" using the GSA 2003 and UFC 2005 Guidelines. Both these guidelines were adopted by *Shalva Marjanishvili* and *Elizabeth Agnew* in their research "Comparison of Various Procedures for Progressive Collapse Analysis [26]". In all these three studies the linear static procedure led to smaller structural deflections than the nonlinear dynamic method. However in this context, the new Load Increase Factors offered by the UFC 2013 and the GSA 2013 were used to calculate the dynamic factors for linear static procedure. Again it should be stated that the conservative load increase factors for linear static analysis offered by the GSA 2013 and the UFC 2013 are the main reason of bigger deflections in this analysis method in comparison with nonlinear dynamic analysis.

For the top floor corner column removal, the load increase factor becomes 3.783 by using the equation 5.2, ($\Omega_{LD} = 0.9\ m_{LIF} + 1.1$) Alternatively following the equation 5.1, $\boldsymbol{G}_{LD} = \Omega_{LD}\,[1.2D + (0.5\ L \text{ or } 0.2\ S)]$, the increased gravity loads for deformation-controlled actions for linear static analysis becomes 4.54×DL+1.8×LL. Obtaining higher bending moments and higher deflections in linear static procedure can be explained when this load combination of linear static method is compared to the nonlinear dynamic load case (1.2×*DL*+0.5×*LL*). It is obvious that new load increase factors in the UFC 2013 and the GSA 2013,

seem to lead the analysis to more conservative results than the nonlinear dynamic procedure which yields to more accurate results.

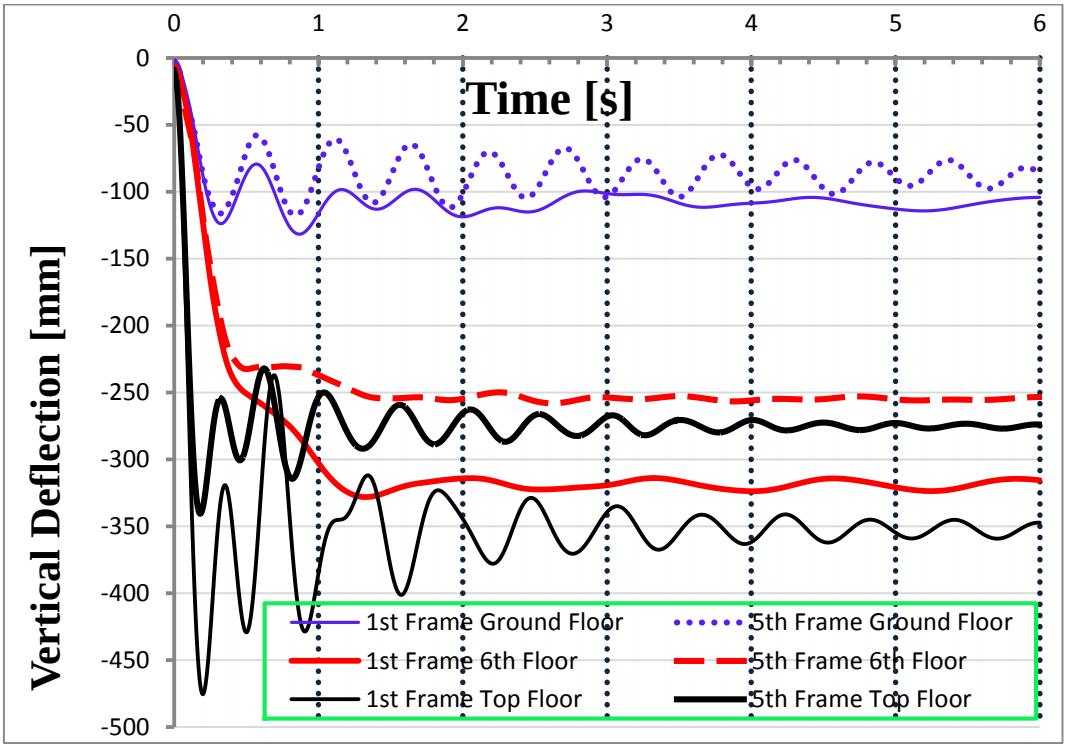


Figure 6.25: Comparison of Vertical Displacements at nodes above the column removal locations in the Original Model

Figure 6.25 compares the vertical displacements of the Original Model for different column removal scenarios. Time-history analyses were carried out for 6 seconds to get the maximum inelastic displacement in all the models. However, it can be seen that maximum deflection in all column removals took place during the first second. As shown in Figure 6.25, the solid and dashed blue lines belong to the ground floor column removal scenarios where the minimum vertical displacements happened. The maximum displacement obtained when a corner column at top floor was removed. As indicated in Figure 6.25, the black solid line represents the maximum displacement for the exclusion of the angle column at

highest floor which is $U_3$= -475 *mm*. Considering Figure 6.25, it can be concluded that the removal of the column at corners made more oscillations when compared to the middle column removal scenarios in the structure and the maximum oscillation happened at top floor corner column removal scenario. Furthermore, the oscillations at the corner of the structure continued until the end of the 6th second and at the end of the time-history analysis the structure was still in turbulence. By contrast, the oscillations at middle of the structure had bigger amplitudes and their duration took more time when compared to the corner column removal scenarios. It was also found out that the structure for the middle column removal scenarios behaved in stable manner before the time-history analysis finished.

It can be concluded that using different column removal sequences will cause to different force redistribution paths. Most researchers discussed on the catenary effects which resist against the progressive collapse. However, *Fu* [19], [30], [31] showed that the catenary effect can only be triggered when plasticity is adequately formed in the relevant beams. Different column removal scenarios will produce different plasticity forming paths which needs to be taken into the consideration in the plastic design of the composite frame buildings in resisting the progressive collapse.

Most of the researchers [18], [26], [32] focused on the progressive collapse analysis of bare steel frames without considering the contribution of the floor systems. Most of the researchers used 2-D models for the progressive collapse analysis and therefore such studies did not simulate the real structural

performance after the column removals. In this study the effect of concrete slab was taken into account in all analyses. For designing the slab, the steel rebar system was used and the Automatic Area Mesh option in the SAP2000 was adopted to force the 3-D model react similarly to real structural performance. Based on the experiments done by *Fu* [31], it was concluded that increasing the steel rebar in the concrete slab can increase the rotation capacity of the composite joint. This allows the plasticization of the steel member and therefore, increases the ductility of the joint. The increasing ductility increases the energy absorption capacity of the joints. Ductile joints allow for redistribution of internal forces within the structural system by enabling large deformations so that they are suitable for progressive collapse mitigation by transition from flexural loading to axial loading in the members and joints and initiating of a catenary action[31].

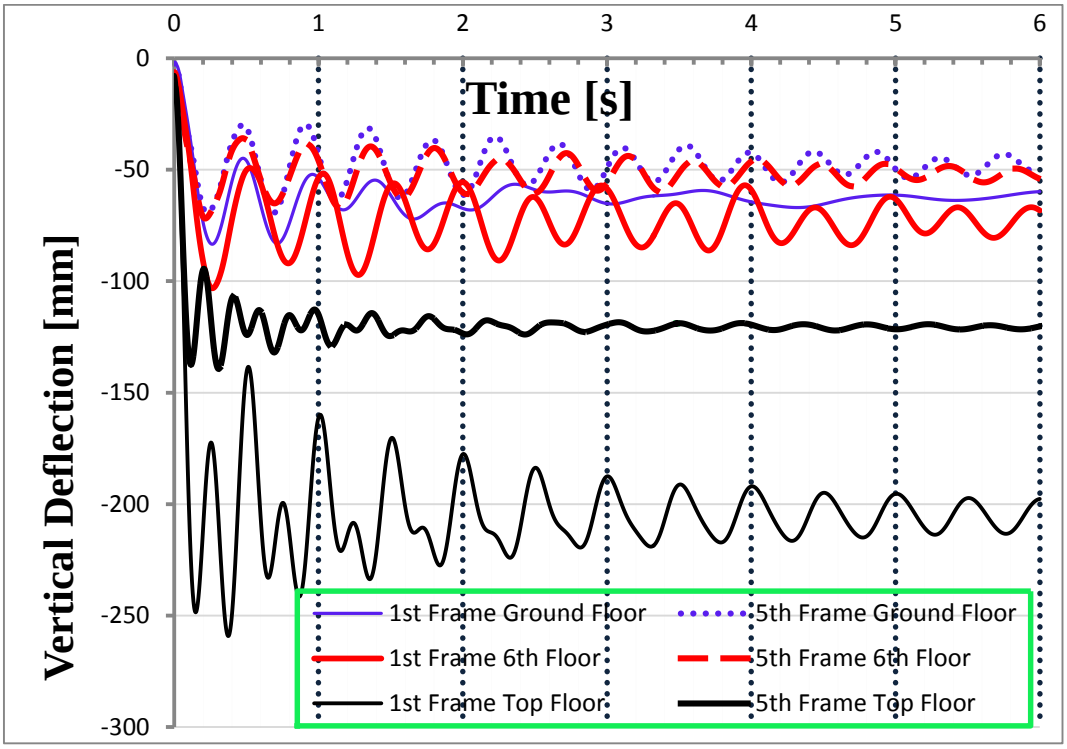


Figure 6.26: Comparison of Vertical Displacements at nodes above the column removal locations in the Retrofitted Model

Figure 6.26 compares the progressive collapse response of the retrofitted structure to different column removal scenarios. In the retrofitted structure, the weak columns (failed in the original structure) where were replaced by stronger sections. The vertical deflection of the structure in all locations has decreased as a consequence and apart from the top floor column removal scenario, deflections are approximately the same for other analysis. As shown in Figure 6.26, the $6^{th}$ floor deflection curve had oscillations for both the corner and middle column removal locations. Comparing this condition with the Fig 6.25, the original structure had fewer oscillations at $6^{th}$ floor. Figures 6.5 and 6.7 show that, the moment frame beams failed due to the plastic hinge formations after sudden column removal whereas in figures 6.5 and 6.11 the inelastic behavior of the changed sections goes under Collapse Prevention (CP) state as required by UFC 2013 [2]. It is very obvious that when the structural collapse happens also the beams are failed. In this case the slab will be more involved to absorb the energy stream distributed around column removal location. In the retrofitted structure, the spandrel beams (moment frame beams) exhibit less inelastic behavior and smaller plastic hinge formations and therefore more energy was transferred into them. In this case the catenary effect of the slab decreases and the structure will be more dependent to steel elements for progressive collapse robustness which leads to more structural oscillation.

The collapse in the truss system could not be only due to the failure of the chords or truss members. Based on AISC 14 design guideline, the truss members had to be connected to the chords by the gusset plates. These gusset plates are welded to the HSS sections and to the truss chords. A detailed analysis was developed in

ABAQUS and it was found that some of the gusset plates showed failure potential when the column was removed as they exhibit had high stresses as well (see Figure 6.27). As shown in Figure 6.27, a plastic hinge was formed on the gusset plate attached to the column, opposite to the removed column). The SAP2000 nonlinear analyses are not able to predict such failure mechanisms in the structure and therefore detailed finite element analysis were conducted and used to catch such failure potentials.

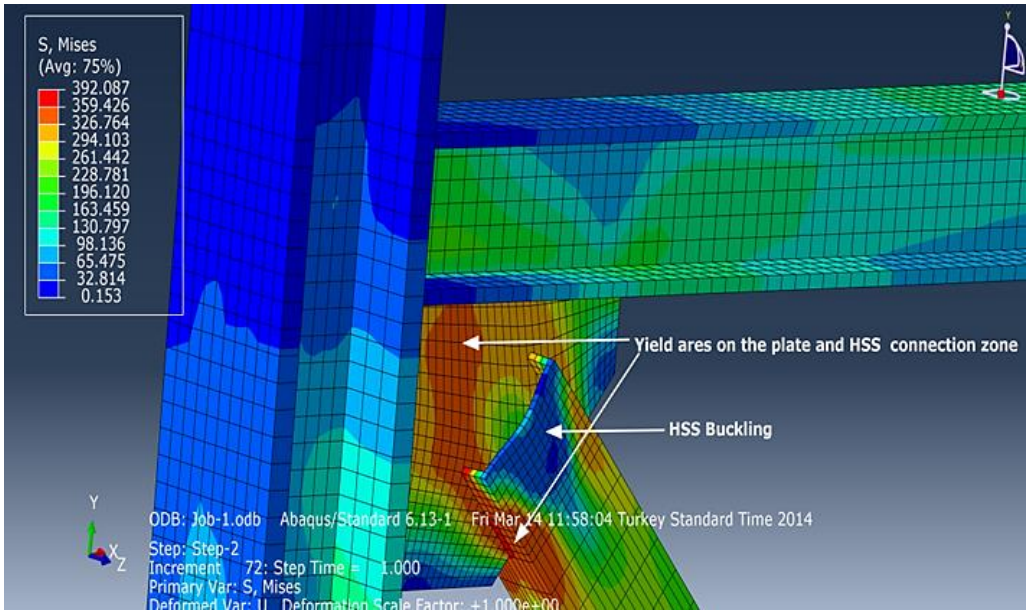

Figure 6.27: plastic hinge formation on the Gusset Plates

## 6.6 Ductility Demand Ratio

Ductility refers to the deformation ability of a component or a structure after yielding. Sudden loss in load bearing element can produce strong force streams throughout the neighboring components of the column removal location. This can lead to severe damages and force the structure to enter into the *elasto-plastic* stage and finally to a total collapse of the structure. Therefore the robustness ability of the structure directly affects the structural performance and repair costs. Ductility,

demand defined as the ratio of ultimate displacement to yield displacement, can be calculated according to Equation 6.1. The yield displacement is the structural deflection when the first plastic hinge activates and the ultimate displacement belongs to maximum plastic deflection due to column removal.

$$\mu = \frac{\boldsymbol{\Delta_u}}{\boldsymbol{\Delta_y}} \tag{6.3}$$

To assess the behavior of STS and MRF systems due to the loss of a bearing member, the ductility demand of both framing systems were calculated for the Original and the Retrofitted models and are illustrated in Table 6.5. According to this table, the ductility demand ratio was high when the angle column was detached. It was also seen that the ductility demand ratio shrinks in the retrofitted model for both framing systems. When compared to the original model In general, the ductility demand ratio of the MRF systems is less than STS. It was observed that for the column removal at top floor in the original structure the ductility demand has overpassed the acceptance criterion of 20 defined by GSA, whereas the ductility ratio of the MRF system was 3.3. It can be concluded that for this column removal case, the collapse process will start from staggered truss system direction.

According to Table 6.5, ductility demand of the STS and MRF systems were very different for the original structure whereas for the retrofitted structure, the ductility demand ratios were approximately the same. The results of nonlinear-dynamic analysis showed that, the first plastic hinges formed in the upper chords

when a column was removed from ground floor but immediately after a short time the next plastic hinges was developed on spandrel beams. However when a column was removed from $6^{th}$ and top floors, plastic hinges were activated on spandrels first and then on chords.

Table 6.5: Comparing Ductility demand Ratios for Different Column removals in Staggered Truss System (STS) and Moment Resisting Frames (MRF)

| Removed Column | Original Structure | | | | | | | | Retrofitted Structure | | | | | | | |
|---|---|---|---|---|---|---|---|---|---|---|---|---|---|---|---|---|
| | STS | | | | MRF | | | | STS | | | | MRF | | | |
| | yield displacement (mm) | Max displacement (mm) | location of first yielding | Ductility | yield displacement (mm) | Max displacement (mm) | location of first yielding | Ductility | yield displacement (mm) | Max displacement (mm) | location of first yielding | Ductility | yield displacement (mm) | Max displacement (mm) | location of first yielding | Ductility |
| 1st frame - 1st floor | 33 | 132 | 5th frame top floor chord | **4** | 66 | 132 | first floor spandrel between 1st and 2nd frames | **2** | 83 | 83 | no plastic hinges activated | **1** | 59 | 83 | first floor spandrel between 1st and 2nd frames | **1.25** |
| 1st frame - 6th floor | 35.4 | 460 | 3rd frame top floor chord | **13** | 84.2 | 460 | 7th floor spandrel between 1st and 2nd frames | **5.46** | 109 | 132 | 1st frame 6th floor chord | **1.2** | 78 | 132 | 7th floor spandrel between 1st and 2nd frames | **1.69** |
| 1st frame - top floor | 20.5 | 574 | 1st frame top chord | **28** | 173 | 574 | top floor spandrel between 1st and 2nd frames | **3.3** | 86 | 218 | 1st frame top floor chord | **2.53** | 151 | 218 | top floor spandrel between 1st and 2nd frames | **1.44** |
| 5th frame - 1st floor | 47 | 116 | 5th frame 9th floor chord | **2.47** | 66 | 116 | both spandrles between 4th-5th and 6th frames at first floor | **1.76** | 69 | 69 | no plastic hinges activated | **1** | 58 | 69 | both spandrles between 4th-5th and 6th frames at first floor | **1.05** |
| 5th frame - 6th flor | 67 | 364 | 6th floor chord | **5.4** | 81 | 364 | both spandrles between 4th-5th and 6th frames at 6th floor | **4.5** | 93.4 | 93.4 | no plastic hinges activated | **1** | 76 | 93.4 | both spandrles between 4th-5th and 6th frames at 6th floor | **1.23** |
| 5th frame top floor | 23 | 427 | 5th frame top chord | **18.6** | 110 | 427 | both spandrles between 4th-5th and 6th frames at top floor | **3.88** | 93 | 175.4 | 5th frame top floor chord | **1.9** | 93 | 175.4 | both spandrles between 4th-5th and 6th frames at top floor | **1.9** |

It was observed that in the original model, spandrel beams failed before the staggered truss chords. Therefore in the original model after a sudden column removal, the spandrel beams will overtake the major portion of the redundant forces distributed throughout the structure and after that these beams are yielded, the chords start to overtake the rest. In the retrofitted model, the ductility of both STS and MRF systems are approximately the same which means that, they will start to yield simultaneously.

From all above mentioned issues it can be concluded that, when a structure is only designed to withstand against gravity and lateral loads may have high collapse potential and the different framing systems may not function respectively.

Contrastingly, in the model designed for regular loading conditions and for criterions allocated by UFC and GSA guidelines, no failure mechanism was observed after removing columns in different locations. The STS-MRF structural framing systems in both directions collaborate accordingly to resist against progressive collapse occurrence. This collaboration will help the structure to regain its robustness after that the structure started inelastic behavior.

# Chapter 7

# CONCLUSION

This work presented the results of an extended study on the Staggered Truss System (STS) building that has been designed and analyzed for the potential progressive collapse mechanism by the removal of several critical load bearing elements. In This study, ten story structure equipped with both STS and MRF structural systems was designed based on regular design procedures following the AISC-LRFD steel design code [4]. Then, the potential of the structure for the progressive collapse were analyzed using both the linear static and nonlinear dynamic time history methods using SAP2000 and ABAQUS software for the staggered truss system. The vulnerable portions of both structural systems due to a column removal were identified according GSA and DOD design guide lines. The results from the collapse analyses, applying both linear static and nonlinear dynamic methods, were used to model and design new structure capable of maintaining its integrity after the removal of the critical column. The developed two new structural models were compared to find out which type of analysis is more precise economical design.

Because the main concern of this study is to evaluate the story height truss system elastic, elasto -plastic and plastic behavior, the ABAQUS finite element software was used to model a full 3-D truss. This was done by modeling a portion of the staggered truss system located between the $5^{th}$ and $6^{th}$ floors of the Original model

using solid sections in ABAQUS. The ABAQUS results were used to compare and assess of the failure mechanisms in the sections and propose a strengthening method for the failed section in a cost effective manner. The results of the analysis are summarized below:

- Both the linear static and nonlinear dynamic analyses results showed that, when the column is removed, the forces are mainly redistributed to the adjacent beams. The beams situated further far from the removed column were less affected. When the stiffness of MRF beams are increased, they participate in structural robustness more than truss chords. The trusses are more involved in structural robustness at outer frames while the moment frame beams (spandrels) are more active to absorb the redundant bending moments resulting from removing a column from central frames.
- Although the Staggered Truss System was designed based on AISC-LRFD and AISC 14 design Giude lines, the structure was still vulnerable to collapse stemming from column removals and needed to be strengthened according to UFC guidelines.
- The maximum vertical displacement happened for a column removal from a corner frame at the top floor
- The maximum displacement defined by linear static and nonlinear dynamic analyses at joints directly above the removed column were 704 mm and 475mm respectively.
- The displacements in linear static analyses were greater than nonlinear dynamic analysis. The new dynamic load factors proposed for linear static analysis by the GSA2013 and UFC2013 led to a conservative results for linear analysis.

- Despite these conservative results for linear static analyses, the sections obtained for refrofitted model using linear static method were also bigger than those obtained by nonlinear dynamic analysis. This suggests that the nonlinear dynamic analysis not only yields in more accurate results to reveal the collapse potential at different portions of the structure, but also it is more economical to allocate this method for designing structures against progressive collapse.
- The linear static analysis identified failure for some columns in the original model where in the nonlinear dynamic analysis, the plastic hinges formed on those column were below the acceptance criteria (LS) required by the UFC 2013.
- It was observed that, the potential for progressive collapse was high when a corner column at the top floor was removed. When a column removal scenario is considered at lower floors, the potential for progressive collapse decreases.
- Both analyses identified the vierendeel openings as a critical zone in story height trusses. However, in linear static analyses the deflection of the truss chords had an inclination trend toward the removal location. By contrast, the nonlinear dynamic analysis showed different truss behaviors. In this case, most critical plastic hinge for adjacent chord took place close to the first vertical member. At the top trusses, the critical plastic hinges happened around vierendeel panels.
- Based on nonlinear dynamic results, the chord attached to the removed column will fail at a point close to the removal location. In this case the neighboring vertical and diagonals have the propensity to transmit the load to the bottom chord and lead it to collapse. For the upper trusses this was different because the critical plastic hinges happened around vierendeel panels. Due to the lack

of a diagonal at this zone the failure of the truss chord may lead to a total collapse of the floor. This can trigger a story progressive collapse in the structure, which may result in the collapse of entire building.

- The structures with and without concrete deck had different plastic behaviors. In the model with concrete slabs a series of models with progressively increasing strength were analyzed, it was found that there is one particular strength where the analysis predicts collapse and a slightly larger strength where the analysis predicts little damage. The catenary effect is one main reason for such contrasted behavior.
- Unlike the earthquake analyses, the progressive collapse analyses need smaller damping percentages (1% or below). This small damping ratio prevented the catenary effects to halt the running analyses with SAP2000.
- The 3-D finite element modeling of a truss located between the $5^{th}$ and $6^{th}$ floors showed that the plastic hinges on chords can take place on either flanges or web or on both of them. In the most vulnerable zones, which are around the vierendeel panels and the neighboring panels to the columns, by using stiffeners as AISC 14 suggests the failure potential in these sections decreases. Therefore an uneconomical section increase will not be needed any more. In the same 3-D analysis, it was seen that plastic hinges could happen on gusset plates especially in welding zones with HSS truss members. In both UFC 2013 and GSA 2013 there is no detailed information about connector plates designing against progressive collapse. But such 3-D modeling can be used to verify the structure's weakness against failure and try to reinforce the sections with high failure potentials like the gusset plates in story-height trusses.

- Because in STS structures there are only two column rows located at outer sides and no columns will be placed in central parts, the nonlinear behavior of the columns in these kinds of structural systems had to be considered in detail. If the columns are made of **I** sections, the strong axis had to be located in moment frame (MRF) direction and therefore the truss chords will be connected to column's weak axis in STS direction. The nonlinear dynamic time-history analyses showed that most of plastic hinge on columns were due to the bending moments along weak axis not due to extra axial loads. In some cases column reinforcing may increase the structural erection costs. Therefore, using different sections such as hollow boxes could be an alternative.
- The structural Ductility demand ratio tends to be high when a column is removed from the corner frames. The Ductility of the STS frames increases as the height of structure increases but for moment resisting frames (MRF), the ductility increases first as the structural height increases then at higher levels again decreases. Overall, the STS frames showed high ductility when compared to the MRF frames.
- When the structure was not designed against progressive collapse potential, the ductility of the STS and MRF frames showed huge variations while, this difference was minor for a structure designed against progressive collapse. In the original model, spandrel beams fail before the staggered truss chords. Therefore in the original model after a sudden column removal, the spandrel beams did overtake the major portion of the redundant forces distributed throughout the structure and after these beams have yielded, then the chords start to overtake the rest. In the retrofitted model, the ductility of both STS and MRF systems were approximately the same and this means that both structural

systems in transverse and longitudinal directions functioned together against potential collapse.

## Recommendations for Future Studies

This was a study done on Staggered Truss Systems and the main goal was to analyze the structural system for the collapse potential due to structural element losses. In this study a 10-story building was designed and investigated which can categorize it between low to midrise buildings. Further study can be performed for taller structures with 30 to 40 stories. Furthermore, the progressive collapse was assumed to trigger by sudden removal of a member. This sudden removal can take place due to a blast or an accident. However, the earthquake incidence can lead to similar problems. During this study, it was shown that catenary action is important for the progressive analysis, and therefore it is vital to have a deep understanding on how the catenary action can improve the structural behavior in collapse analysis. Therefore, a new study on collapse behaviors of high-rise staggered truss structures due to earthquake loads regarding catenary effects is recommended hereby.

# REFERENCES

[1] National Institute of Standards and Technology. (February 2007). Technology Administration. U.S. Department of Commerce (NISTIR 7396). Best Practices for Reducing the Potential for Progressive Collapse in Buildings.

[2] Unified Facilities Criteria (UFC). Design of Buildings to Resist Progressive Collapse. (Including Change 2 – 1 June 2013). U.S. Army Corps of Engineers-Naval Facilities Engineering Command-AIR FORCE Civil Engineer Support Agency.

[3] Chang, Kun, Chen. WeiZhang. (2011).Experimental study of the mechanical behavior of steel staggered truss system under pool fire conditions. Thin-Walled Structures.49, 1442–1451.

[4] AISC-LRFD, Manual of Steel Construction Load & Resistance Factor Design. (1994).

[5] ASCE 7-10 Minimum Design Loads for Buildings and Other Structures. (2010).

[6] UBC 97, Volume 2, Structural Design Requirements. (1997).

[7] ASCE/SEI 41-06, American Society of Civil Engineers. (2007). Seismic Rehabilitation of Existing Buildings.

[8] AISC Steel Design Guide Series 14, Staggered Truss Framing Systems. American Institute of Steel Construction October 2003.

[9] Changkun Chen. (November 2010). Simplified Model for Fire Resistance Analysis on Steel Staggered-truss System under Lateral Force.

[10] Michael P, Cohen. (June 1986). Design Solutions Utilizing the Staggered-steel Truss System.

[11] Jinkoo Kim & Joonho Lee. (Geneva, Switzerland, 3-8 September 2006). Seismic behavior of Staggered Truss Systems. First European Conference on Earthquake Engineering and Seismology (a joint event of the 13th ECEE & 30th General Assembly of the ESC).

[12] John B, Scalzi. (May 6, 1971).The Staggered Truss System—Structural Considerations.

[13] XuhongZhou. Yongjun, He. LeiXu. QishiZhou. (17 April 2009).Experimental study and numerical analyses on seismic behaviors of staggered-truss system under low cyclic loading. Thin-Walled Structures 47(2009)1343–1353.

[14] GSA. (OCTOBER 24, 2013). General Service Administration Alternative Path Analyses & Design Guidlines for Progressive Collapse Resistance.

[15] Federal Emergency Management Agency. FEMA 356. (November 2000). Prestandard and Commentary for the Seismic Rehabilitation of Buildings.

[16] Feng Fu. (2009) .Progressive collapse analysis of high-rise building with 3-D finite element modeling method. Journal of Constructional Steel Research 65, 1269-1278.

[17] Xinzheng, Lu. Xiao, Lu. Hong, Guan. Wankai, Zhang. Lieping, Ye. (2013). Earthquake-induced collapse simulation of a super-tall mega-braced frame-core tube building. Journal of Constructional Steel Research 82 59–71. Contents lists available at Sci Verse Science Direct.

[18] Jinkoo Kim. Taewan Kim. (2009). Assessment of progressive collapse-resisting capacity of steel moment frames. Journal of Constructional Steel Research 65, 169–179.

[19] Jinkoo Kim. Jon-Ho Lee. Young-Moon Kim. (2007). Inelastic Behavior of Staggered Truss Systems. The Structural Design of Tall and Special Buildings.

[20] YueYin, Fei. Huang, Naidong Chu. XingyeLiu. (2005). Study on Application of Staggered Truss Systems. Elsevier Ltd.

[21] Wu Xu. Lin,Hai Han. Zhong Tao. (2014). Flexural behaviour of curved concrete filled steel tubular trusses. Journal of Constructional Steel Research 93, 119–134.

[22] XuhongZhou. YongjunHe. LeiXu, QishiZhou. (2009). Experimental study and numerical analyses on seismic behaviors of staggered-truss system under low cyclic loading. Thin-Walled Structures 47, 1343–1353.

[23] CSI-SAP2000 Online Manual. https://wiki.csiamerica.com/display/kb/Home. (2014).

[24] Graham Powell. P.E. (2005).Progressive Collapse: Case Studies Using Nonlinear Analysis.

[25] Seweryn Kokot. Armelle Anthoine. Paolo Negro. George Solomos. (2012). Static and dynamic analysis of a reinforced concrete flat slab frame building for progressive collapse. Engineering Structures 40, 205–217.

[26] Shalva Marjanishvili. P.E. M.ASCE. Elizabeth Agnew. (2006). Comparison of Various Procedures for Progressive Collapse Analysis. M.ASCE.

[27] Chang, Kun Chen. Wei Zhang. (2012). Comparative experimental investigation on steel staggered-truss constructed with different joints in fire. Journal of Constructional Steel Research 77, 43–53

[28] Abaqus 6.13. Abaqus/CAE User's Guide. (2013).

[29] Center for the Protection of National Infrastructure (CPNI). (October 2011). Review of international research on structural robustness and

disproportionate collapse. Department for Communities and Local Government.

[30] Feng Fu. (2012). Response of a multi-story steel composite building with concentric bracing under consecutive column removal scenarios. Journal of Constructional Steel Research 70, 115–126.

[31] Feng Fu. (2010).3-D nonlinear dynamic progressive collapse analysis of multi-story steel composite frame buildings — Parametric study. Engineering Structures 32, 3974–3980.

[32] H.R, Tavakoli. A, Rashidi Alashti. (24 October 2012) Evaluation of progressive collapse potential of multi-story moment resisting steel frame buildings under lateral loading.

[33] J, Kim. Y, Jun. J, Park. (2009).Performance of Building Structures with Outrigger Trusses Subjected to Loss of a Column. 2nd Specialty Conference on Disaster Mitigation.

[34] Bobbi Marstellar, P.E. Tom Faraone, P.E. Anatomy of a Staggered Truss. (1976).

[35] American Association State Highway and Transportation Officials Standard (AASHTO). (2004). Standard Test Methods for Tension Testing of Metallic Materials.

[36] Leslaw Kwasniewski. (2010). Nonlinear dynamic simulations of progressive collapse for a multistory building. Engineering Structures. 32, 1223-1235.

[37] Hyun,Su Kim. Jinkoo Kim .Da,Woon An. (2009). Development of integrated system for progressive collapse analysis of building structures considering dynamic effects. Advances in Engineering Software 40, 1–8.

[38] David C.Stringer.( 1982). Staggered Truss and Stub Girder Framing Systems in Western Canada.Canadian Structural Engineering Conference.

[39] Meng,Hao. Tsai. Bing,Hui Lin. (2008) . Investigation of progressive collapse resistance and inelastic response for an earthquake-resistant RC building subjected to column failure. Engineering Structures 30, 36193628.

[40] Gökhan Pekcan. Christin Linke. Ahmad Itani. (2008). Damage avoidance design of special truss moment frames with energy dissipating devices. Journal of Constructional Steel Research.

[41] Alessandra Longo. Rosario Montuori. Vincenzo Piluso. (2013).Theory of plastic mechanism control of dissipative truss moment frames. Engineering Structures.